TECHNISCHE UNIVERSITÄT WIEN
Vienna University of Technology

Diploma Thesis

Isocyanate-Based High Performance Photopolymers

conducted at the

Research Group for Polymer Chemistry and Technology,

Institute of Applied Synthetic Chemistry (IAS)

at the Vienna University of Technology (TU Vienna)

under the supervision of

Univ.Prof. Dipl.-Ing. Dr.techn. Robert Liska

Univ.Ass. Dr.techn. Katharina Ehrmann, MSc

by

Selina Diendorfer, BSc

01527073

Selina Diendorfer, BSc

Danksagung

An erster Stelle bedanke ich mich bei **Prof. Robert Liska** für die Möglichkeit meine Diplomarbeit in seiner Forschungsgruppe durchführen zu dürfen. Du hast es mir ermöglicht, an einem aktuellen Thema zu arbeiten, das mich sehr begeistert und auch eine spannende Anwendung hat. Besonders hervorzuheben ist auch die angenehme und offene Arbeitsatmosphäre, auf die Du immer großen Wert legst. Vielen Dank!

Dr. Katharina Ehrmann gilt ebenso ein besonderer Dank. Danke dass Du als direkte Betreuerin meiner Arbeit mir immer mit gutem Rat zur Seite gestanden bist. Egal ob hier in Wien oder auf der anderen Seite der Welt, du hast dir immer Zeit genommen um mir zuzuhören und nur durch deinen Input zur richtigen Zeit konnte meine Diplomarbeit sich zu ihrer heutigen Form entwickeln.

Bei **Dr. Patrick Steinbauer** möchte ich mich für die Betreuung während meiner Bachelorarbeit bedanken. Du hast mir nicht nur das spannende Gebiet der Polymerchemie gezeigt, sondern auch mein praktisches Wissen zur Synthesechemie umfangreich erweitert.

Auch Herr **Dr. Markus Kury** möchte ich Danken, der mir die Polymerchemie im Rahmen der Laborübung organische Technologie schmackhaft gemacht hat. Ohne Dich wäre ich nie in der FBMC gelandet und würde diese Diplomarbeit nicht verfassen!

Vielen Dank möchte ich auch **Dipl. Ing. Klaus Ableidunger** und **Raffael Wolff** aussprechen, die mir beim Einstieg in die Thematik meiner Diplomarbeit, sowie der praktischen Durchführung eine große Hilfe waren.

Vielen Dank an alle **Mitglieder der FBMC**, für eure wertvollen Ratschläge, Engagement und ermutigenden Worte. Ein besonderer Dank gilt auch **Jelena und Kaja**, die mir als meine direkten Laborkolleginnen immer mit Rat und Tat zur Seite standen und den Arbeitsalltag im Labor bereichert haben. Ich freue mich auch in Zukunft mit euch als meine Laborkolleginnen den spannenden und anstrengenden Laboralltag zu meistern.

Da bekanntlich das Beste zum Schluss kommt, möchte ich mich am Ende bei meiner Familie bedanken. Danke **Marcel**, dass du immer für mich da bist, immer an mich glaubst und mich stätig mir gutem Essen für die Mittagspausen versorgt hast. Ich kann niemals in Worte fassen, wie dankbar ich meiner Mama **Petra** und meinem Papa **Leopold** für die nie endende Unterstützung bin. Ohne euch wäre ich heute nicht da wo ich jetzt bin!

Table of Contents

Table of Contents		**9**
Introduction		**1**
1. Industrial coatings and additive manufacturing		1
2. Photopolymers		4
3. Polyurethane chemistry		12
Objective		**22**
State of the Art		**23**
Results and Discussion	**R&D**	**Exp.**
1. Model systems for catalytic cyclodimerization and cyclotrimerization of isocyanates with free bases	31	71
1.1. General procedure for the investigation	32	71
1.2. 1,5-Diazabicyclo[4.3.0]non-5-ene	33	71
1.3. Tetramethyl guanidine	37	71
1.4. Triethylamine	40	72
1.5. Tributylphosphine	42	72
1.6. Triphenylphosphine	44	72
1.7. 1,2-Dimethylimidazole	46	72
1.8. 1-(2-Ethyl hexyl)-2-butyl-imidazole)	48	73
1.8.1. Synthesis of 1-(2-Ethyl hexyl)-2-butyl-imidazole)	48	73
1.8.2. Investigation of 1-(2-Ethyl hexyl)-2-butyl-imidazole)	49	74
2. Synthesis and stability of Photobase Generators	51	74
2.1. General procedure for the investigation	52	74
2.2. Photo-1,5-diazabicyclo[4.3.0]non-5-ene	53	-
2.3. Photo-tetramethyl guanidine	55	75
2.3.1. Synthesis of photo-tetramethyl guanidine salt	55	75
2.3.2. Photoactivity and stability of photo-tetramethyl guanidine salt	56	-
2.4. Photo-tributylphosphine	58	76
2.4.1. Synthesis of photo-tributylphosphine salts	58	76
2.4.1.1. Synthesis of photo-keto-tributylphosphine salt	58	76
2.4.1.2. Synthesis of photo-borate-tributylphosphine salt	59	76
2.4.1.3. Synthesis of photo-benzophenone-tributylphosphine salt	61	78
2.4.2. Photoactivity and stability of photo-tributylphosphine salts	62	-

2.5. Photo-dimethylimidazole 64 79
2.5.1. Synthesis of photo-dimethylimidazole salt 64 79
2.5.1.1. Synthesis of photo-keto-dimethylimidazole salt 64 79
2.5.1.2. Synthesis of photo-borate-dimethylimidazole salt 64 80
2.5.2. Photoactivity and stability of photo-dimethylimidazole salt 65 -
2.6. Photo-1-(2-ethyl hexyl)-2-butyl-imidazole 68 80
2.6.1. Synthesis of photo-1-(2-ethyl hexyl)-2-butyl-imidazole) salt 68 80
2.6.2. Photoactivity and stability of photo-1-(2-ethyl hexyl)-2-butyl-imidazole) salt 69 -
Summary and Conclusion **82**
Materials and Methods **87**
References **89**
Appendix **S1**

Abstract

The development of radiation-based curing has had a big impact on coating industry and additive manufacturing. It offers the possibility to manufacture technically advanced products in an economical way. Contrary to thermal curing, where heat exposure is mandatory to cure the formulation, radiation-based curing typically does not utilize thermal treatment. Radiation-based curing triggers the curing process through light, which is an easy, fast and energy efficient possibility to obtain innovative products.

Currently, industrially used materials for radiation-based curing are limited considering their mechanical properties, resulting in very brittle materials. Therefore, current research focuses on the toughening of these brittle networks. A possible improvement of the mechanical properties of the network offer the inclusion of urethane functionalities. Urethane groups inside the polymer network provide the formation of non-covalent inter- and intramolecular interactions, which further improve the modulus and the toughness of the formed network. Nowadays industrially used urethane containing radiation curable materials are (meth)acrylate which exhibit due to their flexible spacers a lower T_g and improved toughness compared to the pure (meth)acrylate polymers. The implementation of materials solely consisting of urethane bonds and accompanying the renunciation of other functionality forming monomers like (meth)acrylate to this selection would be a beneficial addition. In comparison, urethane-based materials, also known as polyisocyanurates, provide impressive thermal and mechanical properties as a result of their structural characteristic of cyclotrimerized isocyanate and would offer a potential new approach to isocyanate-based high performance photopolymers.

Aim of this work was to synthesize and investigate new isocyanate-based high performance materials via photopolymerization. To achieve this, the catalytic conditions for the cyclodimerization and cyclotrimerization of aliphatic and aromatic monofunctional isocyanates were investigated. The free bases 1,5-diazabicyclo(4.3.0)non-5-en, 1,1,3,3-tetramethylguanidin, triethylamine, tributylphosphine, triphenylphosphine, 1,2-dimethyl imidazole and 2-butyl-1-ethylhexyl imidazole were used for investigation of the cyclodimerization and cyclotrimerization of phenyl isocyanate and hexyl isocyanate.

For successful cyclization experiments with the free bases, the corresponding photobase generators (PBGs) were synthesized to investigate the analogue light-activated reaction with respect to photopolymerization efficiency and thermal stability in the dark. A photobase

generator is an organic compound, which generates upon irradiation with light an active species which further catalyzes the desired reaction. As a result of the high reactivity of isocyanates the majority of the synthesized PBGs exhibited dark reactivity in the presence of the isocyanates already at ambient temperatures. However, we identified a promising imidazole PBG, which afforded a stable reaction mixture. In future work, their solubility and reactivity will be optimized to afford cyclodimerization and cyclotrimerization of isocyanates suitable for coating applications and potentially even light-based 3D printing.

Kurzfassung

Die Entwicklung der strahlungsbasierten Härtung hatte einen großen Einfluss auf die Beschichtungs sowie die 3D-Druck Industrie. Strahlenbasierten Härtung bietet die Möglichkeit, technisch anspruchsvolle Produkte wirtschaftlich herzustellen. Im Gegensatz zur thermischen Härtung, bei der zur Aushärtung der flüssigen Formulierung eine Wärmeeinwirkung erforderlich ist, kommt es bei der strahlungsbasierten Härtung zu keinen thermischen Einwirkungen. Der Härtungsprozess der strahlenbasierten Aushärtung wird mit Hilfe von Licht ausgelöst und ist eine einfache und schnelle energiesparende Möglichkeit innovative Produkte zu erhalten.

Derzeit sind industriell genutzte Materialien für die strahlenbasierte Härtung aufgrund ihrer spröden Eigenschaften begrenzt. Aktuelle Forschung fokussieren sich daher auf die Verringerung der spröden Eigenschaften im Polymernetzwerk. Eine mögliche Verbesserung der mechanischen Eigenschaften des polymeren Netzwerkes bietet die Einbindung von Urethanfunktionalitäten in das Netzwerk. Urethangruppen innerhalb des Polymernetzwerkes sorgen für die Bildung nichtkovalenter inter- und intramolekularer Wechselwirkungen, die das Elastizitätsmodul und die Zähigkeit des gebildeten Netzwerks verbessern. Heutzutage werden industriell lichthärtende urethanhaltige (Meth)acrylate verwendet, die aufgrund ihrer flexibleren Spacer einen niedrigere T_g und eine verbesserte Zähigkeit im Vergleich zu reinen (Meth)acrylaten aufweisen. Der Einsatz von Materialien, die ausschließlich aus Urethanbindungen bestehen und einhergehend der Verzicht auf andere funktionalitätsbildende Monomere wie (Meth)acrylate, wäre eine sinnvolle Ergänzung zu dieser Auswahl. Im Vergleich dazu bieten Materialien auf Urethanbasis, auch Polyisocyanurate genannt, aufgrund ihrer strukturellen Eigenschaften von cyclotrimerisiertem Isocyanat beeindruckende thermische und mechanische Eigenschaften und würden einen potenziellen neuen Ansatz für Hochleistungsphotopolymere auf Isocyanatbasis bieten.

Ziel dieser Arbeit war die Synthese und Untersuchung neuer photopolymerisierbarer Hochleistungsmaterialien auf Isocyanatbasis. Um dies zu erreichen, wurden die katalytischen Bedingungen für die Cyclodimerisierung und Cyclotrimerisierung von aliphatischen und aromatischen monofunktionellen Isocyanaten untersucht. Als potentielle Katalysatoren der Cyclodimerisierung und Cyclotrimerisierung von Phenylisocyanat und Hexylisocyanat wurden die freie Basen 1,5-Diazabicyclo(4.3.0)non-5-en, 1,1,3,3-Tetramethylguanidin, Triethylamin,

Tributylphosphin, Triphenylphosphin, 1,2-Dimethylimidazol und 2-Butyl-1-ethylhexylimidazol verwendet.

Für erfolgreiche Cyclisierungsexperimente mit den freien Basen wurden die entsprechenden Photobase Generatoren (PBGs) synthetisiert, um die analoge lichtaktivierte Reaktion hinsichtlich Photopolymerisationseffizienz und thermischer Stabilität im Dunkeln zu untersuchen. Ein Photobasengenerator ist eine organische Verbindung, die bei Bestrahlung mit Licht eine aktive Spezies erzeugt, die die gewünschte Reaktion katalysiert. Aufgrund der hohen Reaktivität von Isocyanaten zeigte der Großteil der synthetisierten PBGs in Gegenwart der Isocyanate bereits bei Umgebungstemperatur eine dunkel Reaktivität. Wir haben jedoch ein vielversprechende Imidazol-PBG identifiziert, die eine stable Formulierung ermöglicht. In zukünftigen Arbeiten werden die Löslichkeit und Reaktivität optimiert, um die Cyclodimerisierung und Cyclotrimerisierung von Isocyanaten zu ermöglichen, die für Beschichtungsanwendungen und möglicherweise sogar für den lichtbasierten 3D-Druck geeignet sind.

Introduction[1]

1. Industrial coatings and additive manufacturing

The use of decorative and protective coating reaches back thousands of years. Around 2000 BC, ancient Chinese artisans implemented decorative and protective layers, utilizing Indian balsams and resins to generate lacquerwork. These enable smooth, glossy surfaces on their daily-use items. The industrial revolution in the 18th century marked the beginning of further development in coating technology, driven by the need to protect buildings and iron materials. In particularly the maritime industry relied on the advancement of effective protective coatings for their watercrafts. Further a variety of resins including vinyl, urea, alkyd and acrylic as well as polyurethane and melamine resins, depicted in Figure 1 emerged. These innovations in coating materials were accompanied by improvements in coating technologies. Finally, also the automation of coatings became prevalent to meet the rising production demands driven by industries like automotive and warfare. Nowadays, there is a variety of coating materials with specifically designed properties for particular purposes.[2]

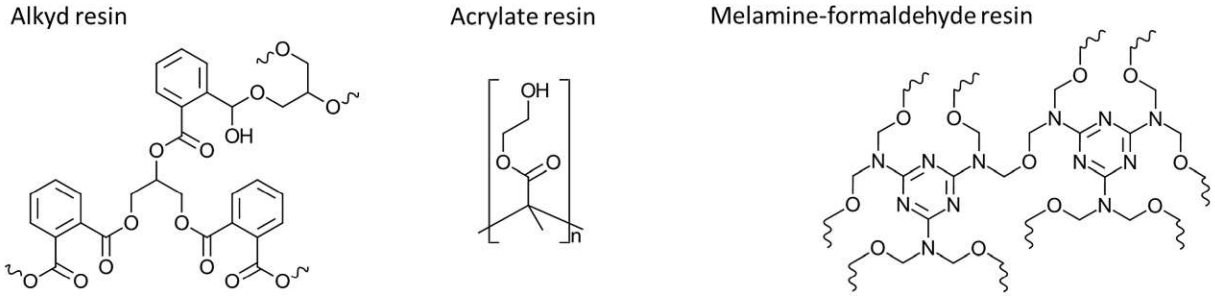

Figure 1: Idealised structures of an alkyd resin derived from glycerol and phthalic anhydride, an acrylate resin of polyhydroxyethyl methacrylate and a melamine-formaldehyde resin

The most common curing procedures for surface coatings are presented in Figure 2, wherein the physical method, to cure solution-based formulations by evaporation of organic solvents, is relinquished steadily due to pollution of the environment, resource limitations and energy savings.[2]

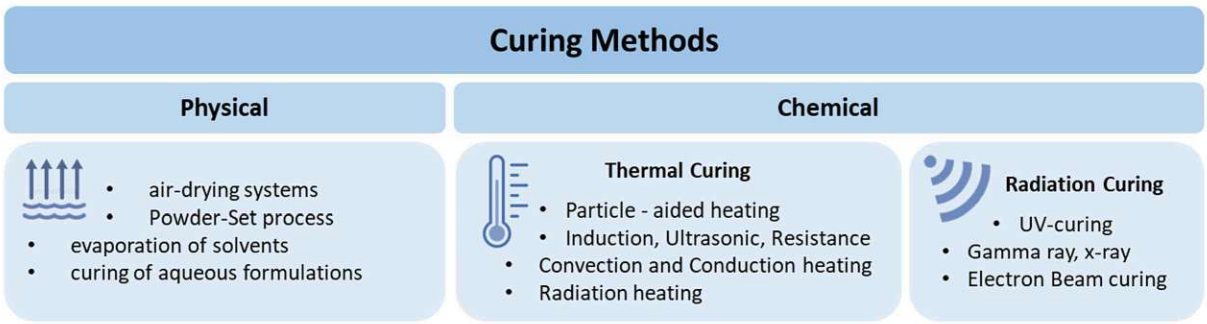

Figure 2: Curing methods for surface coatings[3]

Chemical curing methods consist of thermal and radiation curing methods. Thermal curing of coatings is the most popular method and can be divided into four different categories according to the heating mechanism. Radiation-based curing provides some advantages over thermal curing, including improved resin stability, handling flexibility, fast curing speed, energy efficiency, considerable control and easy processable complex and large structures.[3] For radiation-based curing it is required to use radiation-sensitive compounds, which initiate curing upon irradiation, commonly known as photoinitiators. The resulting photo-cured compounds are thermed photopolymers and photopolymer networks.

An additional application of photopolymerization and herein discussed photopolymers is additive manufacturing (AM), commonly known as 3D printing. Additive manufacturing technologies (AMTs) have been introduced in the 1980s, and since have influenced existing manufacturing methods increasingly.[4] In AMTs, objects are first designed virtually using computer-aided design (CAD) and saved as 3D models in standard transformation language (STL) files, which further are sliced into layered representations with a slicing software. Finally, AMTs utilize this data to produce the physical object through a layer-by-layer approach (Figure 3).[5,6]

Figure 3: AMT process flow[6]

The advantages of ATMs in comparison with other traditional manufacturing techniques like subtractive manufacturing or formative manufacturing, range from the ability to create complex shapes in various orientations to minimal material waste and hence, from an ecological point of view, this could promote material saving as well as long-life products due to the possible selection of the most suitable material for the intended purpose. Additionally, AMTs require lower initial investment costs considering the absence of cost- and labour-intensive tools. However, the production output is comparatively lower with regard to costs per piece compared to other manufacturing techniques, and while other manufacturing techniques becomes more cost-effective with higher production volumes, AMTs maintain almost consistent in costs regardless of production volume. This makes AM very attractive for small-scale production of customized, highly complex and small volume items as well as for the increasing demand for high-performance materials.[4,5,7]

Since the first achievements of AM, AMTs have been expanding rapidly as a result of their enormous freedom of design as well as ecological advantages. A selection of common AMTs is presented in Figure 4.[8]

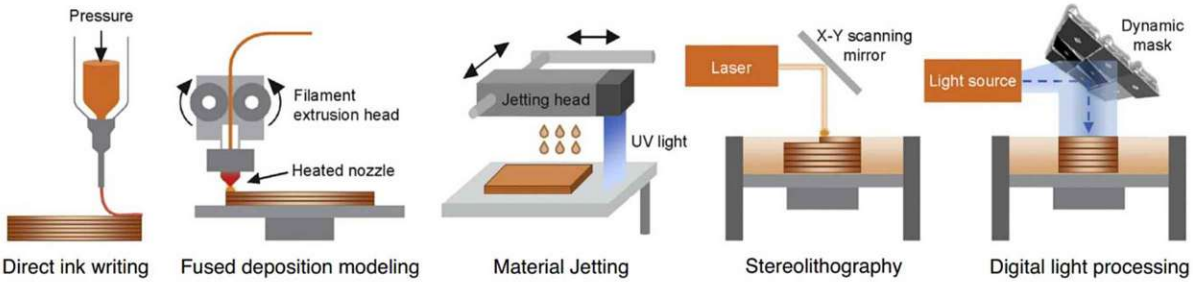

Figure 4: Schematics of five different additive manufacturing techniques including direct ink writing (DIW), fused deposition modeling (FDM), material jetting (MJ), stereolithography (SLA) and digital light processing (DLP)[9]

DIW and FDM are methods in which the final three dimensional object is processed solely through physical processes. During these process, the viscosity of the materials are lower through higher temperatures and reshaped. In contrast, MJ, SLA and DIW are examples for AMTs where the obtained three dimensional object is produces through a chemical reactions of the used formulation and do not necessarily need high temperatures. MJ, SLA and DIW are based on a light induces curing of a liquid formulation to obtain a so called photopolymer. Except for MJ, where selective droplets of the photopolymer are deposited and then cured, this light based polymerizations are commonly known as 'vat photopolymerization'. As the name implies, in vat photopolymerization a liquid photo curable formulation is stored in a vat. A platform is submerged into the liquid formulation and a light source cures the formulation

on the platform. In case of SLT a defined laser is used as light source to obtain high printing resolution or in the case of DLP a broad light source is used to simultaneously cure a whole region at once. Following, the platform is lowered further into the formulation, liquid formulation overlays the cured layer and the light source cures the new layer, to obtain in a layer by layer approach a three dimensional object.[8,9]

A remarkable achievement of lithographic base AMTs is the possibility of hot lithography. Hot lithography is based on the principals of SLA and DLP but at operating temperatures up to 140 °C.[10] This enables the processing of high viscosity formulations and herein the usage of high molecular weight or urethane group containing resins and formulations filled with thermoplastics to significantly improve the thermomechanical properties of the obtained three dimensional object.[11] Accompanying the reduction of the viscosity through higher temperatures enable a higher mobility of the formulation lead to an acceleration of the printing process.

2. Photopolymers

Photopolymers were first introduced in the 1940s. The initial challenge of low curing depth could be improved throughout the last decades, to go from millimeter depth protective and decorative coatings of paper, wood, metals or plastics to higher curing depths in dental fillings, biocompatible and biodegradable polymers used in medical applications, optical materials, adhesives and lithography-based additive manufacturing technologies.[12-18]

Photopolymerization is known for benefits such as rapid curing at ambient temperature, high spatial resolution, minimal release of volatile substances, solvent-free polymerization, energy efficiency and cost-effectiveness. Additionally, the adoption of LEDs as a replacement for conventional mercury lamps further reduces the energy consumption during curing drastically.[12,14-16]

In general photopolymerization is the process of a polymerization initiated by light as the energy source for the polymerization of functional monomers, oligomers and polymers. The photosensitive formulation used for photopolymerization contains a variety of different compounds to fulfil the requirements of the particular purpose of the polymerized formulation. The essential main components of every photosensitive formulation are monomers and a photoinitiator (PI). A PI is a photosensitive compound, which generates an active species upon irradiation with light. The active species of the PI can be a radical or an ion

(cation or anion) and the photopolymerization either follow a chain-growth mechanism or a step-growth mechanism, see Figure 5.[19]

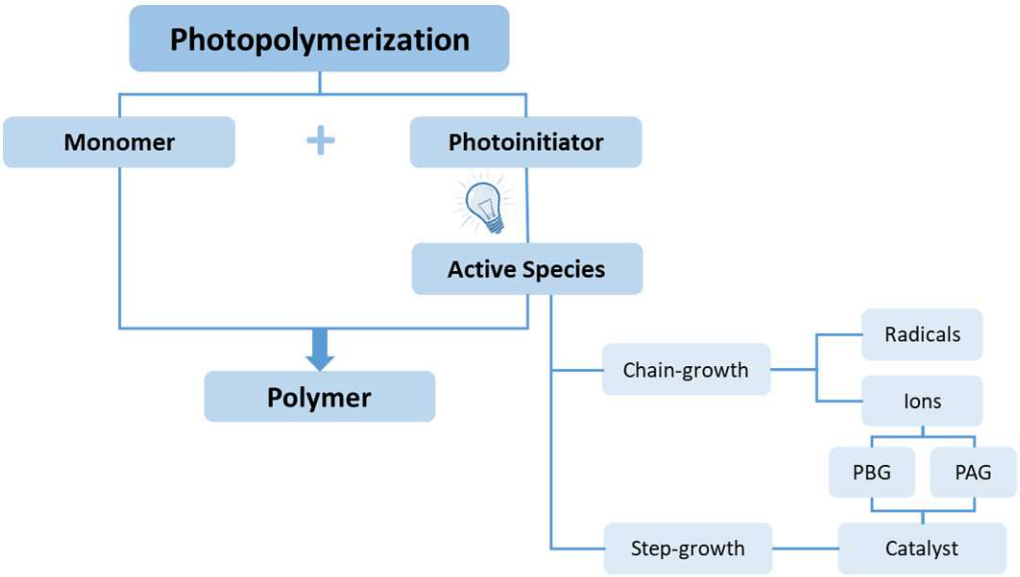

Figure 5: Required compounds for a photopolymerization and the different polymerization mechanism which can be achieved be generating different active species

The key difference between these two polymerization mechanisms is how the polymerization degree changes as the reaction proceeds (Figure 6). The polymerization degree describes the number of sequential monomers in a macromolecule and herein the molecular weight of the polymer chains. In a chain-growth polymerization, long polymer chains exist even at low conversion rates. In contrast, in a step-growth polymerization shorter molecules including dimers, trimers and oligomers are initially formed. To obtain a high degree of polymerization and consequently a high molecular weight, a high conversion is necessary.[20]

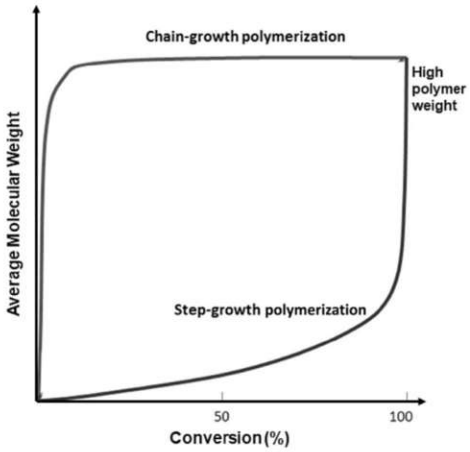

Figure 6: Schematic representation of the molecular weight as a function of the conversion of a chain-growth and step-growth polymerization[20]

A photopolymerization following a chain-growth mechanism characterises a reaction in which monomers add to the active chain end of a growing polymer chain.[19] The process of a chain-growth photopolymerization is depicted schematically in Figure 7.

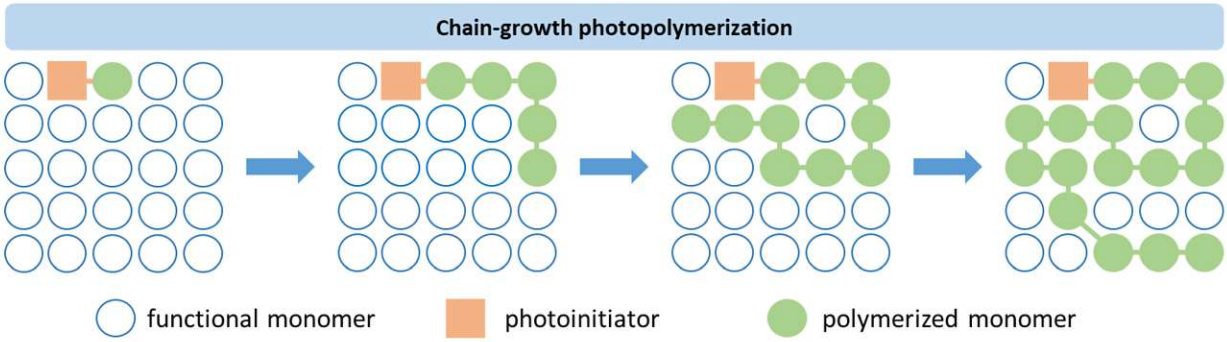

Figure 7: Schematic representation of a photopolymerization following a chain-growth mechanism

The chain-growth photopolymerization includes three different steps, the initiation, the propagation and at least the termination and can be initiated throw a PI, by generating a radical or an ion triggered by light. A radical chain-growth photopolymerization is very sensitive against oxygen, which inhibits the polymerization. Additionally, functionality in the main chain is uncommon and accompanying the adjustment of the properties of the obtained polymer via a radical mechanism is limited.[21] Figure 8 depicts common used radical photoinitiators Ivocerin, TPO-L and BAPO and typical acrylates and methacrylates used as monomers for radical chain-growth polymerization.

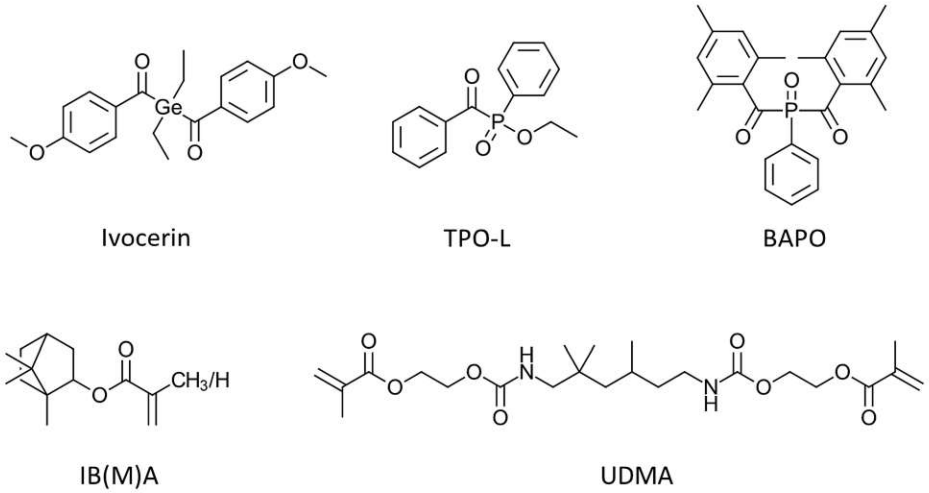

Figure 8: Chemical structures of photoinitiators ivocerin, 2,4,6-trimethylbenzoyldi-phenylphosphinate (TPO-L), phenylbis(2,4,6-trimethylbenzoyl)phosphine oxide (BAPO), and structures of typical monomers isobornyl (meth)acrylate (IB(M)A) and urethane diemethacrylate(UDMA)[21,22]

In relation to an ionic active species, the photopolymerization can be initiated with a cationic or an anionic active species resulting in a cationic or anionic chain-growth photopolymerization.[23] To induce cationic or anionic chain-growth photopolymerizations, photoacid generators (PAG) and photobase generators (PBG) can be used. Typically used PAG for cationic photopolymerization and some common used monomers, like epoxides and oxetanes are depicted in Figure 9.[21,22]

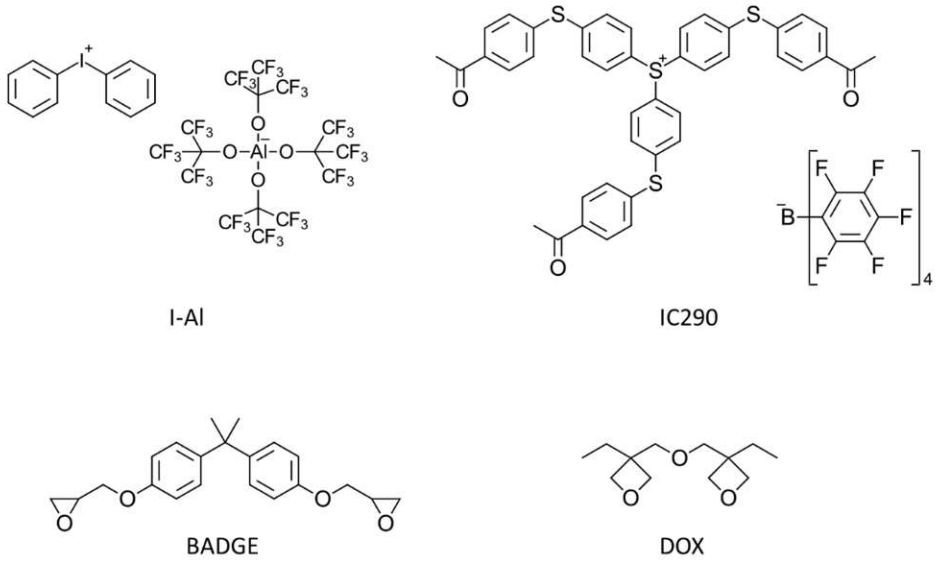

Figure 9: Chemical structures of PAG: iodonium aluminate (I-Al), borate-based triarylsulfonium salt Irgacure® 290 (IC290) and structures of typical monomers aromatic bisphenol-A glycidyl ether (BADGE) and 3,3'-[oxybis(methylene)]bis[(3-ethyl)oxetane] (DOX)

In a reaction defined by a step-growth mechanism, photopolymerization occurs whereby endgroups of di- or multifunctional monomers undergo chemical reactions with each other to form oligomeric intermediates and ultimately polymers (Figure 10).[19] In general a step-growth polymerizations do not necessarily need an initiator but to achieve a step-growth photopolymerization a photoactive compound is required to catalyse and initiate the step-growth photopolymerisation in a radical or ionic way.[24]

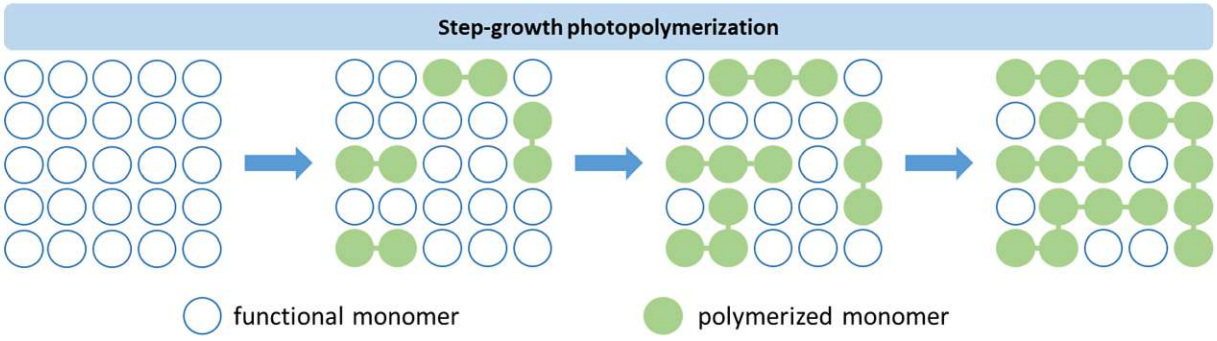

Figure 10: Schematic representation of a photopolymerization following a step-growth mechanism

Thiol-ene chemistry is an ongoing research topic and an example for a possible step-growth photopolymerization via chain transfer agents (CTA). Thiols act as CTA, donating a hydrogen to the active radical chain end and accompanying generate a thiyl-radical. Subsequently, the resulting highly reactive thiyl-radical initiates the formation of another chain. Depending on the monomer electron density, the photopolymerization shift from chain-growth to step-growth. Electron-rich monomers, such as those with norbornene or allyl functionalities, commonly undergo step-growth photopolymerization.[21]

Photobase generator

In the last decade, intensive research has been conducted in the synthesis and characterization of PAGs and PBGs, with synthesis and characterization of PBGs being rare compared to PAGs.[25,26] The concept of organic photobase generators was first introduced in 1990 by Cameron and Frechet, who employed a photosensitive carbamate compound to generate basic amines.[27]

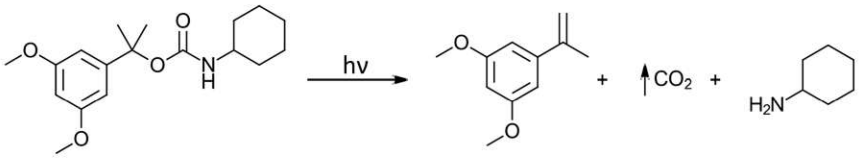

Figure 11: Photosensitive carbamate compound and generation of cyclohexylamine via photodecarboxylation[27]

Cameron developed the concept of PBG derivated from the existing concept of PAG. A PBG generates an organic base as active species upon irradiation with light in the UV range and the generated base initiate the base catalyzed polymerization. Since this thesis will focus on the synthesis and characterization of PBG Scheme 1 depicts the irradiation of a photobase generator and generation of an organic base to further catalyses the photopolymerization.[28] Additionally Figure 12 depicts common boron based PBG and Figure 13 represents the mechanism of the base generation with a boron anion or via photodecarboxylation of a xanthone.

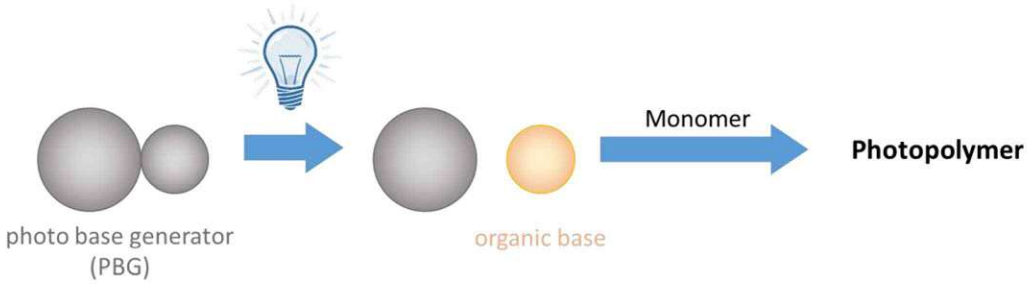

Scheme 1: Irradiation of a photobase generator and generation of an organic base, which further initialises the step-growth photopolymerization

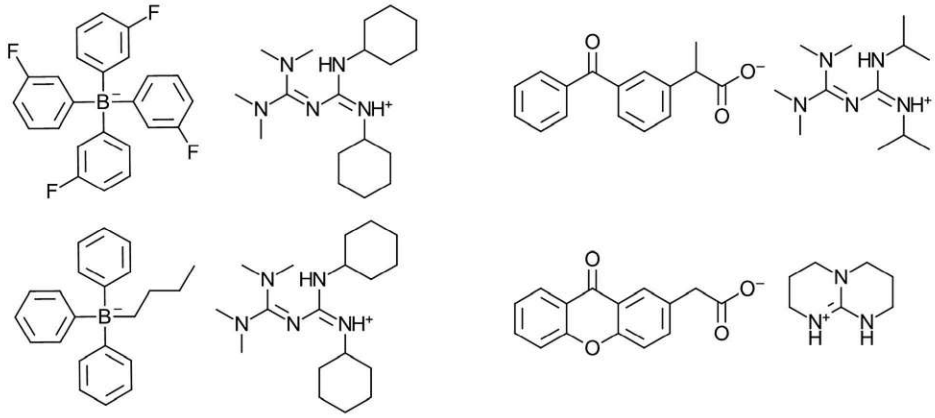

Figure 12: Common used PBG based on borate and guanidine (left) and decarboxylating PBG of ketoprofen (right top) and xanthone (right bottom)[29,30]

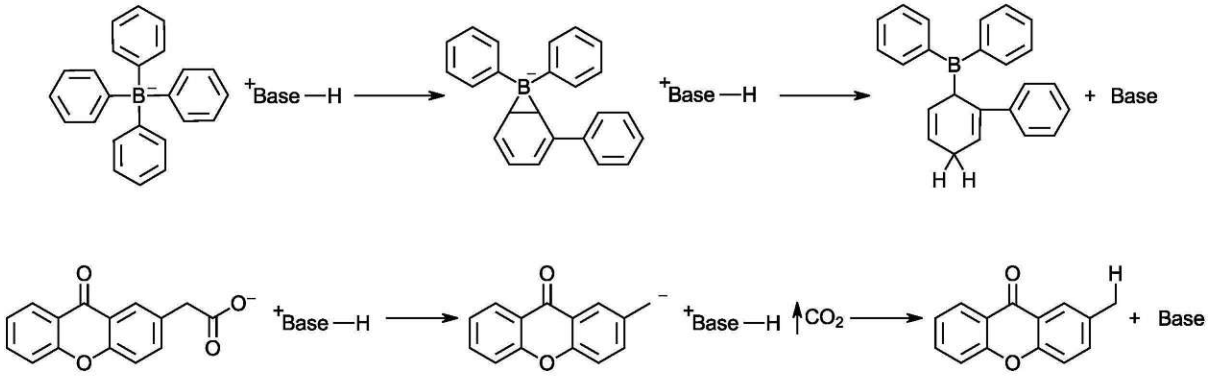

Figure 13: Mechanism of the base generation with UV light of a borate PBG (top) and mechanism of a base generation via photodecarboxylation of a xanthone PBG[26,26]

One advantage of PBGs and PAGs is their insensitivity towards oxygen. Therefore, they can be used in air, which is a considerable advantage compared to free radical polymerization. Another advantage of PBGs, compared to PAGs, is their non-reactivity with metals, which makes PBGs suitable for applications which contain metals, like the automotive and electronic industries.[28]

High performance materials

The origin of high-performance polymers (HPPs) can be traced back to the 1950s and was pushed due to the need for thermally stable polymers in particular in the aircraft and electronics industries. During the 1960s, the first HPP-based on polyimide, which is still widely recognized today as DuPont's Kapton™, became commercially accessible. Following this, in the 1970s, additional HPP, such as the aromatic polyamide Kevlar™ and the thermoplastic polyetherimide Ultem™, were introduced to the market. The structures of these HPP are depicted in Figure 14. In the 90s further development was promoted for the use of HPP in the membrane production or aerospace. Also in the field of microelectronics such as interlayer dielectrics or photoresist HPP still has a lot of potential for new developments.[31]

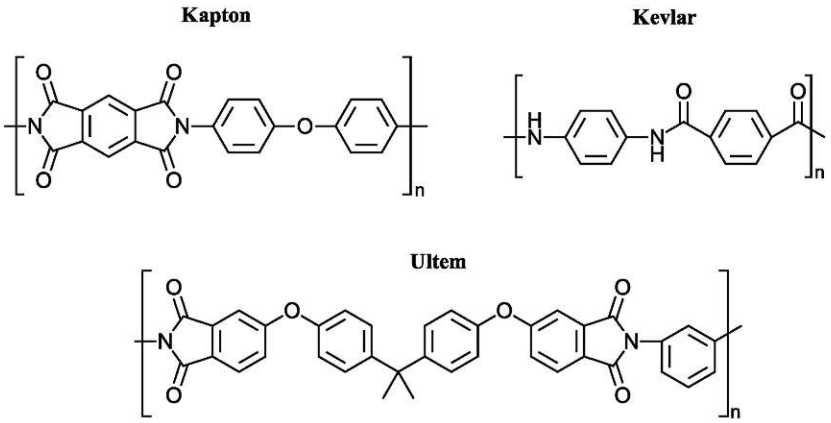

Figure 14: Structures of HPP of Kapton, Kevlar and Ultem

High-performance polymers are generally characterized as polymers capable of enduring and performing effectively under harsh conditions. In general, HPPs distinguish themselves from standard polymers and engineering polymers, by delivering exceptional performance at temperatures exceeding 150 °C, see Figure 15. Standard polymers are produced in large quantities for applications below 100 °C and engineering polymers, which are small quantity products are suitable for temperature between 100-150 °C. While thermal resistance is a key factor, HPPs are also distinguished by their chemical, mechanical, electrical and various physical properties. However, the variety of different properties and their tradeoffs makes it challenging to precisely define the boundaries of HPPs.[31,32]

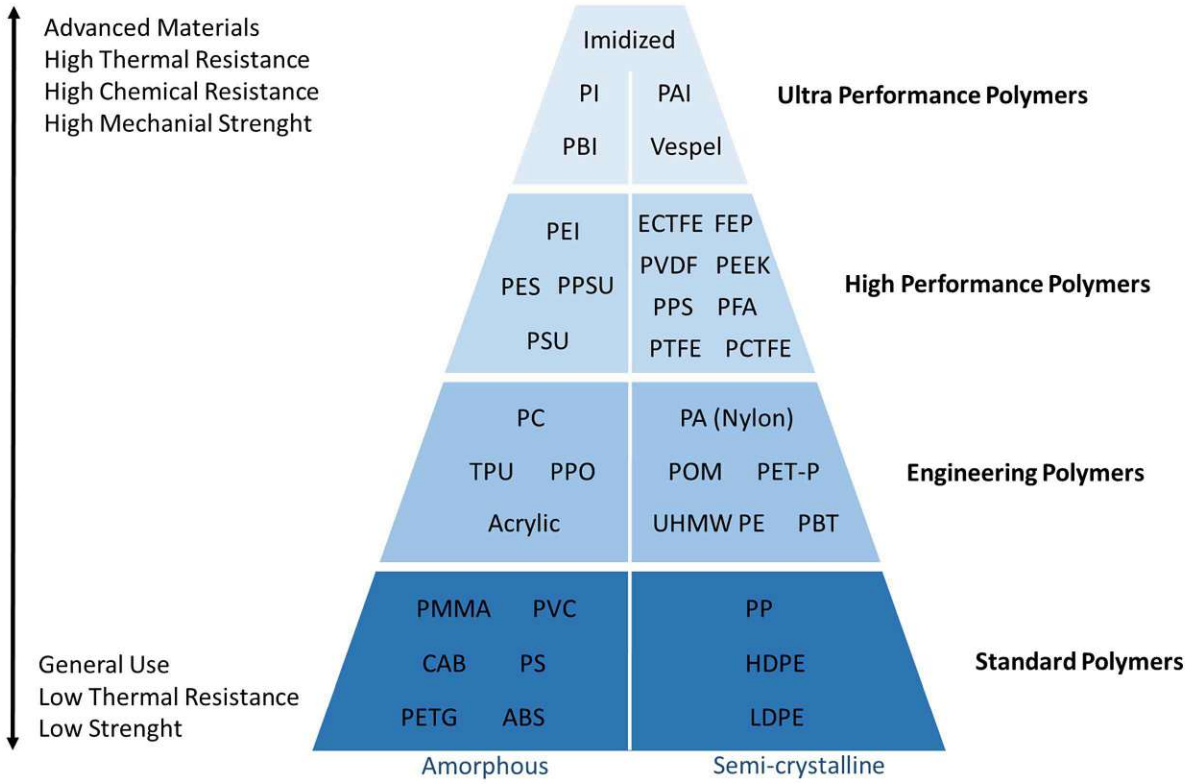

Figure 15: Classification of polymers according to their performance in the areas of temperature, chemical and mechanical stability[32]

High-performance polymers can be divided into two categories. The first category consists of amorphous polymers, including polyetherimides (PEI), polyethersulfone (PES), polyphenylenesulphones (PPSU), polysulphones (PSU), polyimides (PI) and polybenzimidazoles (PBI). The second category contains semi-crystalline polymers, which include polyaryleneetherketones like polyetheretherketone (PEEK), as well as fluoropolymers such as ethylenechlor trifluorethylen (ECTFE), fluorethylenpropylen (FEP), polyvinylidene difluoride (PVDF), perfluoralkoxy-polymere (PFA), polytetrafluoroethylene (PTFE or Teflon), polychlortrifluorethylen (PCTFE), aromatic sulfides or aromatic polyimides like polyphenylene sulfide (PPS) and Vespel. Polymers that undergo imidization, like polyaromatic imides (PAI), PBI and PI are sometimes classified as ultra-performance polymers and arranged above the category of high-performance polymers considering their unique combination of properties, including significantly higher continuous use temperatures and the absence of a melting point.[32]

Kapton™ is obtained through a polycondensation of tetracarboxylic acid dianhydrides and diamines. It is used in industry for electrical isolation, adhesive film and labels for high temperature applications, laminates, heat protection and carrier for film or flexible materials

due to its excellent thermal resistance from -269 °C to +400 °C, the ability of flame retardation and self-extinguishing behaviour accompanied by the absence of a melting point and starting carbonization at 800 °C.[33] The polyamide Kevlar™ is a polycondensation product of terephthaloyl dichloride and para phenylenediamine and is known for the use as bullet-resistant protective clothing because of the very high tensile strength.[34] Ultem™ is obtained through polycondensation of bisphthalic anhydride with 1,3-diaminobenzene.[35] It is flame-retardant with barely any smoke development and has good dielectric strength with consistent dielectric properties and is therefore used in food industry and medicine.[36]

Since HPPs are of great interest in industry and therefore a huge research topic nowadays, some HPPs cannot be categorised yet, e.g., rigid polyurethanes and polyurethanes with a high polyisocyanurate content.[32,37-40]

3. Polyurethane chemistry

Polyurethanes (PUs) represent a unique category of polymeric materials used for many different applications including flexible and rigid foams, paints, liquid coatings, insulations, elastomers, elastic fibers and integral skins.[41,42]

Polyurethanes are produced by reacting an isocyanate with a polyol.[43] Besides the synthesis of polyurethanes, isocyanates are well-known for their ability to dimerize and trimerize catalytically as well as to form ureas, biurets and allophanates, depicted in the following Scheme 2.[44] The formation of urethan, urea, uretdione and isocyanurate already occurs at ambient and moderate temperatures, whereas the formation of biurets and allophanates in general needs temperatures about 150 °C.[45]

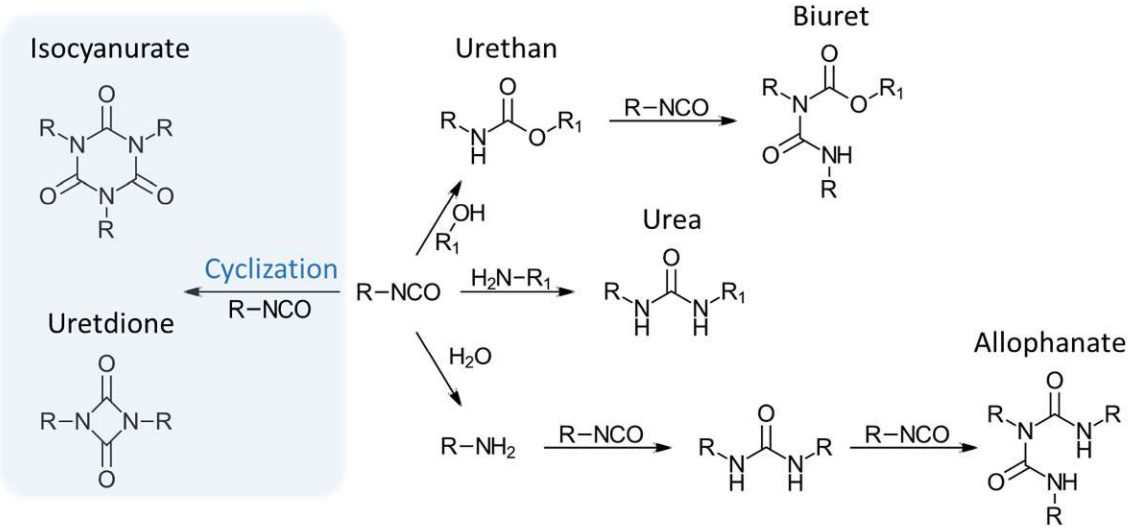

Scheme 2: Basic reactions of an isocyanate group with itself and with other reaction partners

The development of PU leads back to World War II, where PUs were used for coatings, specifically for impregnated paper and chemically resistant coatings for metal, wood, stonework and as high gloss finishes for aircrafts. The production of mustard gas and corrosion resistant clothes made out of PU leads to big advances in the armaments industry. Further, PUs were widely used in the 1950s in elastomers, rigid foams and adhesives and later in the 1950s, comfortable and convenient cushions out of flexible foam became commercially available. The invention of flexible foam from cheap starting materials additionally lead to an enormous enhancement for applications in the automotive and upholstery industries that still remain significant nowadays.[46]

Polyurethanes are commonly synthesised through the reaction of a polyol or diol and a diisocyanate.[46] Scheme 3 depicts the synthesis of a linear PU from difunctional monomers.

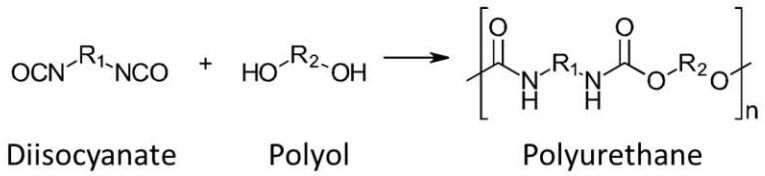

Scheme 3: Synthesis of polyurethane through a diisocyanate and a polyol

Depending on the used isocyanates, polyols and diols, and various additives, which significantly influence the ultimate properties of polyurethanes PUs, PUs can be categorized into five distinct classifications: thermoplastic PU (TPU), flexible PU (FPU), rigid PU (RPU), PU ionomers (PUI) and water-born PU (WPU).[46]

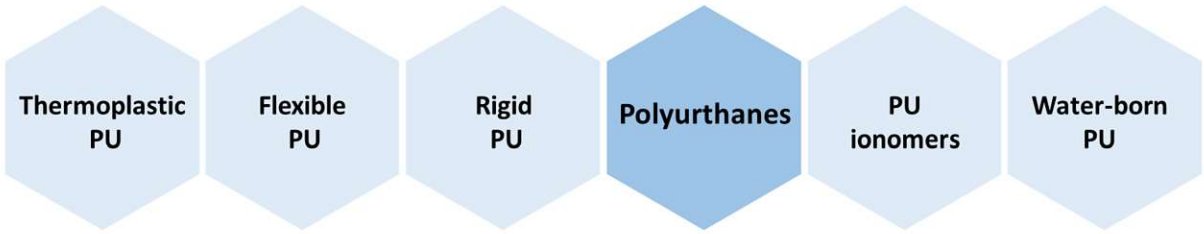

Thermoplastic polyurethanes (TPUs)

TPUs offer a unique combination of physical characteristics, including flexibility and elasticity, resulting in excellent impact, abrasion, and weather resistance, as a result of their hard and soft block structure. Their melt-processability facilitates various processing methods like extrusion, blow molding, compression molding and injection molding as well as the possibility for coloring making TPUs versatile for a wide range of applications.[47-49] Moreover considering

the water-insolubility, no ionic and inert characteristics of TPU, they have found effective use in medical applications. This includes usage in vaginal rings due to their ability of controlled drug release and their suitability for medical tubing due to their impressive mechanical strength, allowing to produce thin walls of tubes without requiring plasticizers.[49,50]

TPUs consist of two main structural units, a hard and a soft block, see Figure 16. The hard block mainly contains the used diisocyanate and a chain extender, whereas the chain extender is a small molecular weight diol or diamine, creating many urethane or urea groups, respectively, which cause 'physical crosslinking' via hydrogen bonding between these groups. The second structural unit, the soft block, consists of a diol. Hard and soft blocks are generally incompatible with each other, leading through physical cross linking via hydrogen bonds to a phase separation of a soft matrix with embedded hard blocks in between.[51] The mechanical and thermal characteristics of TPUs are linked to the chemical structure of the used monomers, the volume fraction of the hard and soft block and the interactions between these two blocks.[52]

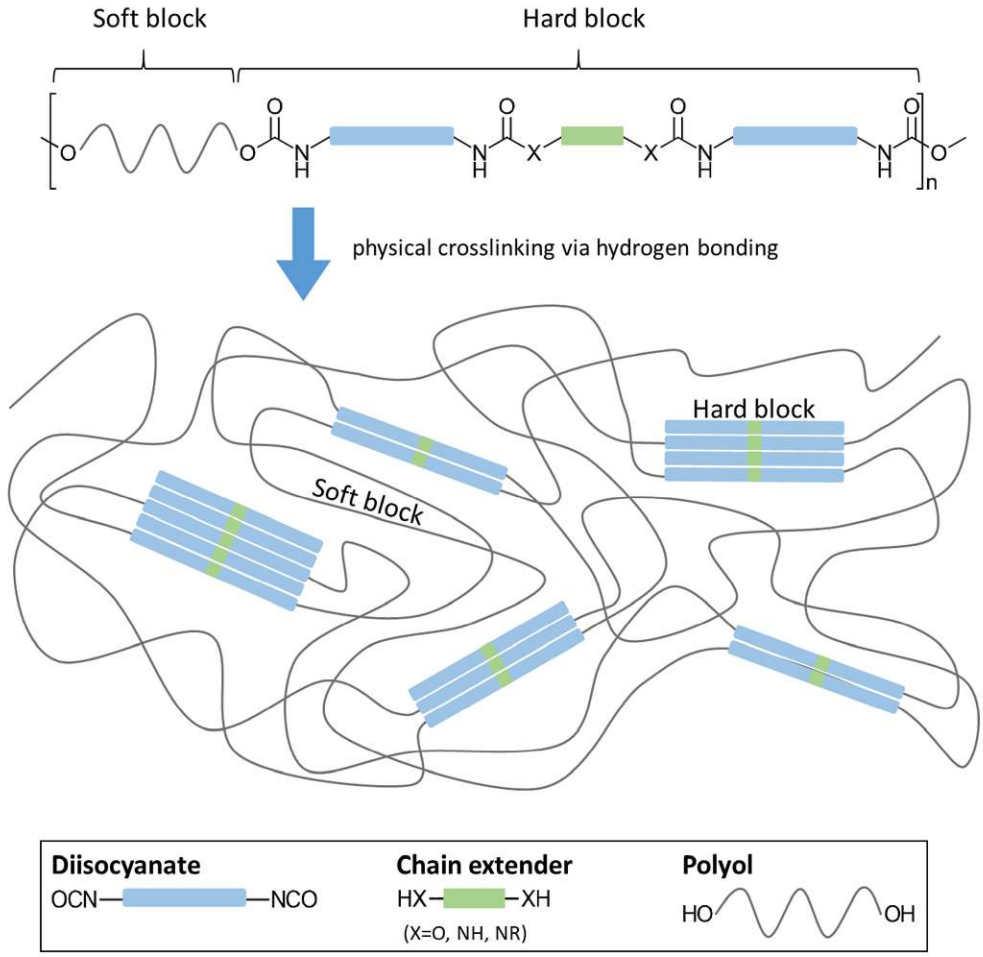

Figure 16: Cartoon of a PU consisting of a soft block (polyol) and hard block (diisocyanate and chain extender) and the phase separation through hydrogen bonding[53]

Flexible polyurethane (FPU) foams, characteristically consist of block copolymers, which obtain their flexibility through the separation of soft and hard blocks like TPUs. The flexible properties of these polyurethane foams can be modified by carefully adjusting the ratios of these two different blocks.[54] Their classification as flexible polyurethanes depends on various physical characteristics such as density, durability, firmness, tear resistance, combustibility, surface elasticity and more. Accompanying good flexibility can be ensured through a combination of these properties. FPU foams are widely used in consumer and commercial products, including carpet underlays, furniture, cushions, bedding, automotive interior parts, packaging, biomedicine and nanocomposites.[46]

Rigid PU (RPU) foams are widely known as versatile and energy-efficient insulation materials. According to reports from "Wien Energie", the major energy consumption of a European household is heating of the living areas. This energy consumption is made up by about 50 % of the total energy consumption of a household.[55] To maintain a consistent temperature and also to reduce the noise level in private households as well as public buildings RPU foams are commonly used in windows, walls and roof insulation as well as in barrier sealants for doors and air control.[46]

The synthesis of **FPU** and **RPU** foams typically consists of two main steps: blowing and gelling, depicted in Scheme 4. The blowing reaction includes the generation and expansion of carbon dioxide and urea through addition of a small amount of moisture, which is entrapped in the reaction mixture. Simultaneously the gelling reaction occurs, involving the formation of urethane linkages between the isocyanate and hydroxyl groups of the polyol.[56,57]

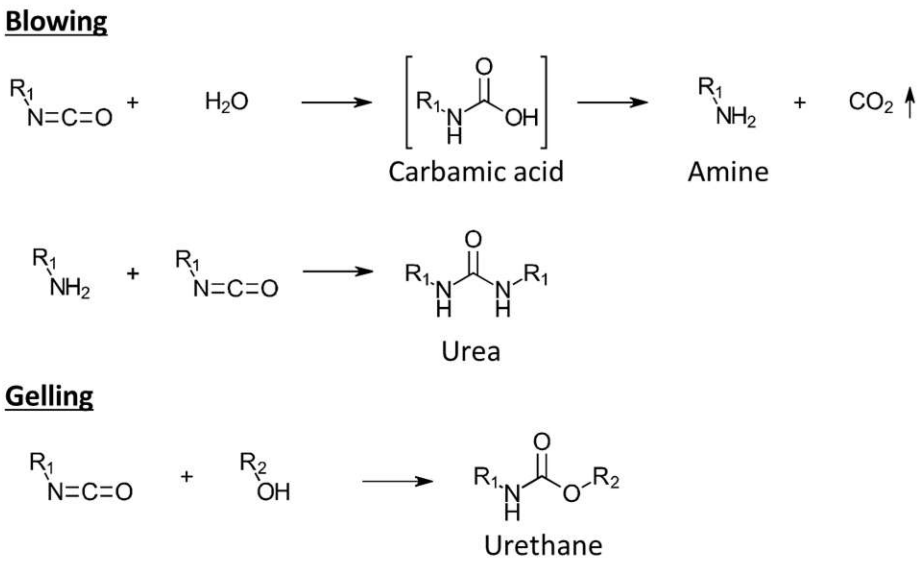

Scheme 4: Blowing and gelling reaction of the synthesis of FPU and RPU[57]

Water born polyurethane (WPU) are coating and adhesives, which primarily use water as a solvent. The main reason for using WPUs is the strict regulations for industry, limiting the use of volatile organic solvents and other potentially hazardous air pollutants. Consequently, in the commercial and industrial sectors many applications make use of WPU dispersions to eliminate hazardous air pollution. WPU dispersions are a two-phase colloidal system including the polyurethane particles and a water-based medium. A big advantage of WPU dispersions is the independence of the viscosity on the molecular weight of the polymer. This enables the accessibility of high solid-content WPUs through a drying process (Scheme 5).[46] However, the drying process is rather slow due to the high boiling point of water.

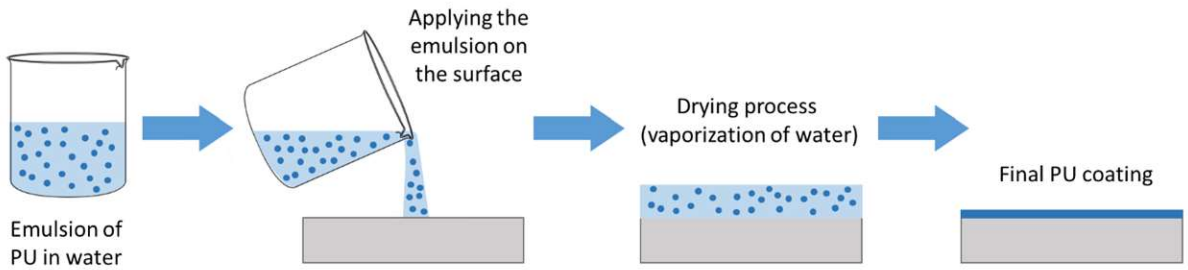

Scheme 5: Schematic representation of a drying process to obtain a PU coating

Besides the typical PU foams FPU and RPU, some literature describes the formation of **polyisocyanurate-polyurethane foams (PIR-PU)**, consisting of polyisocyanurate crosslinked networks.[58-60] PIR-PU show better flame-retardant properties and greater dimensional and thermal stability than PU foams. These exceptional properties are attributed to the formation of the isocyanurate structure, which is preferentially formed when using an excess of isocyanate compared to the hydroxyl groups of the polyol (Figure 17).[61]

Figure 17: Cyclotrimerization of an isocyanate to form an isocyanurate

Presently, three different synthesis methods are described to obtain a polyurethane network within isocyanurate building blocks.[60] In the first method, shown in Scheme 6a, a slight molar excess of the difunctional isocyanate is polymerised with a polyol to obtain linear polyurethanes with an isocyanate functionality at the end. These isocyanate end groups

perform the cyclotrimerization to obtain a PIR-PU network. The formation of the isocyanurate is introduced as an intended side reaction during the synthesis of polyurethane.[62,63]

The second method for the synthesis of PIR-PU, shown in Scheme 6b, is contrary to the first model. Here the first step of the cyclotrimerization is conducted without the polyol in the formulation. In the second step the polyol is added to already formed isocyanurates to obtain the final PIR-PU.[60]

The third and most recently described synthesis method combines the functionalisation of a polyol with an isocyanate to obtain a prepolymer, then removes the unreacted isocyanate and finally trimerizes the isocyanate to get the final PIR-PU, shown in Scheme 6c.[60]

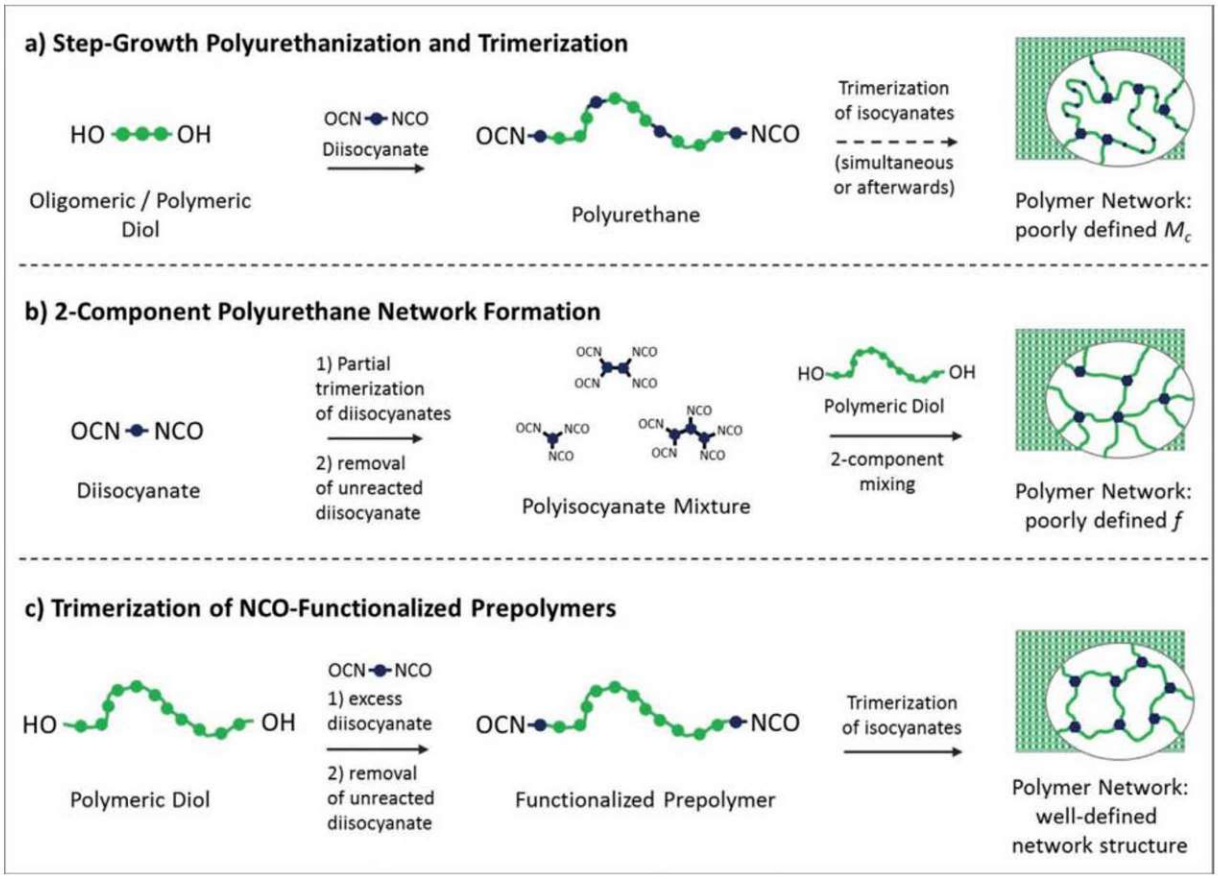

Scheme 6: Simplified graphical representation of the discussed synthesis methods for PIR-PU[60]

The advantages and disadvantages of the three described synthesis methods are: for synthesis method Scheme 6a[60]

+ the crosslinking units (isocyanurate) are well defined and trifunctional
- the molecular weight of the linear polyurethane between the isocyanurate groups has a polydispersity of 2 (due to the step-growth character of the polymerization)

for synthesis method Scheme 6b:

+ the molecular weight between the isocyanurate functionalities are well defined (according to the used polyol)
- low conversion to polyisocyanate and a broad molecular weight distribution of polyisocyanate accompanying with a varying quantity of isocyanate functionalities on the polyioscyanate due to trimers and higher-molecular weighted oligomers of isocyanate leading to a stoichiometric issue in the following network formation step with polyols

The third synthesis method Scheme 6c combines the advantages of the prior mentioned ones leading to well defined polymer networks:

+ narrow molecular weight distribution of the isocyanate end functionalised prepolymer
+ the molecular weight between the isocyanurate functionalities is well defined (according to the used polyol)
+ the crosslinking units (isocyanurate) are well defined and trifunctional

Isocyanates are besides polyols one of the two main components in PUs. The structures of commonly used isocyanates are illustrated in Figure 18. The most commonly used aromatic isocyanates are methylene diphenyl diisocyanate (MDI) and toluene diisocyanate (TDI). These aromatic diisocyanates are usually used for production of flexible and rigid foams due to their low cost and excellent reactivity and find application as molded foams for car seats, as slabstocks for mattresses, refrigerator insulations or shoe soles. For applications like coatings, where transparency or special coloring is mandatory, aliphatic and cycloaliphatic isocyanates are used because aromatic isocyanates darken the final PU when exposed to light. Typically used aliphatic or cycloaliphatic isocyanates are isophorone diisocyanate (IPDI), 4,4´-diisocyanato dicyclohexylmethane (hydrogenated MDI) and 1,6-hexamethylene diisocyanate (HMDI).[46]

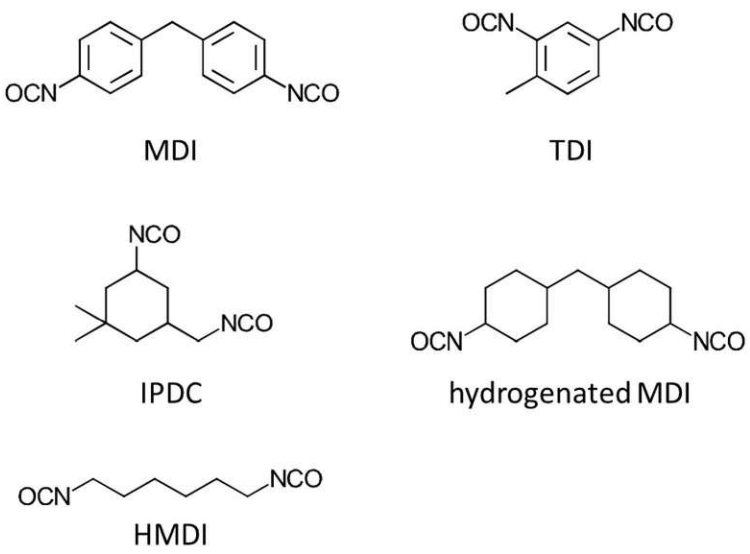

Figure 18: Structures of commonly used isocyanates methylene diphenyl diisocyanate (MDI), toluene diisocyanate (TDI), isophorone diisocyanate (IPDI), 4,4´-diisocyanato dicyclohexylmethane (hydrogenated MDI) and 1,6-hexamethylene diisocyanate (HMDI) for PU synthesis

The second main component of PUs are polyols. A polyol characterises a compound, which has at least two hydroxyl groups. Polyols can be divided into two main categories: polyether polyols and polyester polyols. Polyether polyols can be synthesised through a reaction between an epoxide and an active hydrogen-containing compound or through a ring-opening polymerization of epoxy monomers.[64,65] The second category of polyols, polyester polyols, are accessible through a polycondensation of hydroxyl compounds and multifunctional carboxylic acids.[66] Less commonly used compounds for polyols are polycarbonate and polysiloxane.[67] Table 1 provides an overview of advantages and disadvantages of commonly used polyols from different sources and Figure 19 depicts structural examples of a polyether polyol, a polyester polyol, a polycarbonate polyol and a polysiloxane polyol.

Table 1: Commonly used polyols and their advantages and disadvantages[46]

Polyol Type	Advantages	Disadvantages
Polyether polyols based on propylene oxide and ethylene oxide	Hydrolytic stability, cost, viscosity, flexibility	Oxidative stability, modulus/strength, thermal instability, flammability
Aliphatic polyester polyols	Oxidative stability, modulus/strength	Viscosity, hydrolytic stability
Aromatic polyester polyols	Flame retardance, modulus/stiffness	Viscosity, low flexibility
Polyether polyols based on tetrahydrofuran	Hydrolytic stability, modulus/strength	Oxidative stability, viscosity, cost
Polycarbonate polyols	Hydrolytic stability, oxidative stability, modulus/strength	Viscosity, cost
Polycarbonate polyols	Hydrolytic/oxidative stability, hardness	Viscosity, cost, low flexibility
Polybutadiene polyols	Low temperature flexibility, solvent resistance	Viscosity, thermal oxidizable (unless hydrogenated), cost

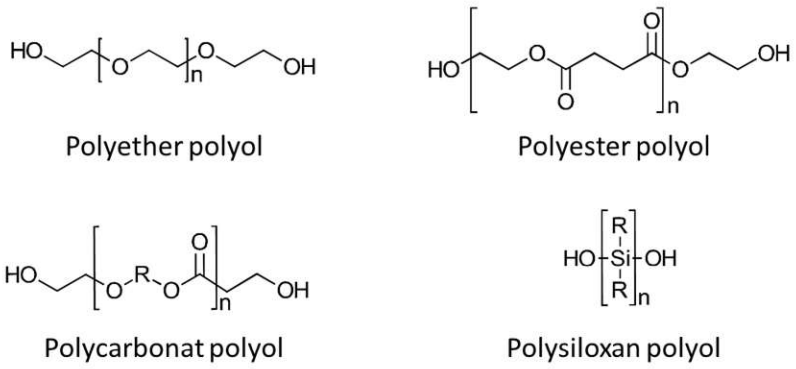

Figure 19: Structural examples of a polyether polyol, a polyester polyol, a polycarbonate polyol and a polysiloxane polyol

Besides the main components for PU, isocyanate and polyols, various additives are used in industry to adapt the final properties. Commonly used additives for the adjustment of the final properties of PU for example are flame retardants, pigments, fillers, blowing agents and surfactants. Table 2 provides an overview of the most common components used in PUs, as well as the reason for the inclusion.[46]

Table 2: Commonly used PU additives and their reason for inclusion[46]

Additives	Reason for inclusion
Isocyanates	Responsible for the PU reactivity and curing properties
Polyols	Contributes flexible long segments, which produces soft elastic polymers
Catalysts	To speed up the reaction between the isocyanate and polyols and to allow reaction at a lower reaction temperature
Plasticizers	To reduce material hardness
Pigments	To produce coloured PU materials, especially for aesthetic purposes
Chain-extender/cross-linker	For structural modification of the PU molecule and to offer mechanical support that will enhance the material properties
Blowing agents/surfactants	To aid the production of PU foams, to help control the formation of bubbles during synthesis and to control the foam cell structure
Fillers	To minimize cost and to improve the material properties, such as stiffness and tensile strength
Flame retardants	To reduce material flammability
Smoke retardants	To reduce the rate of possible smoke generation when the material is burn

Objective

The aim of this thesis is to synthesize and investigate isocyanate-based high performance materials with their formation triggered by light. Radiation-based polyisocyanurate formation can create efficient production conditions in curing industry and lithographic additive manufacturing due to the time and energy efficiency as well as eco-friendliness. The resulting polyisocyanurate offers exceptional thermal and mechanical properties and herein enable a potential new access to high performance materials via photopolymerization.

The synthesis of polyisocyanurate should be based on a cyclodimerization and cyclotrimerization reactions of isocyanates initiated by a catalytic amount of a photobase generator (PBG). A PBG releases a base upon irradiation with light, which further catalyzes the desired reaction. Therefore, the photochemical catalytic reaction conditions of the cyclodimerization and cyclotrimerization of isocyanates will be investigated. To achieve this, model reactions catalyzed by free bases will be performed to gather information about the conditions of the cyclodimerization and cyclotrimerization of isocyanates. In the next step, the PBGs corresponding to the prior investigated free bases will be synthesized and their photoactivity and stability in darkness at elevated temperatures will be determined. Furthermore, the synthesized PBGs will be investigated about their ability to catalyze the cyclodimerization and cyclotrimerization of isocyanates.

On the basis of these characterizations an implementation of the model reactions into a polymer system will be investigated. Therefore, in the case of cyclodimerization and cyclotrimerization, multifunctional isocyanates will be designed and potentially synthesized according to the previously found reactive reagents. Their ability to form crosslinked polyisocyanurate polymers will be investigated. Finally, the suitability of these isocyanate-based reactions for coatings or additive manufacturing applications will be determined.

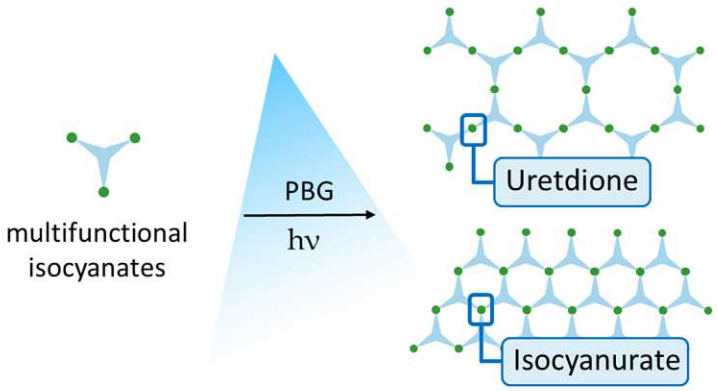

State of the Art

During the period 1885 - 1900, the fundamental properties of isocyanates were discovered. Since then, isocyanates have become indispensable in industrial applications, particularly in the field of polymers and especially polyurethanes.[68]

Polyurethanes (PUs) are presently one of the most prevalent, adaptable and extensively researched materials worldwide due to their combination of durability and toughness of metals with the elasticity of rubber, qualifying them as suitable replacements for metals, plastics and rubber in numerous engineered products.[69-71] Their remarkable properties including hardness, elongation, strength and modulus, making them very interesting for application in biomedical, construction, automotive, textile, and various other industries.[44,70,72-76] Figure 20 represents the most common types of PUs and some conventional applications.

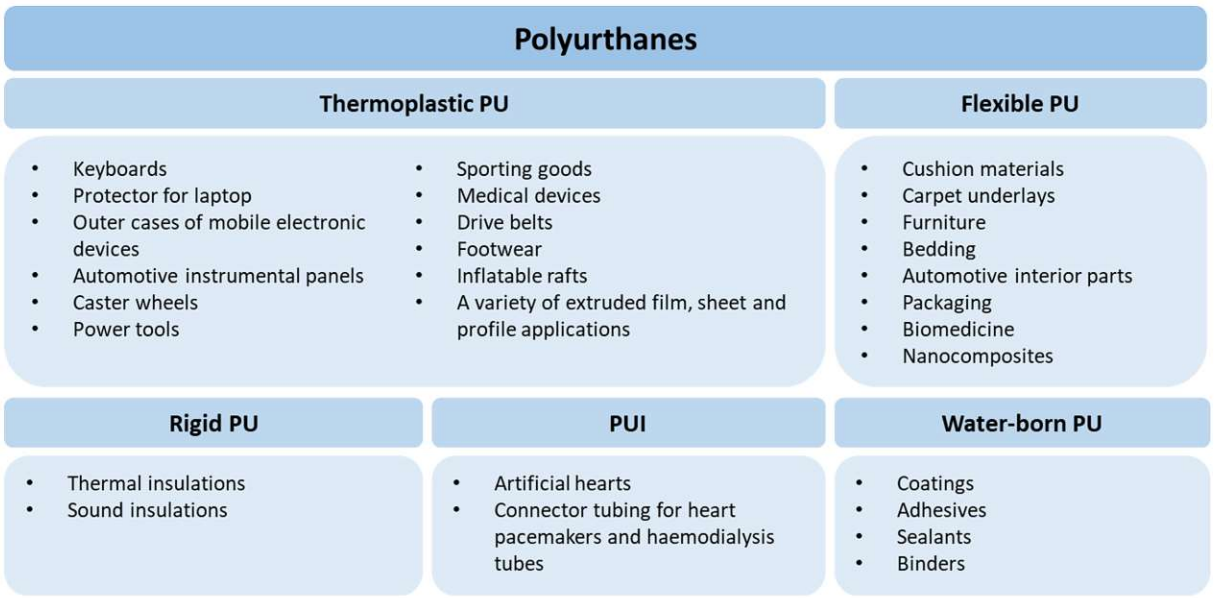

Figure 20: Important types of PUs and common examples of their applications[46]

Modern industry especially values isocyanate-based coatings because they offer flexibility and reduced hardness compared to other coating systems like epoxies.[77] Derived from the mechanical and thermal improved properties of PIR-PU, polyisocyanurates might be a promising new material class for the coating industry due to their improved thermal and solvent stability, which can be achieved through poly-trimerization of isocyanates or polyisocyanates.[61]

Regarding the synthesis of isocyanurates, Guo et al. listed 129 catalysts for the trimerization of isocyanates including 59 catalysts operating via a Lewis basic mechanism and 70 metal containing catalysts. According to the aim of this thesis, to achieve a photo base catalysed cyclotrimerization of isocyanates, the catalysts which do not operate via a Lewis basic mechanism as well as the catalysts which do not catalyses the trimerization of isocyanates in bulk will not be discussed further. Guo et al. reported 22 suitable catalysts via a Lewis basic mechanism in bulk for the cyclotrimerization of isocyanates including carboxylates, tertiary amines, fluoride and phosphorous compounds, carbens and alkenes (Figure 21).[78]

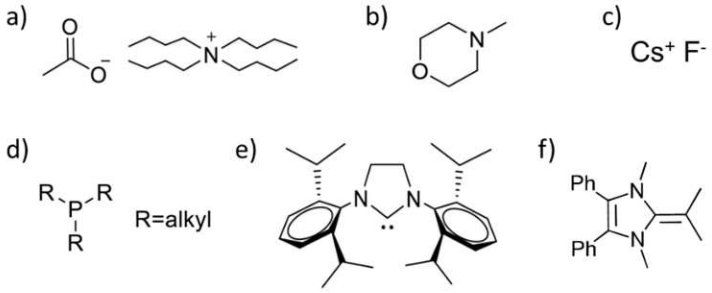

Figure 21: Structures of a) carben: tetrabutylammonium acetate, b) tertiary amine: n-methylmorpholine, c) fluoride: caesium fluoride, d) phosphoroes compound: trialkylphosphine, e) carben: 1,3-bis-(2,6-diisopropylphenyl)-4,5-dihydroimidazol-2-ylidene, f) alkene: 1,3-dimethyl-4,5-diphenyl-2-(propan-2- ylidene)-2,3-dihydro-1H-imidazole

Catalysts that induce the cyclotrimerization through a Lewis basic mechanism are typically anions, zwitterions or other functional groups possessing lone electron pairs. The cyclotrimerization is commonly initiated by a simple nucleophilic addition of an anion or the lone electron pair from the catalyst to the electrophilic isocyanate carbon, resulting in the formation of an anionic intermediate. Subsequently, in a step-growth mechanism the intermediate reacts further with a second and a third isocyanate leading to the formation of an isocyanurate through ring closure and the removal of the catalyst. Scheme 7 represents the proposed anionic mechanism of the cyclotrimerization of isocyanates.[78]

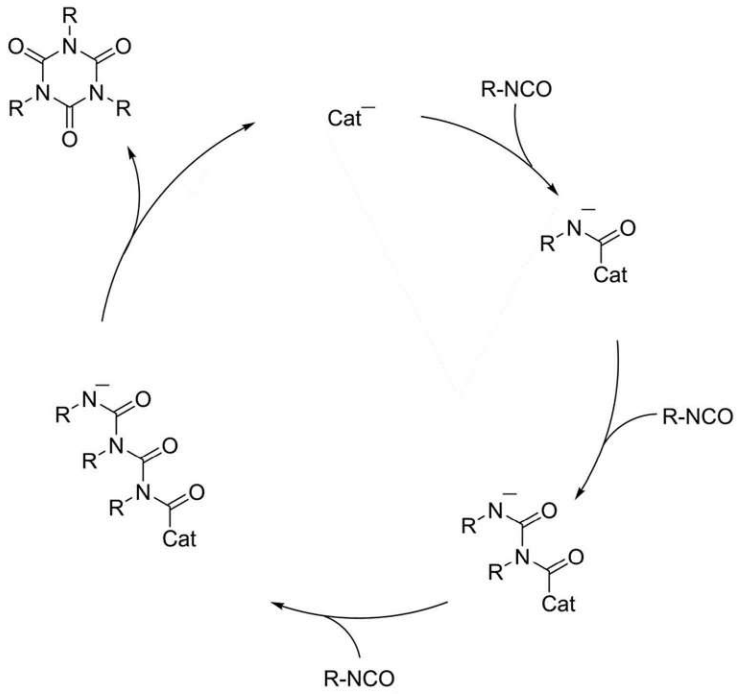

Scheme 7: Proposed mechanism for the anionic cyclotrimerization of ioscyanates[78]

Siebert et at. studied the catalytic cyclotrimerization with tetrabutylammonium acetate, shown in Figure 22 left. They reported a fast cyclotrimerization at ambient temperatures of aryl and alkyl isocyanates in bulk.[79] A second carboxylate was reported by Wu et al. They investigated various acid or base conjugates, based on organocatalyzed bases and Brønsted acids and found $HTBD^+OAc^-$ as a suitable catalyst for aryl isocyanates at ambient temperatures with only 0.5 mol% catalyst used. The cyclotrimerization with $HTBD^+OAc^-$ could be observed within seconds to minutes (Figure 22 right).[80]

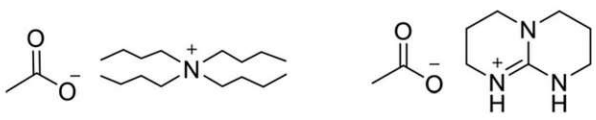

Figure 22: Structures of tetrabutylammonium acetate (left) and $HTBD^+OAc^-$ (right)

$HTBD^+OAc^-$ worked efficient under nitrogen or under air atmosphere. In the context of their study, it was proposed that hydrogen bonding interactions between HTBD and the oxygen atom of the isocyanate resulting in increased electronegativity of the oxygen, leading to the nucleophilic attack of the acetate anion on the carbon atom of the isocyanate. Subsequently, the anionic intermediates reacts further with a second and a third isocyanate leading to the

formation of an isocyanurate in a step-growth mechanism. Scheme 8 represents the proposed anionic mechanism of the cyclotrimerization of isocyanates by $HTBD^{+}OAc^{-}$.[80]

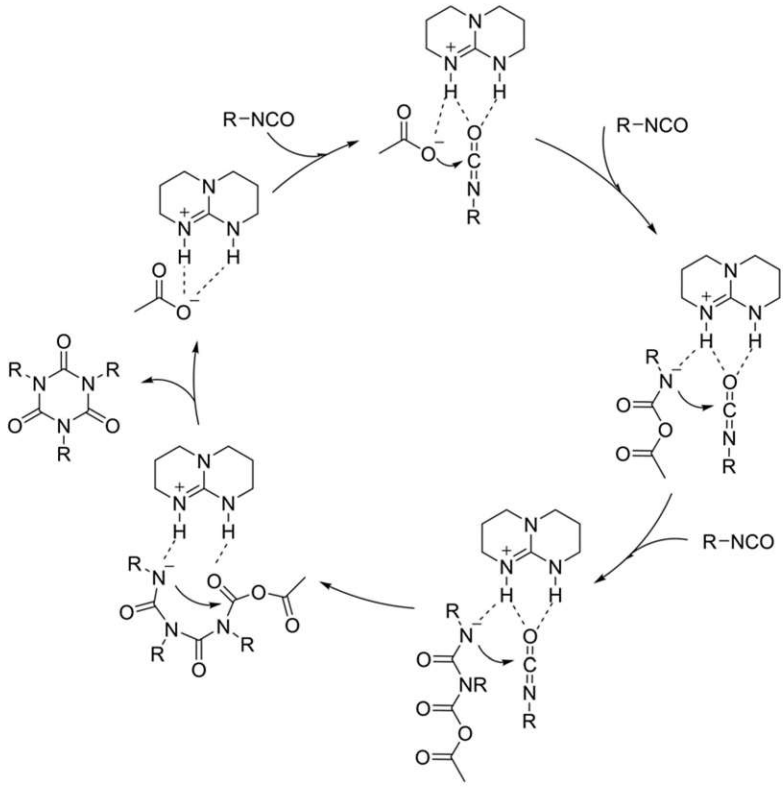

Scheme 8: Proposed mechanism for the anionic cyclotrimerization of isocyanates by $HTBD^{+}OAc^{-}$ [80]

Zeng et al.[81] and Dekamin et al.[82] studied the catalytically ability of the trimerization of isocyanates of two other carboxylates. Zeng et al. reported the trimerization of the alkyl isocyanate pentamethylene diisocyanate with 0,04 w% of 2 hydroxypropyl trimethylisooctanoate ammonium salt at 75 °C within 2 h (Figure 23 top left). Noted that neither yellowing or high viscosity could be observed. Dekamin et al. reported tetraethylammonium 2-(carbamoyl) benzoate, which was capable of catalysing with only 0.25 w% catalyst the cyclotrimerization of aryl, allyl and alkyl isocyanates within seconds at ambient temperatures (Figure 23 bottom left). This can be attributed to the catalyst structure that provides in addition to the nucleophile also a possibility of a hydrogen bonding interaction with the oxygen of the isocyanate or the negative nitrogen of the intermediate. Figure 23 left represents the proposed anionic mechanism of the cyclotrimerization of isocyanates by tetraethylammonium 2-(carbamoyl) benzoate.

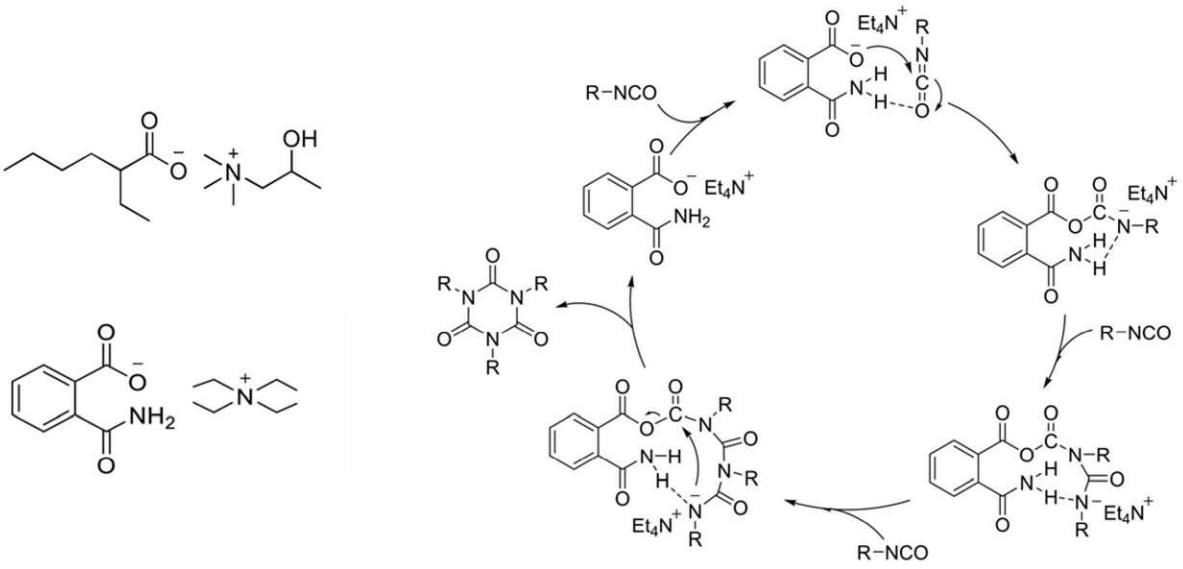

Figure 23: Structures of 2- hydroxypropyl-trimethylisooctanoate ammonium salt (top left), carboxylate tetraethylammonium 2-(carbamoyl) benzoate (bottom left) and the proposed mechanism for the cyclotrimerization of isocanates by the carboxylate tetraethylammonium 2-(carbamoyl) benzoate (right)

In contrast to the carboxylates, also two tertiary amines were reported of being suitable as a catalyst for a bulk cyclotrimerization of isocyanates. N-methylmorpholine[83] and methyl amino sulfenate[84] were able to catalyse the cyclotrimerization in bulk but high pressure was mandatory and in case of N-methylmorpholine also a proton donor such as alcohols, phenols or carbamates were necessary and temperatures of 120 °C for 16 hours (Figure 24).

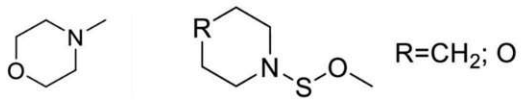

Figure 24: Structures of N-methylmorpholine (left) and methyl amino sulfonate (right)

Nitrate, sulfinate, sulfite, or sulfate have also been reported as catalysts for the cyclotrimerization owing to their negative charged oxygen. A catalytic systems was reported which use tetrabutyl ammonium as a cation with a phtalimide-N-oxid which enables the cyclotrimerization of aryl, alkyl and allyl isocyanates in bulk within seconds at ambient temperatures (Figure 25).[82] Tetrabutyl ammonium iodide was further reported as a co-catalyst of sodium saccharin (catalysing the cyclotrimerization at 110 °C),[85] sodium p-toluenesulfinatea (catalysing the cyclotrimerization at 140°C),[86] as well as potassium sulfate[87] and sulphite[88] promoting the cyclotrimerization of aryl and alkyl isocyanates (Figure 25). Potassium sulfate and sulphite implement the cyclotrimerization at 70 °C within 1 hour. Additionally sodium or potassium nitrite,[89] which catalyzes the cyclotrimerization at 140 °C,

or piperidinedithiocarbamate,[89] which catalyzes the cyclotrimerization at 110 °C, were also documented as catalyst for the cyclotrimerization of aryl and alkyl isocyanates (Figure 25).

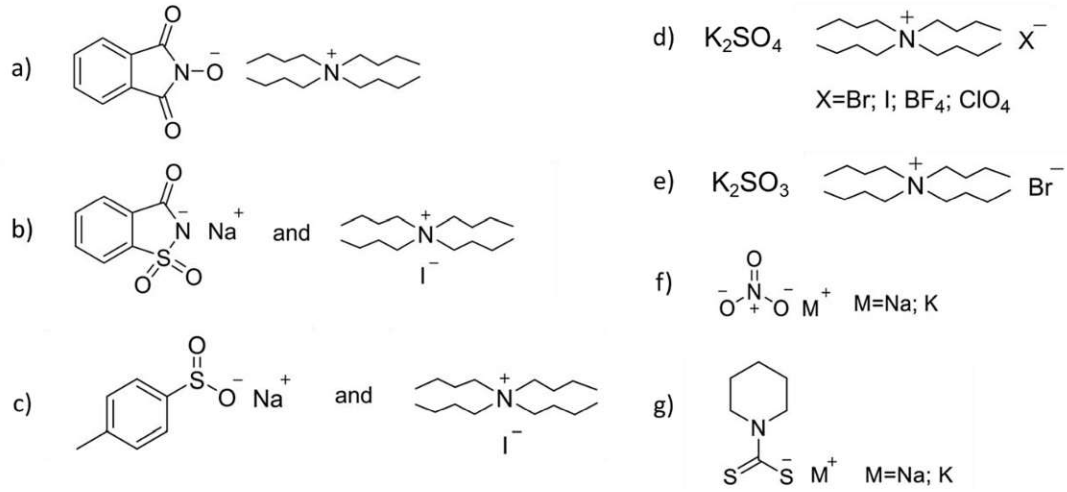

Figure 25: Structures of tetrabutyl ammonium phtalimide-N-oxyl (a), sodium saccharin and tetrabutyl ammonium iodide (b), sodium p-toluenesulfinatea and tetrabutyl ammonium iodide (c), potassium sulfate (d) and sulphite (e) with a tetrabutyl ammonium ion, sodium or potassium nitrit (f) and sodium or potassium piperidinedithiocarbamate (g)

Another anion, the fluorid anion, was reported for the cyclotrimerization from Nambu et al. They studied caesium fluoride and tetrabutylammonium fluoride, depicted in Figure 26 for an anionic pathway of the cyclotrimerization of aryl isocyanates. Bothe fluoride compounds catalyzes the cyclotrimerization already at ambient temperatures, and especially tetrabutylammonium fluoride catalysed cyclotrimerization occurred within 5 minutes.[90]

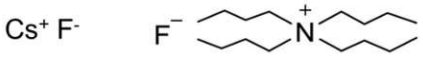

Figure 26: Structures of caesium fluoride (left) and tetrabutylammonium fluoride (right)

Furthermore phosphine are reported various times to be able to catalyse the cyclotrimerization of isocyanates. Besides the formation of Lewis basic salts, phosphines are strong nucleophiles. Herein catalysing the cyclotrimerization in an anionic pathway over the formation of a zwitterion with the isocyanate. Tang et al. and Raders et al. documented proazaphosphatrane with different substituents as catalysts for the cyclotrimerization. With 0.1 w% of the different substitated proazaphosphatrane catalyst they reported a conversion of more than 91% of aryl, alkyl and allyl isocyanates at ambient temperatures.[91-93] Additionally trialkylphosphines with different alkyl substituents were reported as catalysts at ambient temperatures.[94] The rate of reaction is highly dependent on the nature of the substituents within the phosphorous catalyst. Although the catalytic efficience of trialkylphosphines were

not as high as with proazaphosphatrane. Figure 27 represents the general structures of proazaphosphatrane and trialkylphosphines.

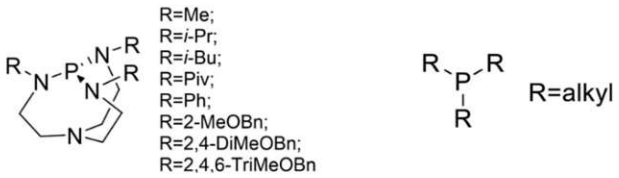

Figure 27: Structures of proazaphosphatrane (left) and trialkylphosphine (right)

Also carbenes are good nucleophiles, according to the lone electron pair, which make them suitable for the cyclotrimerization of isocyanates via an anionic mechanism. In literature 1,3-bis-(2,6-diisopropylphenyl)-4,5-dihydroimidazol-2-ylidene[95] and CO_2-protected N-heterocyclic carbine[96] were documented as catalysts for the cyclotrimerization of isocyanates (Figure 28). 1,3-Bis-(2,6-diisopropylphenyl)-4,5-dihydroimidazol-2-ylidene promotes the cyclotrimerization already at ambient temperatures within a few minutes, whereas the CO_2-protected N-heterocyclic carbine requires temperatures of 65 °C over a period of 60-90 minutes.[95,96]

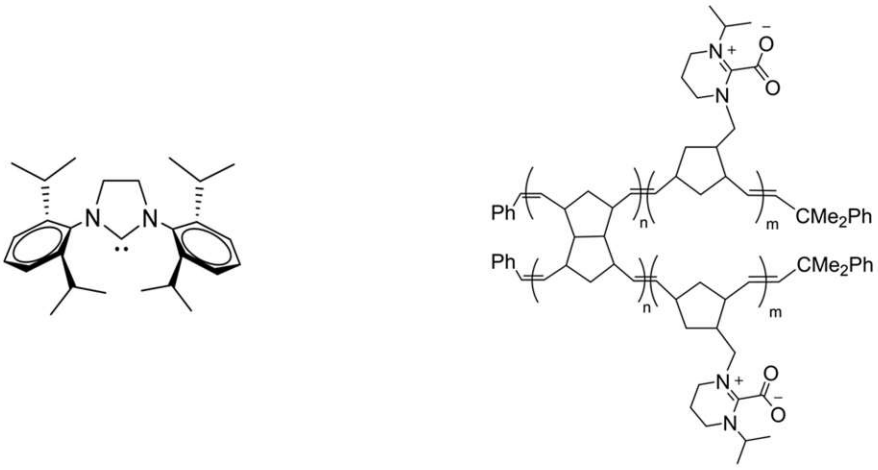

Figure 28: Structures of 1,3-bis-(2,6-diisopropylphenyl)-4,5-dihydroimidazol-2-ylidene (left) and CO_2-protected N-heterocyclic carbene (right)

Besides carbenes, electron-rich alkenes have been reported as catalysts for the cyclotrimerization of isocyanates in bulk, see Figure 29. The suggested mechanism starts with the reaction of an isocyanate with the alkene to form a zwitterion, and further the cyclotrimerization proceeds along an anionic pathway. It was documented that 1,3-dimethyl-4,5-diphenyl-2-(propan-2-ylidene)-2,3-dihydro-1H-imidazole[97] catalysed the cyclotrimerization of aryl, alkyl and allyl isocyanates, tetrakis(dimethylamino)ethylene[98]

catalysed the cyclotrimerization of aryl and alkyl isocyanates and 1,2-dimethylimidazole[99] catalysed the cyclotrimerization of alkyl isocyanates (Figure 29). These three electron-rich alkenes catalysed the cyclotrimerization at ambient temperatures within a few seconds to minutes.

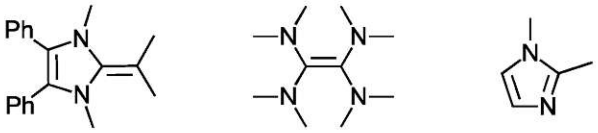

Figure 29: Structures of 1,3-dimethyl-4,5-diphenyl-2-(propan-2- ylidene)-2,3-dihydro-1H-imidazole (left), tetrakis(dimethylamino)ethylene (middle) and 1,2-dimethylimidazole (right)

While the cyclotrimerization of isocyanates is literature known and widely used in polyurethane chemistry, a way to obtain polyisocyanurate without the polyurethane matrix is for our best knowledge not reported yet. In this approach, the crosslinking process involves polytrimerization of isocyanates which leads to the formation of isocyanurate groups rather than urethanes (Scheme 9). This method results in highly compact networks, that offer enhanced resistance to solvents and heat, surpassing the properties of traditional urethane networks.[77]

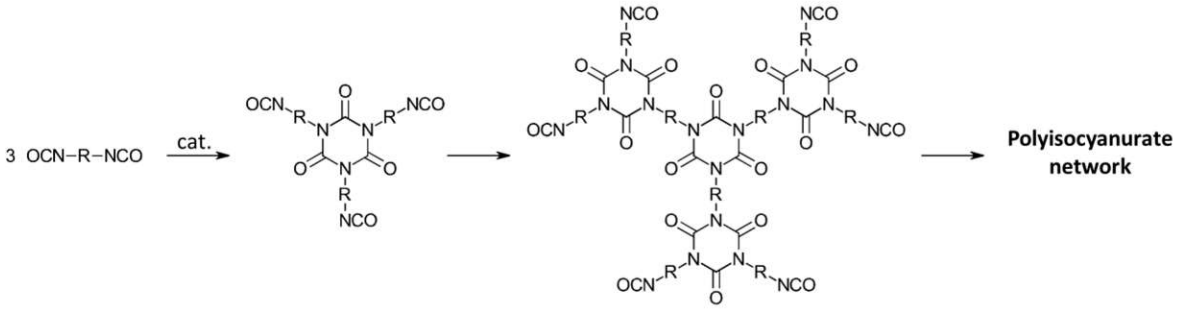

Scheme 9. Synthesis of a polyisocyanurate network

The results in this research should move PU chemistry to the next level by implementing a photochemical and catalytic cyclotrimerization of isocyanates to obtain potentially new high performance photopolymers.

Results and Discussion

Based on literature search, the free bases 1,5-diazabicyclo(4.3.0)non-5-ene,[100] 1,1,3,3-tetramethylguanidin,[80] triethylamine,[101] tributylphosphine,[102] triphenylphosphine,[102] 1,2-dimethyl imidazole[99] and 2-butyl-1-ethylhexyl imidazole were investigated about their catalytic ability for the cyclodimerization and cyclotrimerization of isocyanates in bulk (Scheme 10).

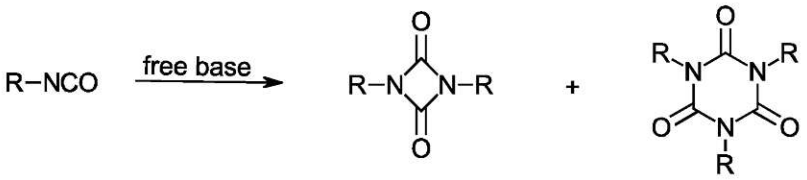

Scheme 10: Cyclodimerization and cyclotrimerization of isocyanates

According to the free bases, which were capable of the catalysis of the cyclodimerization and cyclotrimerization, the corresponding photobase generator should be synthesized. The synthesized photobase generator can further be investigated about their photoactivity and stability via ^{1}H-NMR as well as the photochemical cyclodimerization and cyclotrimerization of isocyanates (Scheme 11).

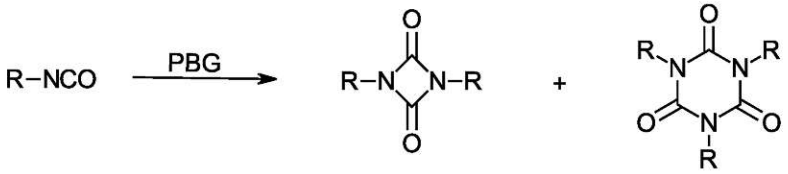

Scheme 11: The PBG catalysed cyclodimerization and cyclotrimerization of isocyanates

1. Model systems for catalytic cyclodimerization and cyclotrimerization of isocyanates with free bases

To exclude the effects of UV irradiation or insufficient base generation on the cyclodimerization and cyclotrimerization, first polymerization attempts were conducted with the free base to focus on the reactivity of the base. Furthermore monofunctional isocyanates were used to enable a simple tracking via NMR of the cyclodimerization and cyclotrimerization, as well as to minimize the steric hindrance on the formed cyclodimers and cyclotrimers. The used isocyanates were purified via distillation, to remove impurities and hydrolysed isocyanate because of moisture. The removal of the hydrolysis products of the

isocyanates are mandatory because the hydrolysed isocyanate, aniline and hexylamine, could undergo unwanted side reactions.

The isocyanate cyclodimerization and cyclotrimerization was investigated with the monofunctional isocyanates phenyl isocyanate and hexyl isocyanate and seven different free bases (Figure 30). The seven free bases were derived from literature-known catalysts for the cyclotrimerization of isocyanates.[80,100-103]

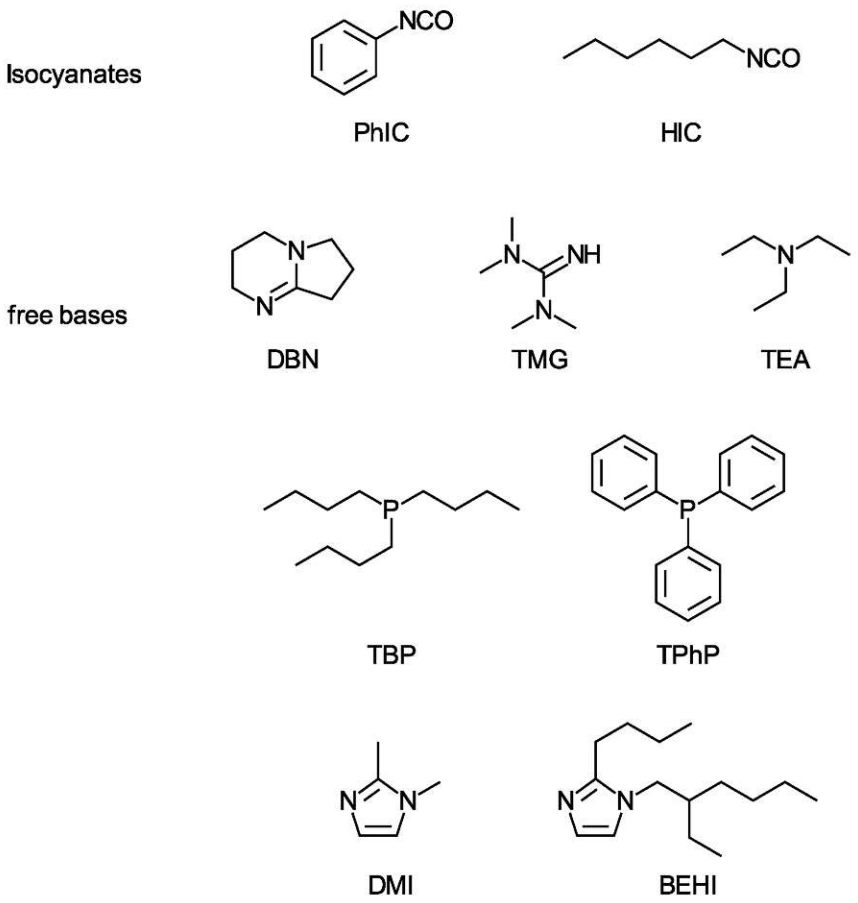

Figure 30: Structures used for investigation of the cyclodimerization and cyclotrimerization: phenyl isocyanate (PhIC) and hexyl isocyanate (HIC), and the free bases 1,5-diazabicyclo(4.3.0)non-5-ene (DBN), 1,1,3,3-tetramethylguanidin (TMG), triethylamine (TEA), tributylphosphine (TBP), triphenylphosphine (TPhP), 1,2-dimethyl imidazole (DMI) and 2-butyl-1-ethylhexyl imidazole (BEHI)

1.1. General procedure for the investigation

The conditions of the cyclodimerization and cyclotrimerization of phenyl isocyanate and hexyl isocyanate were studied with different base concentrations (5 mol%, 10 mol%, equivalent) at ambient temperatures in bulk. Therefore, phenyl isocyanate and hexyl isocyanate were purified via distillation and stored for maximal five days under argon atmosphere and molecular sieve at 5 °C. The distilled phenyl isocyanate or hexyl isocyanate were transferred via an Eppendorf Pipette into brown glass vail under constant argon flow. The brown glass vail

was prior purged with argon to ensure inert gas atmosphere. Additionally the corresponding free base was added to the isocyanate under constant argon flow via an Eppendorf Pipette. After addition of the isocyanate and the free base, the brown glass vails were closed off and stored at ambient temperatures for 24 hours. The resulting reaction mixtures were characterized via attenuated total reflection-fourier-transform-infrared spectroscopy at ambient temperatures (ATR-FTIR), nuclear magnetic resonance (^{1}H-NMR) and liquid chromatography-mass spectroscopy (LC-MS) as soon as the reaction mixtures cooled down to ambient temperatures again and solidification was observed. If no heat release and solidification within 30 minutes could be observed the reaction mixtures were characterized after 24 hours. The used equivalents and NMR solvents are noted in the respective chapters.

1.2. 1,5-Diazabicyclo[4.3.0]non-5-ene

First cyclodimerization and cyclotrimerization attempts with 1,5-diazabicyclo[4.3.0]non-5-ene (DBN) according to literature (Scheme 12).[100] They reported the cyclotrimerization of aryl isocyanates with 1,8-diazabicyclo[5.4.0]undec-7-ene in acetonitrile at 50 °C (Figure 31).

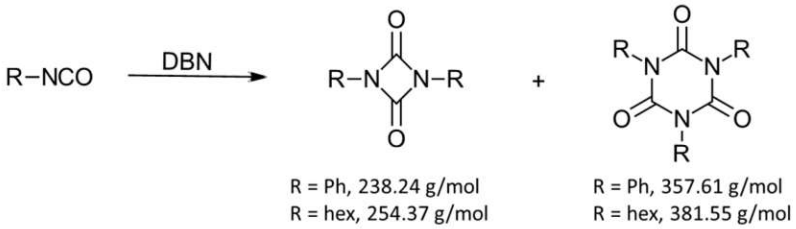

Scheme 12: Cyclodimerization and cyclotrimerization of phenyl isocyanate and hexylisocyanate with 1,5-diazabicyclo[4.3.0]non-5-ene (DBN)

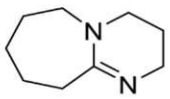

Figure 31: Structure of 1,8-diazabicyclo[5.4.0]undec-7-ene (DBU)

Therefore, phenyl isocyanate and 5 mol% DBN were reacted at ambient temperature. The reaction mixture immediately solidified under heat release upon the addition of phenyl isocyanate. The ATR-FTIR of the reaction mixture showed complete conversion of phenyl isocyanate, according to the disappearance of the isocyanate vibration (Figure S 1). Additionally, the ATR-FTIR showed characteristic bands of the dimer at 1774 cm^{-1}, 1750 cm^{-1}, 1601 cm^{-1}, 1423 cm^{-1} and the trimer at 1498 cm^{-1} and 1415 cm^{-1} of phenyl isocyanate. The

characteristic vibrations of an isocyanate, the phenyl isocyanate dimer and the phenyl isocyanate trimer are listed in Table 3.

Table 3: Characteristic vibrations of an isocyanate, phenyl uretdion and phenyl isocyanurate[104]

Isocyanate vibration	Phenyl uretdion (dimer)	Phenyl isocyanurate (trimer)
2260 cm^{-1}	1779 cm^{-1}	1710 cm^{-1}
	1755 cm^{-1}	1498 cm^{-1}
	1604 cm^{-1}	1415 cm^{-1}
	1505 cm^{-1}	
	1423 cm^{-1}	

The ^{1}H-NMR of the reaction mixture exhibited no complete conversion of phenyl isocyanate and exhibited new signals at 7.39 ppm and 7.55 ppm (Figure 32). The new signals could potentially be assigned to the trimer and dimer as suggested in Figure 32.

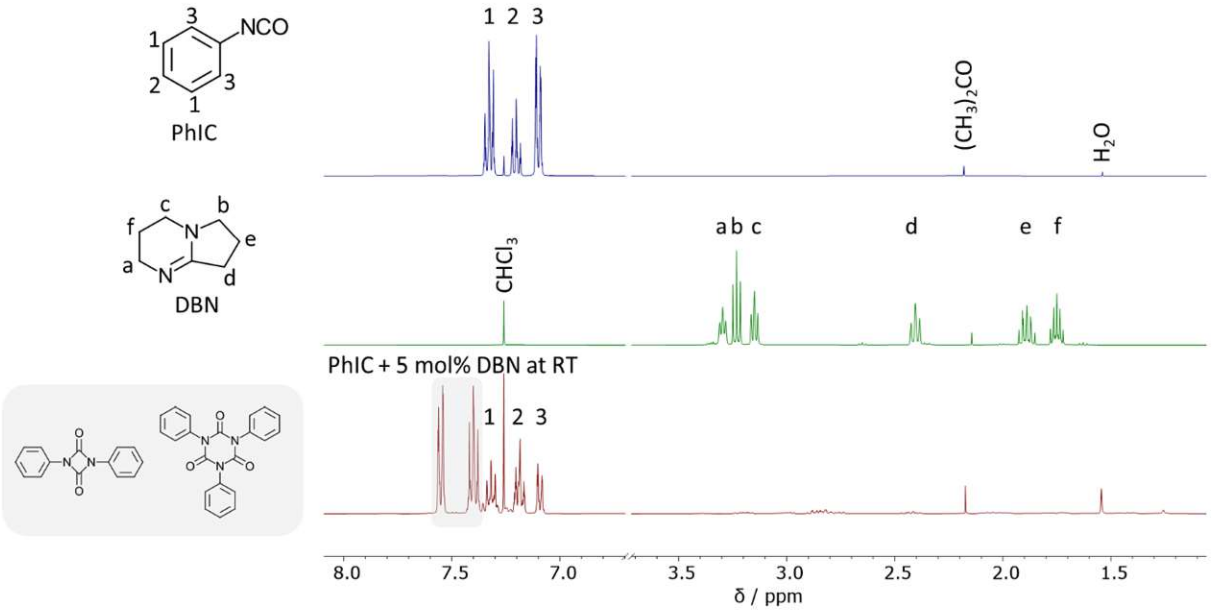

Figure 32: ^{1}H-NMR spectra (400 MHz, $CDCl_3$) of phenyl isocyanate in (blue), DBN (green) and reaction mixture with phenyl isocyanate and 5 mol% DBN (red) at ambient temperature. First tentative interpretation of the new signals is indicated through grey assignments

The LC-MS measurements of the reaction mixture indicated the presence of diphenylurea due to a m/z value of 213 in positive mode, which corresponds to the molecular weight of 212 g mol^{-1} of diphenylurea. This is attributed to the incomplete conversion of phenyl isocyanate in the aqueous solution for LC-MS measurements, which leads to partial hydrolysis of phenyl isocyanate and further to the formation of diphenylurea from the isocyanate and

hydrolyzed amine. The formation of such urea compounds of the isocyanates and their corresponding hydrolysis products could be observed in all experiments with phenyl isocyanate as well as with hexyl isocyanate if the conversion was incomplete.

The formation of the dimer or trimer could not be proven with LC-MS. According to literature a cyclisation reaction between an isocyanate and DBN was reported (Scheme 13).[105] The corresponding molecular weight of the adduct between two equivalents of isocyanate and one equivalent of DBN (362 g mol^{-1}) match with the indicated molecular weight of the LC-MS measurements of 363 g mol^{-1} in positive mode.

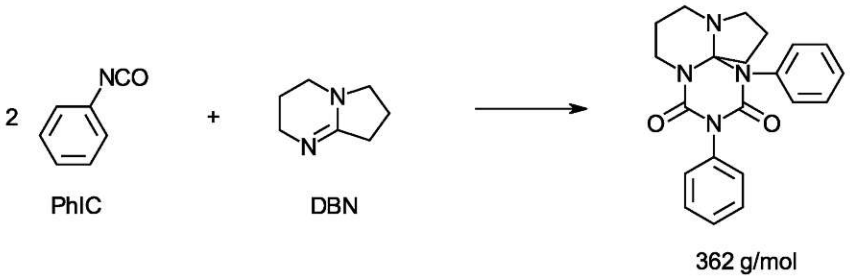

Scheme 13: Reaction of two equivalents of phenyl isocyanate (PhIC) and one equivalent 1,5-diazabicyclo[4.3.0]non-5-ene (DBN) to form a cyclic adduct

This leads to the assumption that the cyclic dimer and the cyclic trimer and also the cyclisation adduct of DBN and two equivalents of phenyl isocyanate were formed. Accompanying a cyclodimerization and cyclotrimerization of phenyl isocyanate and DBN was possible but with an unavoidable side reaction of phenyl isocyanate and DBN and thus a deactivation of the catalyst DBN.

Additionally, the aliphatic hexyl isocyanate was investigated analogously with 5 mol% DBN at ambient temperature. This reaction mixture remained liquid after adding hexyl isocyanate. The ATR-FTIR of the reaction mixture showed that hexyl isocyanate was still present after the reaction due to the presence of the isocyanate vibration at 2260 cm^{-1} (Figure S 2). Consistent with this finding, the ^{1}H-NMR of the reaction mixture indicated the presence of hexyl isocyanate (Figure 33). Additionally, a new triplet at 3.65 ppm as well as DBN signals changed and one even disappeared (**d**).

The LC-MS measurement gave an m/z value of 379 in positive mode, which indicated the molecular weight of the adduct of one equivalent of DBN with two equivalents of hexyl isocyanate (Scheme 14).

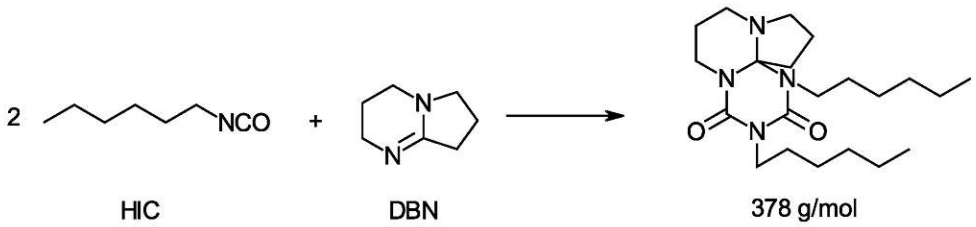

Scheme 14: Reaction of two equivalents of hexyl isocyanate and one equivalent 1,5-diazabicyclo[4.3.0]non-5-ene (DBN) to form a cyclic adduct

To confirm the hypothesis and first experimental indications for the stoichiometric reaction of DBN with hexyl isocyanate, a reaction mixture containing two equivalents of hexyl isocyanate and one equivalent of DBN was reacted at ambient temperature. Immediately after adding hexyl isocyanate, an exothermic reaction and gelation of the reaction mixture could be observed. The ATR-FTIR of the crude product showed a complete conversion of hexyl isocyanate due to the disappearance of the isocyanate vibration at 2260 cm^{-1} (Figure S 3). The ^{1}H-NMR showed the characteristic peaks of the adduct according to literature and the LC-MS also indicates the presence of the adduct due to an m/z of 379 in positive mode, which matches the molecular weight of the anticipated adduct (Scheme 14).[105]

This further corroborates that the formation of an adduct of two equivalents of hexyl isocyanate and one equivalent of DBN in the reaction mixture with hexyl isocyanate and 5 mol% DBN occurs (Figure 33). Accompanying a catalytic cyclodimerization and cyclotrimerization of hexyl isocyanate and DBN was not possible.

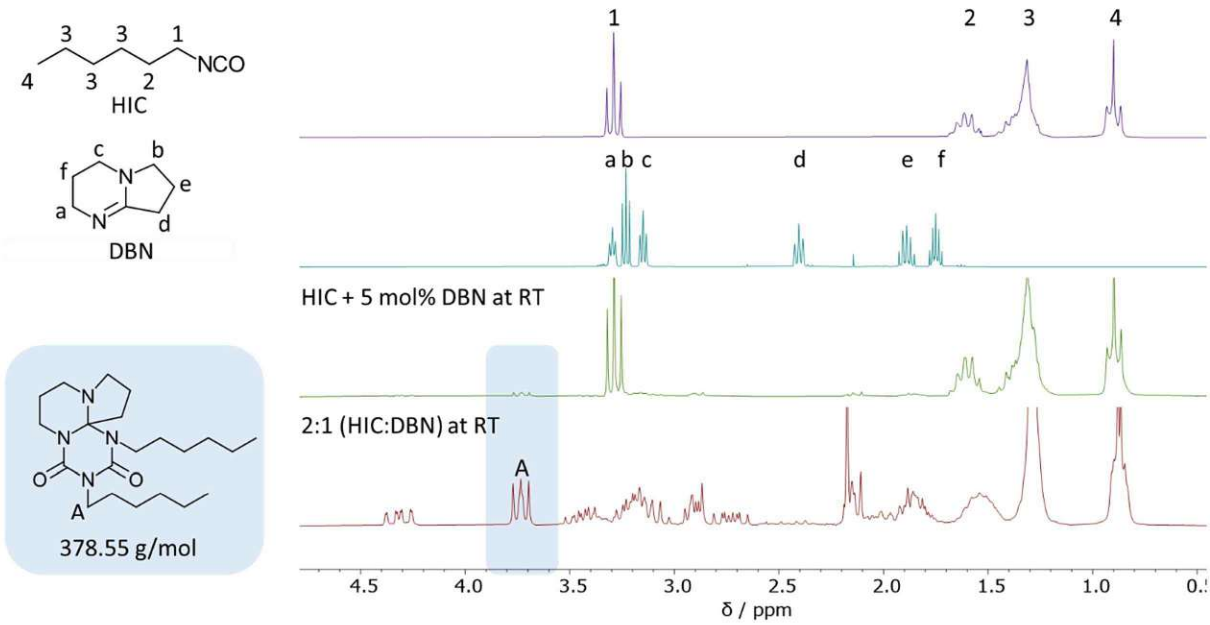

Figure 33: ^{1}H-NMR spectra (400 MHz, $CDCl_3$) spectra of hexyl isocyanate (purple), DBN (blue), reaction mixture with hexyl isocyanate and 5 mol% DBN at ambient temperatures (green), reaction mixture with hexyl isocyanate and DBN (2:1) at ambient temperatures (red) and the formed adduct between two equivalents of hexyl isocyanate and one equivalent of DBN

The experiments of phenyl isocyanate and hexyl isocyanate with DBN showed no complete catalytic cyclodimerization and cyclotrimerization. A side reaction of the formation of an adduct of two equivalents isocyanate and one equivalent DBN could be observed (Scheme 14). This adduct formation enables an interesting way to obtain a photocurable stoichiometric copolymer of isocyanates and DBN.

1.3. Tetramethyl guanidine

The second investigated free base for the cyclodimerization and cyclotrimerization is tetramethyl guanidine (TMG), derived from literature, which used 1,5,7-triazabicyclo(4.4.0)dec-5-en carboxylate for the cyclotrimerization of aryl isocyanates (Scheme 15 and Figure 34). They reported the cyclotrimerization at ambient temperatures with HTBD$^+$OAc$^-$ within seconds to minutes.[80]

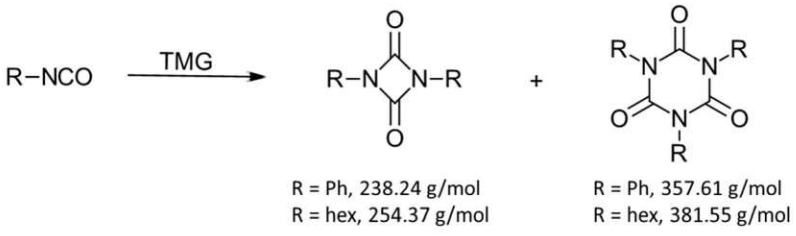

Scheme 15: Cyclodimerization and cyclotrimerization of phenyl isocyanate and hexylisocyanate with tetramethyl guanidine (TMG)

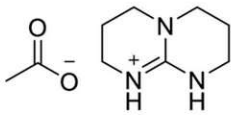

Figure 34: Structure of 1,5,7-triazabicyclo(4.4.0)dec-5-ene carboxylate (HTBD^{-}OAc^{+})

Therefore, phenyl isocyanate and 5 mol% tetramethyl guanidine (TMG) were reacted at ambient temperature. The reaction mixture solidified under heat release immediately when adding phenyl isocyanate. The ATR-FTIR of the reaction mixture showed complete conversion of phenyl isocyanate due to the disappearance of the isocyanate vibration at 2260 cm^{-1} (Figure S 4). Consistent with this finding, the ^{1}H-NMR of the reaction mixture exhibited complete conversion of phenyl isocyanate (Figure 35). Additionally, many new signals in the aromatic region could be observed. LC-MS measurements provided the m/z values 192, 354 and 332 in positive mode.

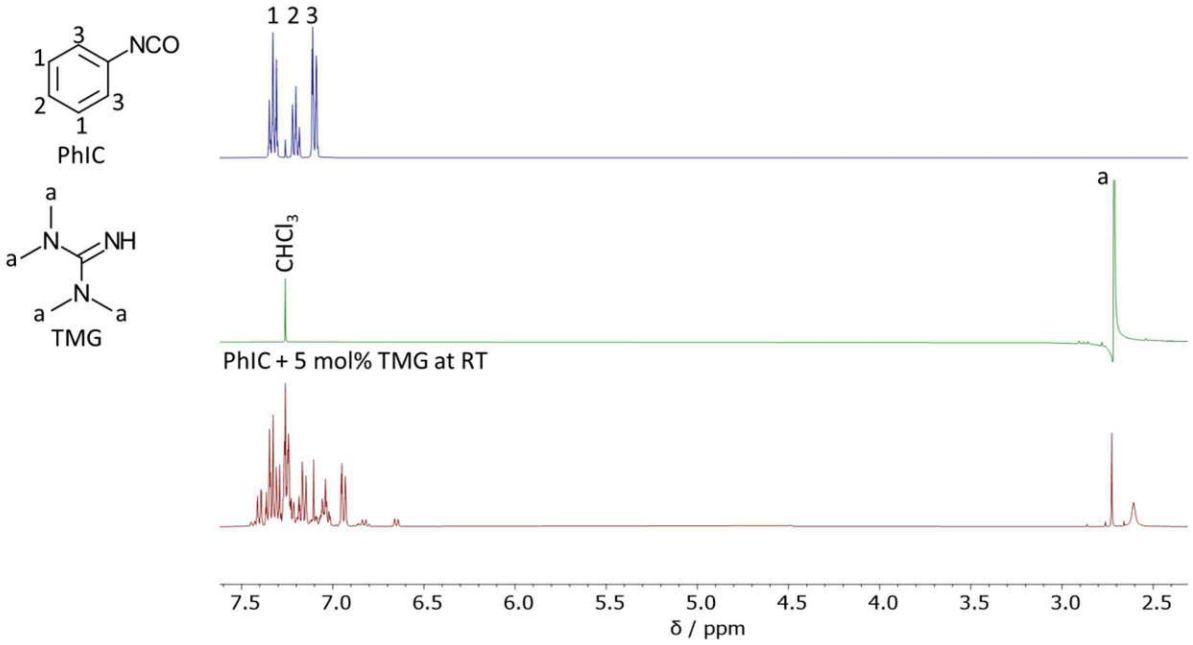

Figure 35: ^{1}H-NMR spectra (400 MHz, $CDCl_3$) of phenyl isocyanate (blue), TMG (green) and reaction mixture with phenyl isocyanate and 5 mol% TMG at ambient temperatures (red)

The reaction of the aliphatic hexyl isocyanate and 5 mol% TMG was also investigated at ambient temperature. The reaction mixture solidified under heat release within 15 minutes. The ATR-FTIR of the reaction mixture showed only incomplete conversion of hexyl isocyanate due to the presence of the isocyanate vibration at 2260 cm^{-1} (Figure S 5). The ^{1}H-NMR of the reaction mixture also exhibited the presence of hexyl isocyanate (Figure 36). Additionally, new

signals at 2.80 ppm and 3.80 ppm as well as a new chemical shift of the TMG signal from 2.71 ppm to 2.41 ppm could be observed.

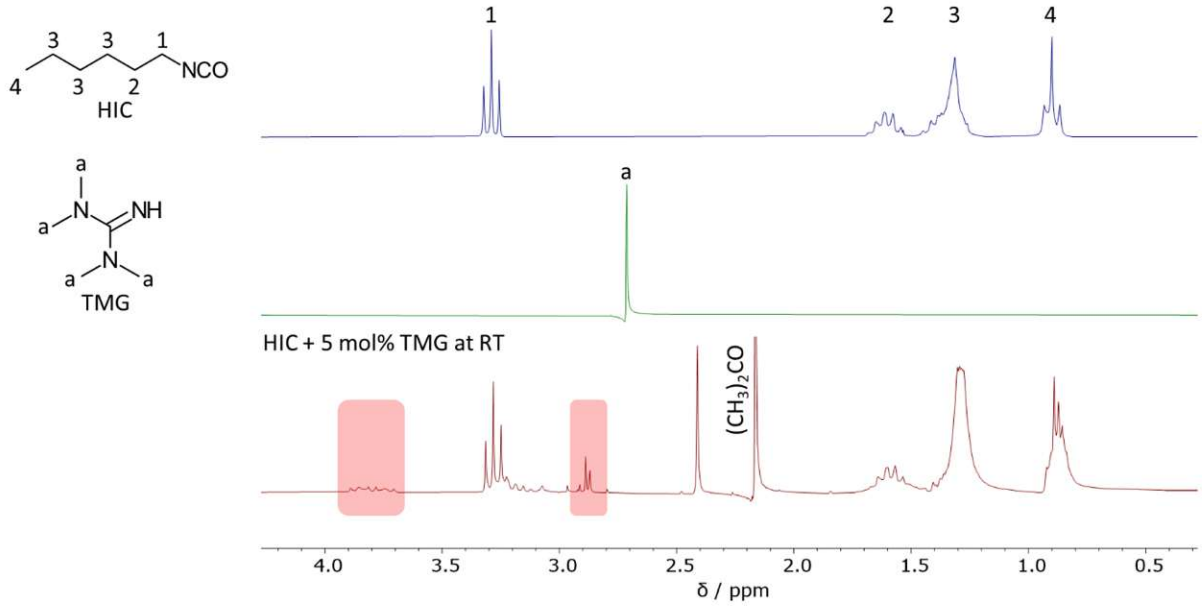

Figure 36: ^{1}H-NMR spectra (400 MHz, $CDCl_3$) of hexyl isocyanate (blue), TMG (green) and reaction mixture with hexyl isocyanate and 5 mol% TMG at ambient temperatures (red). The new signals at 2.80 ppm and 3.80 ppm are highlighted in red.

As discussed previously, the LC-MS measurements of the reaction mixture indicated the presence of 1,3-dihexylurea due to the incomplete conversion of hexyl isocyanate. The m/z value of 200, 243, 286 and 370 at positive mode could be observed additionally.

In literature, a cyclisation reaction between an isocyanate and TMG was reported, which could partly explain these findings (Scheme 16).[105] The suggested mechanism and the corresponding molecular weights of the intermediate and products, which match the m/z values obtained from LC-MS measurements of the reactants, are shown in Scheme 16. The molecular weights highlighted in green concur with the supposed molecular weights of the LC-MS measurements of the reaction mixture containing phenyl isocyanate or hexyl isocyanate and 5 mol% TMG.

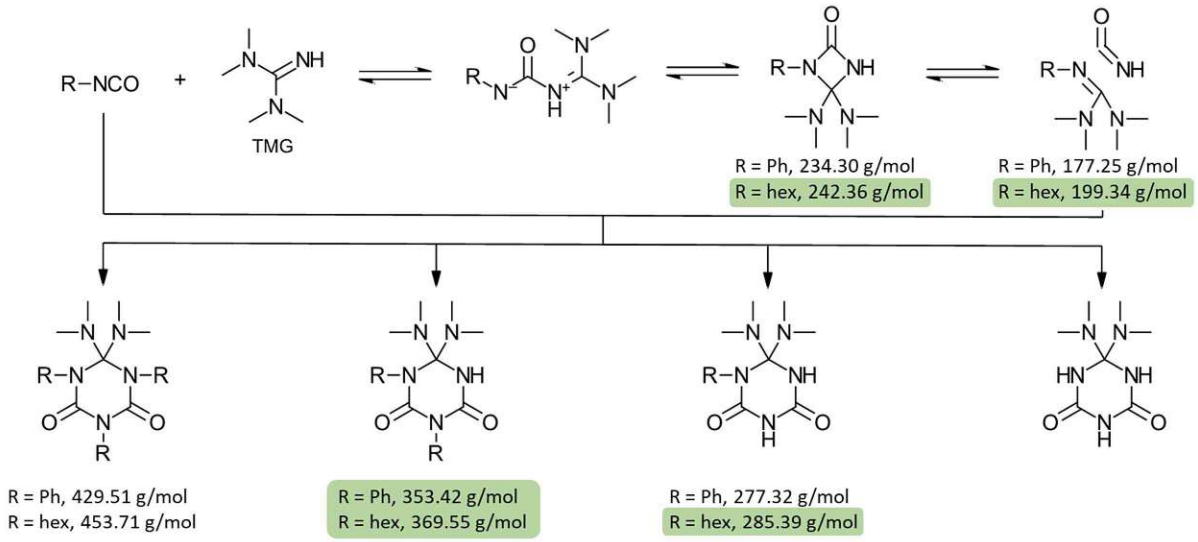

Scheme 16: Supposed mechanism[105] for the cyclisation of an isocyanate and 1,1,3,3-tetramethylguanidin (TMG) at ambient temperatures and the corresponding intermediates and cyclisation product of phenyl isocyanate and hexyl isocyanate

Concluding a catalytic cyclodimerization and cyclotrimerization of phenyl isocyanate or hexyl isocyanate and TMG was not possible. The observed addition reactions and the formation of six membered rings enables an interesting way to obtain a photocurable stoichiometric copolymer of isocyanates and TMG.

1.4. Triethylamine

According to literature, which reported the cyclotrimerization of isocyanates with triethylamine (TEA) under high pressure (500 MPa) at 40 °C, phenyl isocyanate and hexyl isocyanate were investigated with TEA for their ability of cyclodimerization and cyclotrimerization at ambient pressure and temperature (Scheme 17).[101]

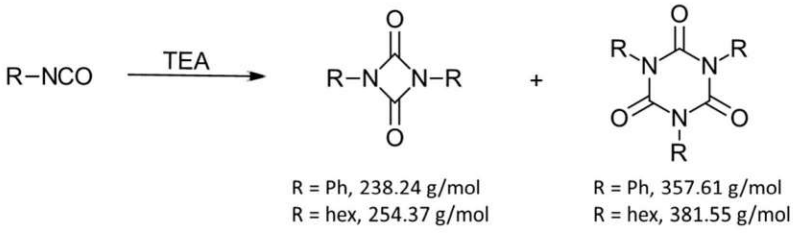

Scheme 17: Cyclodimerization and cyclotrimerization of phenyl isocyanate and hexylisocyanate with triethylamine (TEA)

Therefore, phenyl isocyanate or hexyl isocyanate were reacted with 5 mol% TEA at ambient temperature. The ATR-FTIR of the liquid reaction mixtures showed no complete conversion of hexyl isocyanate or phenyl isocyanate due the isocyanate vibration at 2260 cm^{-1} (Figure S 6 and Figure S 7). Additionally, the ^{1}H-NMR of these reaction mixtures show no change in multiplicity and chemical shifts, corresponding to the pure reactants.

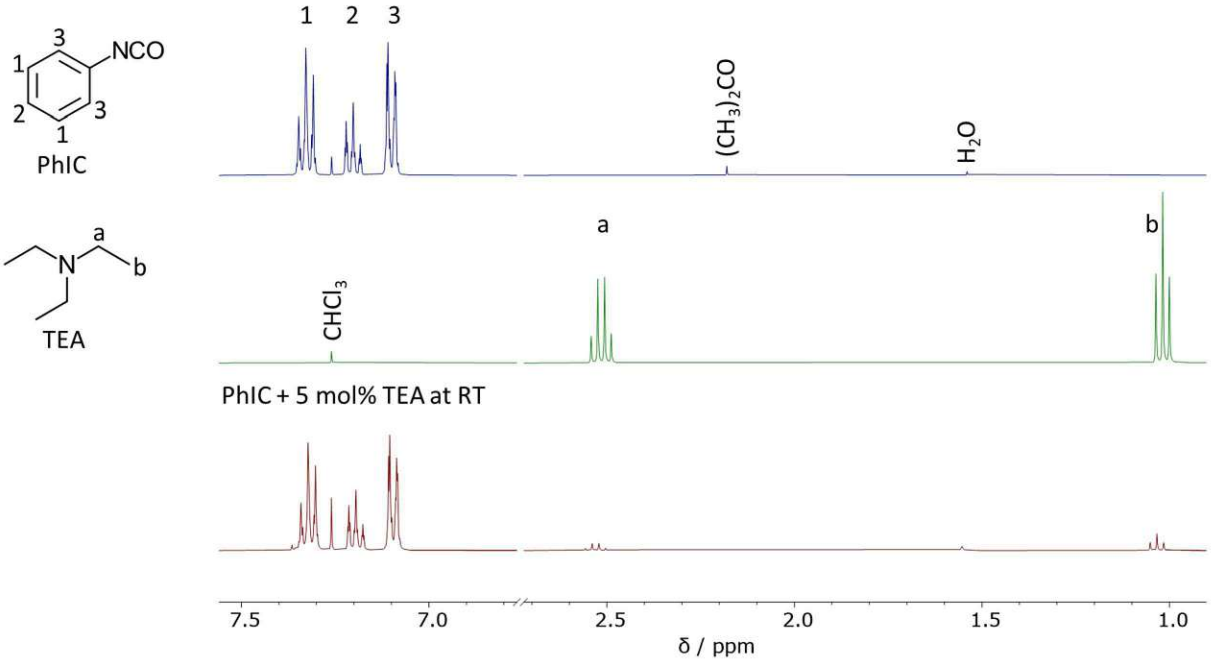

Figure 37: ^{1}H-NMR spectra (400 MHz, $CDCl_3$) of phenyl isocyanate (blue), TEA (green) and reaction mixture with phenyl isocyanate and 5 mol% TEA at ambient temperatures (red)

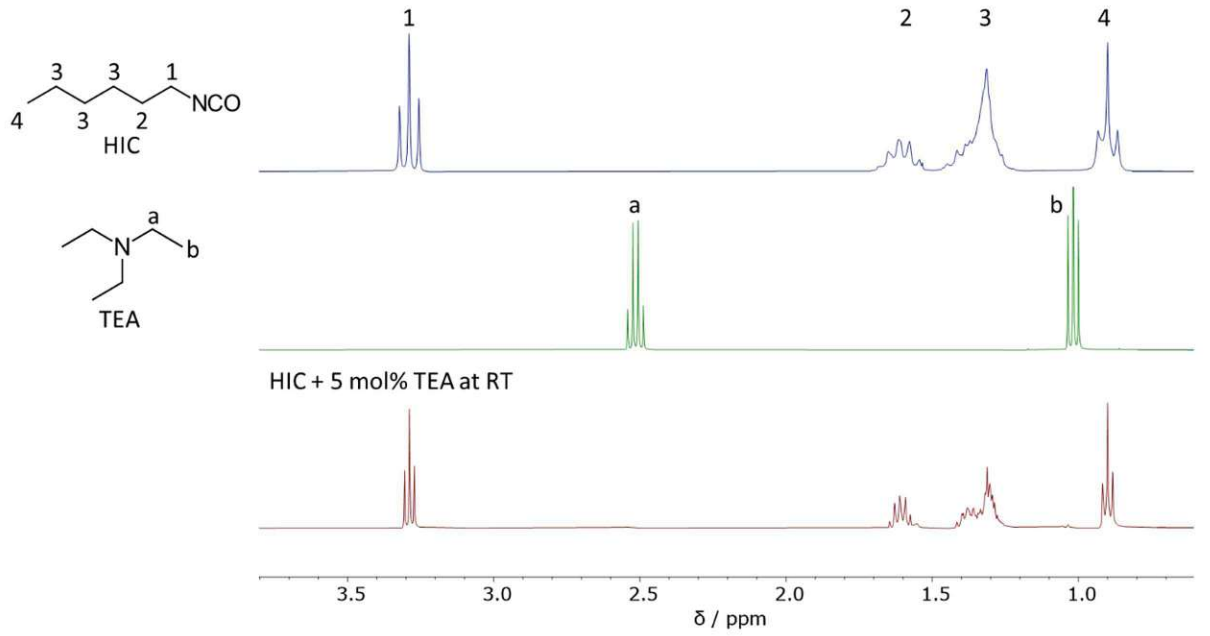

Figure 38: ^{1}H-NMR spectra (400 MHz, $CDCl_3$) of hexyl isocyanate (blue), TEA (green) and reaction mixture with hexyl isocyanate and 5 mol% TEA at ambient temperatures (red)

It can be concluded that TEA does not catalyze the cyclodimerization and/or cyclotrimerization of phenyl isocyanate or hexyl isocyanate nor any other side reactions at ambient pressure and temperature. Accompanying a PBG of TEA was not synthesized.

1.5. Tributylphosphine

Tributylphosphine (TBP) was investigated for its ability to catalyze cyclodimerization and cyclotrimerization of phenyl isocyanate and hexyl isocyanate as reported in literature (Scheme 18). They reported the cyclotrimerization at 60 °C with TBP within minutes.[102]

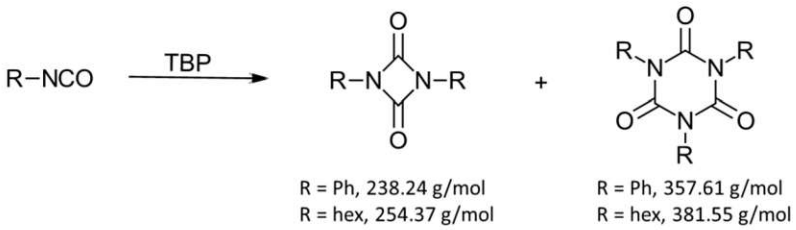

Scheme 18: Cyclodimerization and cyclotrimerization of phenyl isocyanate and hexylisocyanate with tributylphosphine (TBP)

Therefore, phenyl isocyanate and 5 mol% TBP were reacted at ambient temperatures and 60 °C in analogy to literature.[106] The ATR-FTIR of the reaction mixtures containing phenyl isocyanate and TBP displayed complete conversion of phenyl isocyanate due to the disappearance of the isocyanate vibration at 2260 cm^{-1} (Figure S 8). The ^{1}H-NMR of these reaction mixtures exhibited a change in multiplicity and chemical shifts, compared to phenyl isocyanate (Figure 39). In contrast to the LC-MS measurements of the reaction mixture at ambient temperatures, which only indicated the molecular weights of the reactants, the reaction mixture reacted at 60 °C indicated the existence of the cyclotrimer, the isocyanurate due to a m/z value of 358 in positive mode. This proved the existence of triphenyl isocyanurate with the molecular weight of 357.61 g mol^{-1} in the reaction mixture with phenyl isocyanate and 5 mol% TBP at 60 °C.

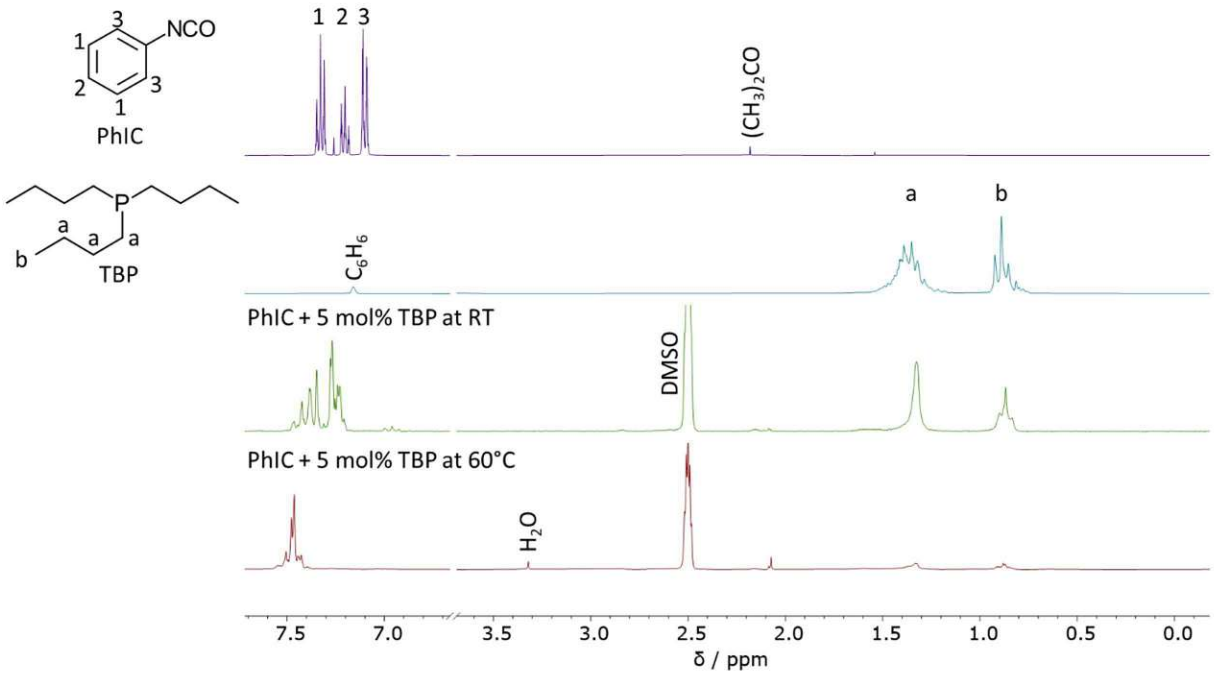

Figure 39: ^{1}H-NMR spectra (400 MHz) of phenyl isocyanate in $CDCl_3$ (purple), tributylphosphine in C_6D_6 (blue), reaction mixture with phenyl isocyanate and 5 mol% TBP in DMSO at ambient temperatures (green) and reaction mixture with phenyl isocyanate and 5 mol% TBP in DMSO at 60 °C (red)

Also, the aliphatic hexyl isocyanate and 5 mol% TBP were investigated at ambient temperatures and 60 °C in analogy to literature.[106] The ATR-FTIR of the reaction mixtures containing hexyl isocyanate and TBP indicated incomplete conversion of hexyl isocyanate due the isocyanate vibration at 2260 cm^{-1} (Figure S 9). The ^{1}H-NMR of these reaction mixtures proved the existence of the hexyl isocyanurate due to the signals at 3.36 ppm, 3.64 ppm and 3.84 ppm (Figure 40). According to literature, these signals are characteristic for the hexyl isocyanurate and the isomer depicted in Figure 40.[106] Although the LC-MS measurements could not prove this assumption, the formation of the isocyanurate and the isomer could be proven with H^1-NMR.

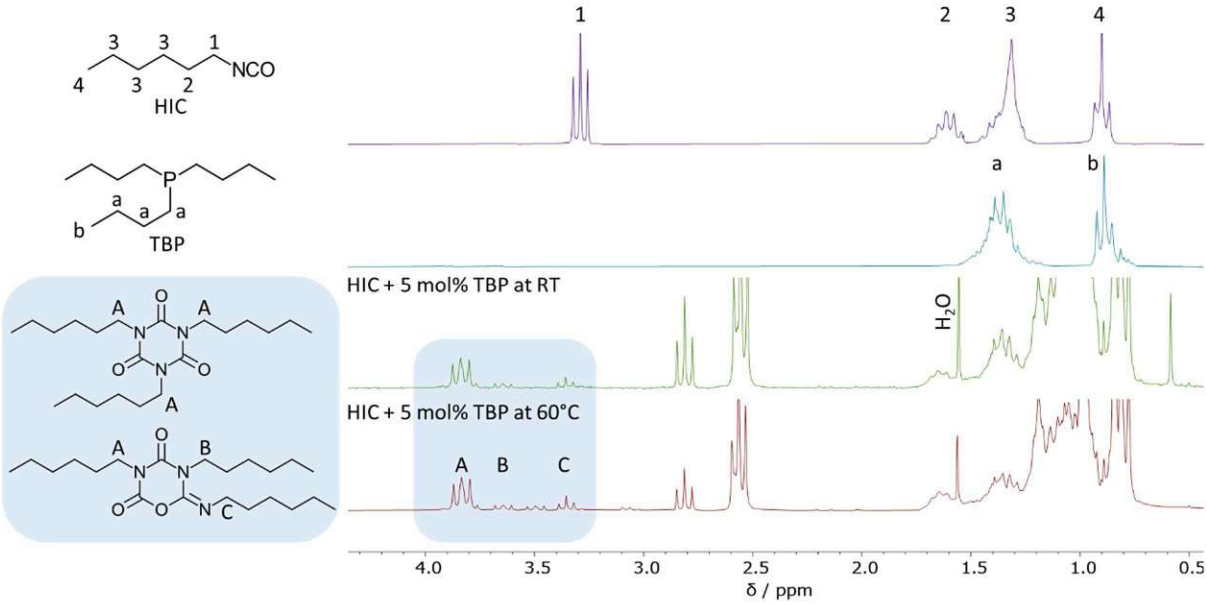

Figure 40: ^{1}H-NMR spectra (400 MHz) of hexyl isocyanate in $CDCl_3$ (purple), tributylphosphine in C_6D_6 (blue), reaction mixture with hexyl isocyanate and 5 mol% TBP in C_6D_6 at ambient temperatures (green) and reaction mixture with hexyl isocyanate and 5 mol% TBP in C_6D_6 at 60 °C (red)

It could be found that, TBP catalyses the cyclodimerization and cyclotrimerization of phenyl isocyanate and hexyl isocyanate in bulk already at ambient temperatures. Therefore TBP is interesting for producing a photobase generator and investigate the photochemical cyclodimerization and cyclotrimerization of isocyanates.

1.6. Triphenylphosphine

Triphenylphosphine (TPhP) was investigated about their cyclodimerization and cyclotrimerization of phenyl isocyanate and hexyl isocyanate derived from tributylphosphine (TBP) according to literature (Scheme 19). They reported the cyclotrimerization at 60 °C with TBP within minutes.[102]

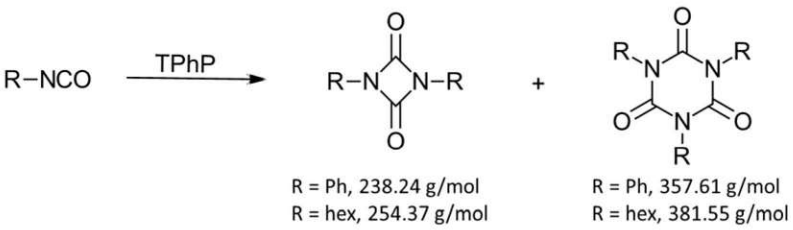

Scheme 19: Cyclodimerization and cyclotrimerization of phenyl isocyanate and hexylisocyanate with triphenylphosphine (TPhP)

Therefore, phenyl isocyanate or hexyl isocyanate and 5 mol% TPhP were investigated at ambient temperatures and 60 °C. The ATR-FTIR of the liquid reaction mixtures showed no complete conversion of hexyl isocyanate nor phenyl isocyanate, due the isocyanate vibration

at 2260 cm^{-1} (Figure S 10 and Figure S 11). The ^{1}H-NMR of these reaction mixtures display characteristic signals of the hydrolyzed educts, the amines aniline and hexylamine depictured in (Figure 41 and Figure 42). The LC-MS measurements supports the results of the ^{1}H-NMR to the hydrolysis to the corresponding amines aniline and hexylamine.

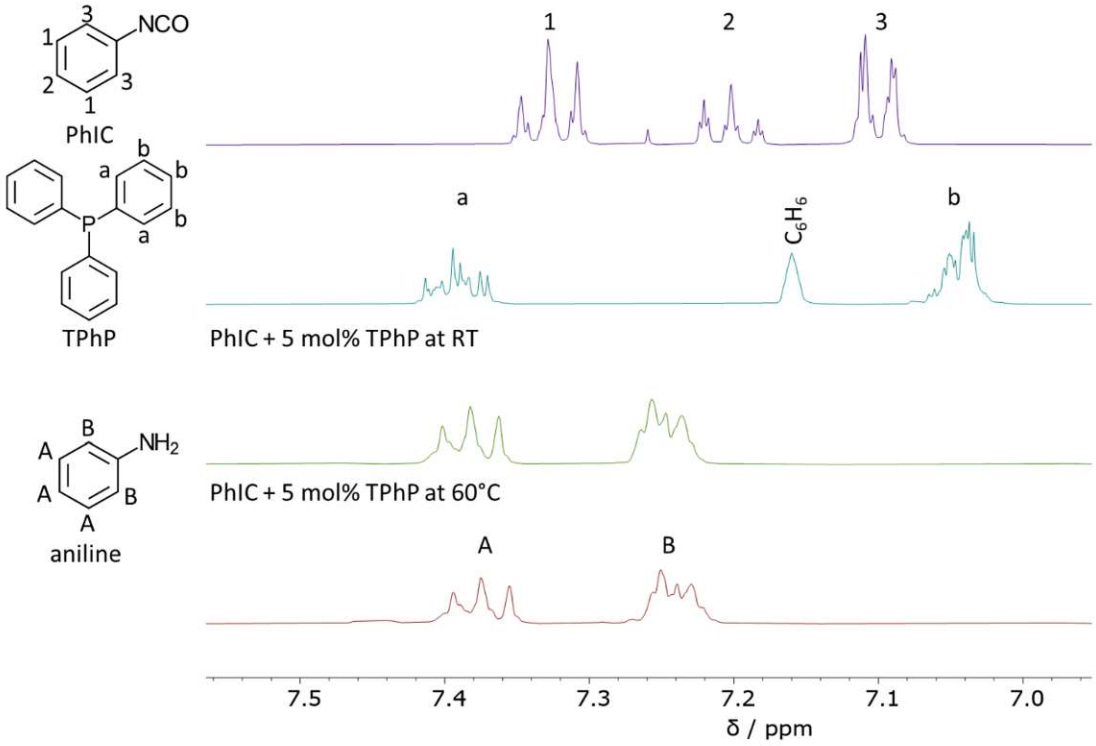

Figure 41: ^{1}H-NMR spectra (400 MHz) of phenyl isocyanate in $CDCl_3$ (purple), triphenylphosphine in C_6D_6 (blue), reaction mixture with phenyl isocyanate and 5 mol% TPhP in DMSO at ambient temperatures (green) and reaction mixture with phenyl isocyanate and 5 mol% TPhP in DMSO at 60 °C (red)

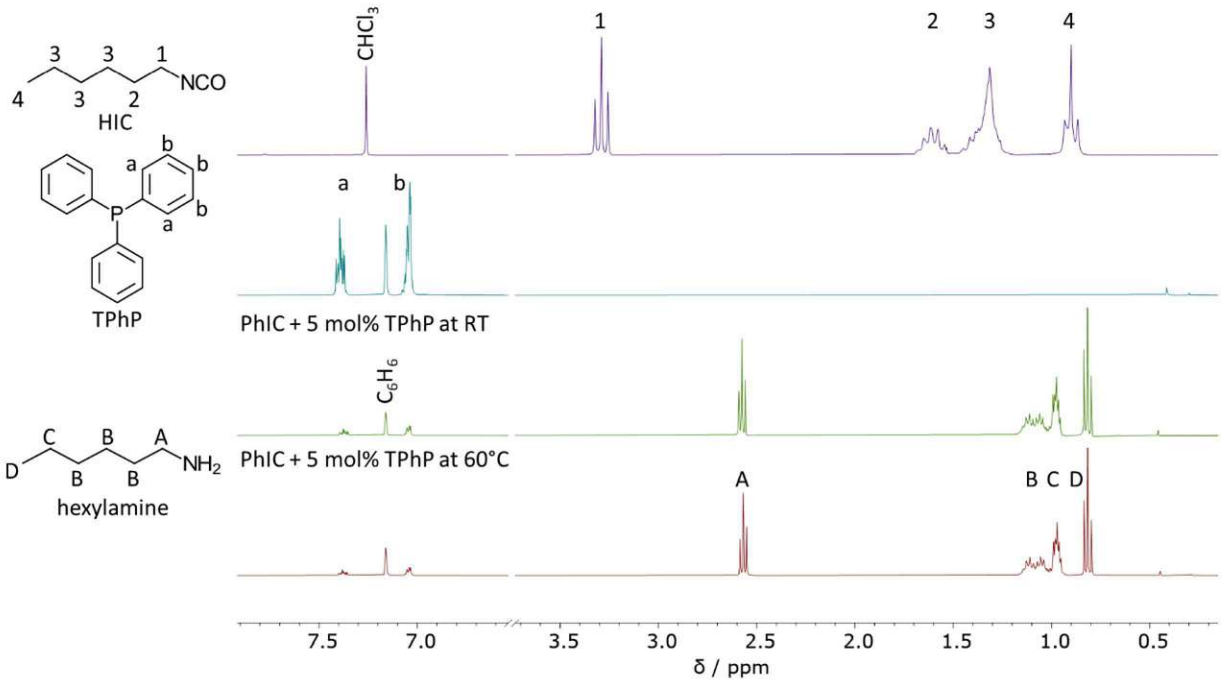

Figure 42: ^{1}H-NMR spectra (400 MHz) of hexyl isocyanate in $CDCl_3$ (purple), triphenylphosphine in C_6D_6 (blue), reaction mixture with hexyl isocyanate and 5 mol% TPhP in C_6D_6 at ambient temperatures (green) and reaction mixture with hexyl isocyanate and 5 mol% TPhP in C_6D_6 at 60 °C (red)

The experiments with TPhP do not show a cyclodimerization or cyclotrimerization of phenyl isocyanate and hexyl isocyanate. Accompanying a PBG of TPhP was not synthesized.

1.7. 1,2-Dimethylimidazole

Based on literature, which reported the cyclotrimerization of isocyanates with 1,2-dimethylimidazole (DMI) at ambient temperatures within a few seconds to minutes, phenyl isocyanate and hexyl isocyanate were investigated with DMI about their cyclodimerization and cyclotrimerization at ambient temperatures (Scheme 20).[99]

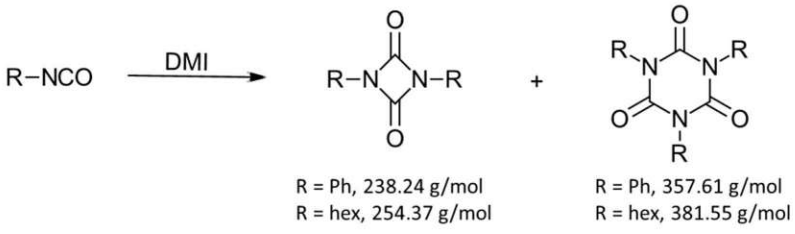

Scheme 20: Cyclodimerization and cyclotrimerization of phenyl isocyanate and hexyl isocyanate with 1,2-dimethylimidazole (DMI)

Therefore, phenyl isocyanate and 10 mol% DMI were investigated at ambient temperatures in analogy to literature.[103] The reaction mixture solidified under heat release within 15 minutes. The ATR-FTIR of the reaction mixture containing phenyl isocyanate and DMI showed

a complete conversion of phenyl isocyanate due to the disappearance of the isocyanate vibration at 2260 cm^{-1} (Figure S 12). Additionally the ATR-FTIR showed characteristic bands of the cyclodimer at 1773 cm^{-1}, 1747 cm^{-1}, 1599 cm^{-1} and the cyclotrimer at 1692 cm^{-1}, 1494 cm^{-1}, 1411 cm^{-1} of phenyl isocyanate.

The ^{1}H-NMR of the reaction mixture exhibited a change in multiplicity and chemical shifts, corresponding to the pure educt phenyl isocyanate (Figure 43). The new signals at 7.18 ppm, 7.39 ppm and 7.54 ppm could potentially be assigned to the trimer and dimer as suggested in Figure 43. However, the LC-MS measurements could not prove this assumption.

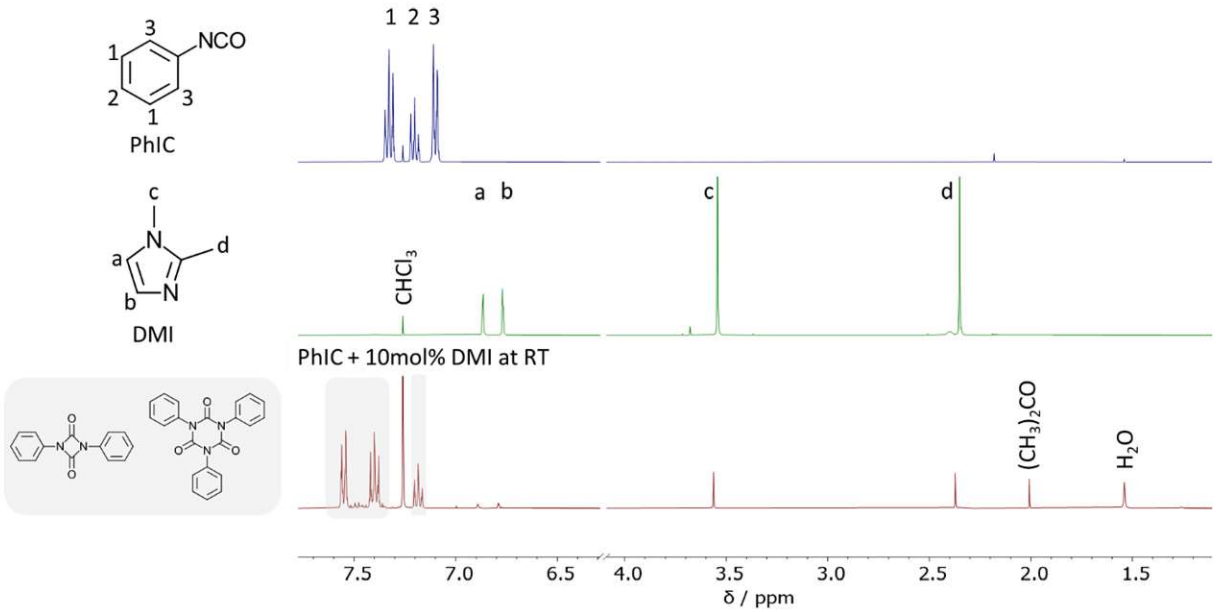

Figure 43: ^{1}H-NMR spectra (400 MHz, $CDCl_3$) of phenyl isocyanate (blue), DMI in $CDCl_3$ (green) and reaction mixture with phenyl isocyanate and 10 mol% DMI at ambient temperatures (red). Second tentative interpretation of the new signals is indicated through grey assignments.

Furthermore, the aliphatic hexyl isocyanate and 10 mol% DMI were investigated at ambient temperatures derived from literature.[103] The ATR-FTIR of the liquid reaction mixture containing hexyl isocyanate and DMI showed no conversion of hexyl isocyanate due to the presence of the isocyanate vibration at 2260 cm^{-1} (Figure S 13). Also, the ^{1}H-NMR of the reaction mixture exhibited no conversion of hexyl isocyanate (Figure 44). The LC-MS measurements of the reaction mixture only indicated the presence of dihexylurea a m/z value of 229 at positive mode, which indicated the molecular weight of 228.37 g mol^{-1} of dihexylurea.

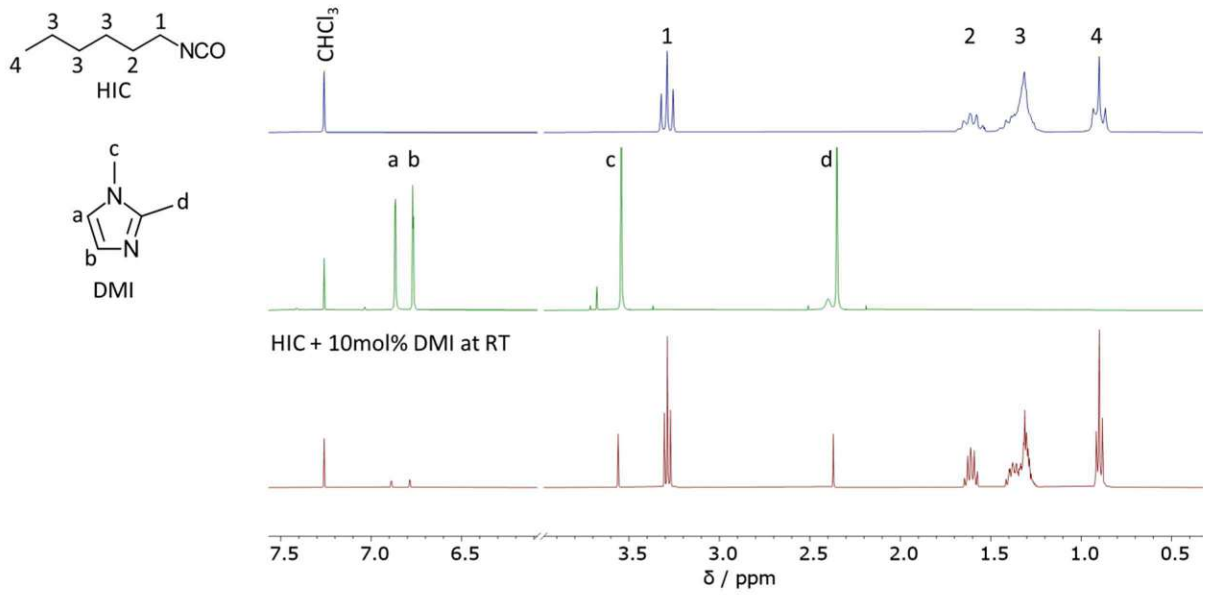

Figure 44: ^{1}H-NMR spectra (400 MHz, $CDCl_3$) of hexyl isocyanate (blue), DMI (green) and reaction mixture with hexyl isocyanate and 10 mol% DMI at ambient temperatures (red)

The results with DMI prove a catalytic cyclodimerization and cyclotrimerization of phenyl isocyanate in bulk and at ambient temperatures. Hexyl isocyanate does not exhibit a catalytic cyclodimerization and cyclotrimerization with DMI. Therefore DMI is interesting for producing a photobase and investigate the photochemical cyclodimerization and cyclotrimerization of aromatic isocyanates.

1.8. 1-(2-Ethyl hexyl)-2-butyl-imidazole)

1.8.1. Synthesis of 1-(2-Ethyl hexyl)-2-butyl-imidazole)

1-(2-Ethyl hexyl)-2-butyl-imidazole) (BEHI) was investigated as a derivative of DMI. The synthesis of 2-butyl-1-ethylhexyl imidazole was based on literature (Scheme 21).[107,108]

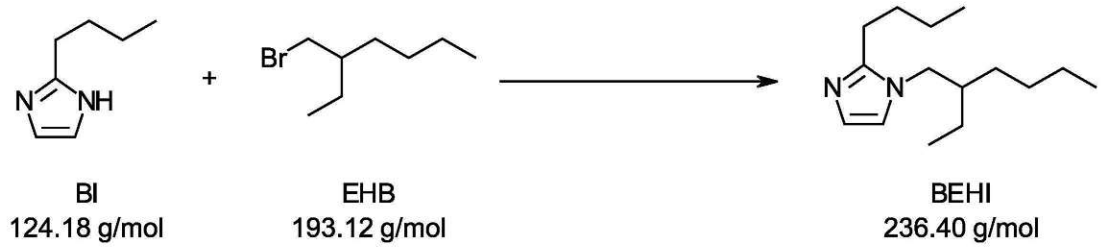

Scheme 21: Reaction of 2-butyl-1H-imidazole (BI) and 2-ethylhexylbromide (EHB) to obtain 1-(2-ethyl hexyl)-2-butyl-imidazole) (BEHI)

The first synthesis route to obtain BEHI was conducted without a phase transfer catalyst. 2-Butyl-1H-imidazole (BI) (1 eq.), 2-ethylhexylbromide (1.3 eq) and NaOH (1.2 eq.) were

dissolved in acetonitrile. After a reaction time of 24 hours at 75 °C the ^{1}H-NMR analysis provided incomplete conversion of BI. This route was not further investigated because BEHI could already be obtained through the second synthesis route.

The second attempt to obtain BEHI utilized phase transfer catalysis with commercially available 2-butyl-1H-imidazole (BI) (1 eq.), 2-ethylhexylbromide (1.1 eq.), tetrabutyl-ammoniumbromide (TBAB) (0.02 eq.) and NaOH (1.2 eq.) in aqueous solution. After a reaction time of 24 hours at 50 °C and purification, the ^{1}H-NMR does not show complete conversion. Therefore, the synthesis was repeated at higher temperatures (75 °C) to obtain a complete conversion of BI (Scheme 21).

1.8.2. Investigation of 1-(2-Ethyl hexyl)-2-butyl-imidazole)

After the successful synthesis of BEHI phenyl isocyanate or hexyl isocyanate and 10 mol% BEHI were investigated at ambient temperatures corresponding to the cyclodimerization and cyclotrimerization (Scheme 22).

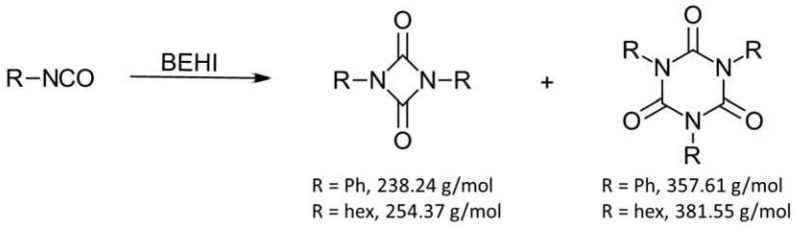

Scheme 22: Cyclodimerization and cyclotrimerization of phenyl isocyanate and hexyl isocyanate with 1-(2-ethyl hexyl)-2-butyl-imidazole) (BEHI)

The ATR-FTIR of the reaction mixture containing phenyl isocyanate and BEHI showed a complete conversion of phenyl isocyanate due to the disappearance of the isocyanate vibration at 2260 cm^{-1} (Figure S 15). The ^{1}H-NMR of the reaction mixture exhibited the same change in multiplicity and chemical shifts as the reaction mixture with phenyl isocyanate and 10 mol% DMI (Figure 45). According to the reaction mixture with phenyl isocyanate and 10 mol% DMI, the signals at 7.18 ppm, 7.39 ppm and 7.54 ppm could potentially be assigned to the trimer and dimer as suggested in Figure 45. It should be noted that the cyclodimerization and cyclotrimerization with a catalytic amount of BEHI was slower than with DMI. With DMI a solidification of the reaction mixture could be observed within 15 minutes. With BEHI the solidification slightly occurs after 1 hour. The reason for the slower cyclodimerization and cyclotrimerization could be the steric hindrance of the imidazole ring

due to the longer and branched aliphatic substituents. However, the LC-MS measurements could not prove the formation of the dimer and trimer.

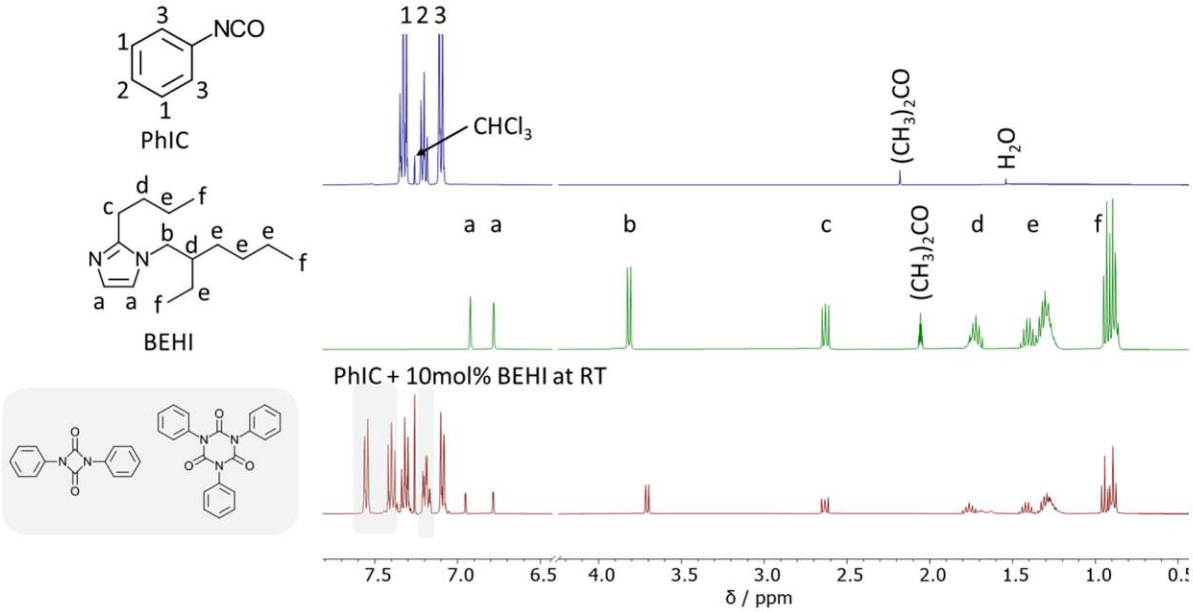

Figure 45: ^{1}H-NMR spectra (400 MHz) of phenyl isocyanate in $CDCl_3$ (blue), BEHI in $(CD_3)_2CO$ (green) and reaction mixture with phenyl isocyanate and 10 mol% BEHI in $CDCl_3$ at ambient temperatures (red). Tentative interpretation of the new signals is indicated through grey assignments.

In contrast to the possible cyclodimerization and cyclotrimerization of phenyl isocyanate with 10 mol% BEHI, the ATR-FTIR of the liquid reaction mixture containing hexyl isocyanate and BEHI showed no conversion of hexyl isocyanate due to the presence of the isocyanate vibration at 2260 cm^{-1} (Figure S 16). An accompanying ^{1}H-NMR of the reaction mixture containing hexyl isocyanate and 10 mol% BEHI does not show any conversion (Figure 46).

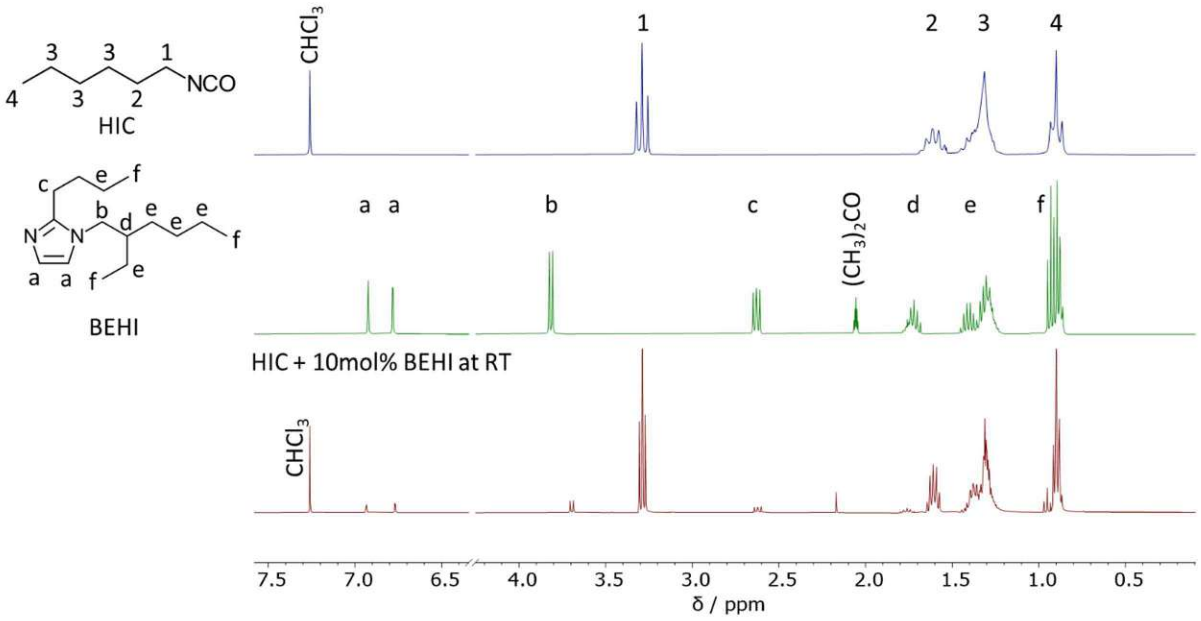

Figure 46: ^{1}H-NMR spectra (400 MHz) of hexyl isocyanate in $CDCl_3$ (blue), BEHI in $(CD_3)_2CO$ (green) and reaction mixture with hexyl isocyanate and 10 mol% BEHI in $CDCl_3$ at ambient temperatures (red)

Concluding, a catalytic amount of BEHI enables a cyclodimerization and cyclotrimerization of phenyl isocyanate in bulk at ambient temperatures. Accompanying BEHI is interesting for producing a photobase and investigate the photochemical cyclodimerization and cyclotrimerization of aromatic isocyanates.

2. Synthesis and stability of Photobase Generators

As concluded from the free base study, with DBN and TMG an adduct formation between the isocyanate and the free base could be proven. Whereas the free bases TBP, DMI and BEHI catalyzed the desired cyclodimerization and cyclotrimerization of isocyanates. Therefore, the corresponding photobase generators of DBN, TMG, TBP, DMI and BEHI were synthesized for investigation of the photochemical cyclic adduct reaction or cyclization reaction. The structures of the free bases used for investigation of the cyclodimerization and cyclotrimerization of hexyl isocyanate and phenyl isocyanate are depicted in Figure 47.

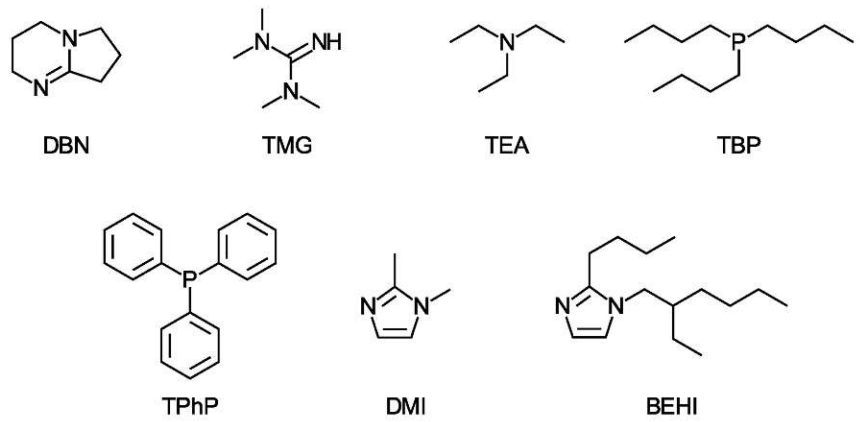

Figure 47: Structures of the free bases used for investigation of the cyclodimerization and cyclotrimerization: 1,5-diazabicyclo(4.3.0)non-5-ene (DBN), 1,1,3,3-tetramethylguanidin (TMG), triethylamine (TEA), tributylphosphine (TBP), triphenylphosphine (TPhP), 1,2-dimethyl imidazole (DMI) and 2-butyl-1-ethylhexyl imidazole (BEHI)

2.1. General procedure for the investigation

The conditions of the photochemical cyclodimerization and cyclotrimerization of phenyl isocyanate and hexyl isocyanate were studied with different PBG (Figure 48). The PBG of DBN, PDBN was already synthesized by co-workers acceding to literature.[109] The PBG of TMG, TBP, DMI and BEHI needed to be synthesised. The investigated concentrations and temperatures were derived from the free base studies.

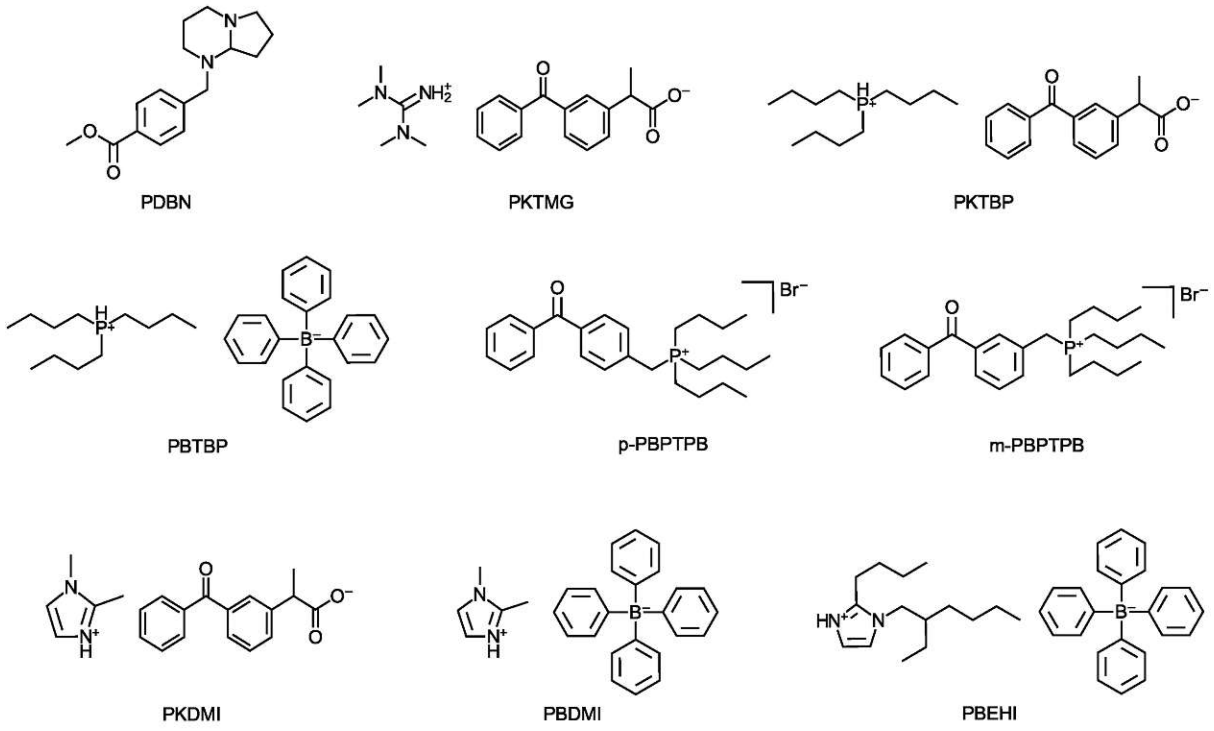

Figure 48: Structures of the photobase generator used for investigation of the photochemical cyclodimerization and cyclotrimerization

Moreover, the photoactivity of the synthesized PBGs under UV irradiation were studied via ^{1}H-NMR. Therefore, the PBGs were dissolved in the NMR-solvent and reacted in the UV oven for 2x200 seconds and with 100% intensity at ambient temperatures.

Furthermore, spontaneous reactions at room temperature without exposure to light will not be suitable for photoinitiated reactions. Therefore, the stability of the reaction mixtures in bulk was studied. Every reaction mixture contained phenyl isocyanate or hexyl isocyanate, a PBG and the sensitizer isopropylthioxanthone (ITX), as described in the respective chapters. The reaction mixtures were prepared under argon atmosphere at ambient temperatures and light exclusion. It has to be noted that phenyl isocyanate and hexylisocyanate were purified bevor usage via distillation and stored for maximal five days under argon atmosphere and molecular sieve at 5 °C. If not otherwise mentioned, the resulting reaction mixtures were stored at ambient temperatures and studied via ^{1}H-NMR as soon as solidification was visible.

2.2. Photo-1,5-diazabicyclo[4.3.0]non-5-ene

Corresponding to the free base studies a catalytic amount of DBN enable the cyclisation of phenyl isocyanate but with an unavoidable side reaction of phenyl isocyanate and DBN (Scheme 13). Therefore, we investigated the reactivity of the corresponding photobase would match these results. The stability of a reaction mixture with 5 mol% of photo-1,5-diazabicyclo[4.3.0]non-5-ene (PDBN), 1 mol% ITX (according to the PDBN) and one equivalent of phenyl isocyanate was investigated at ambient temperatures. The ^{1}H-NMR of the reaction mixture showed a reaction within 1 hour without exposure to light. Hence, no stable reaction mixture of PDBN and phenyl isocyanate could be achieved.

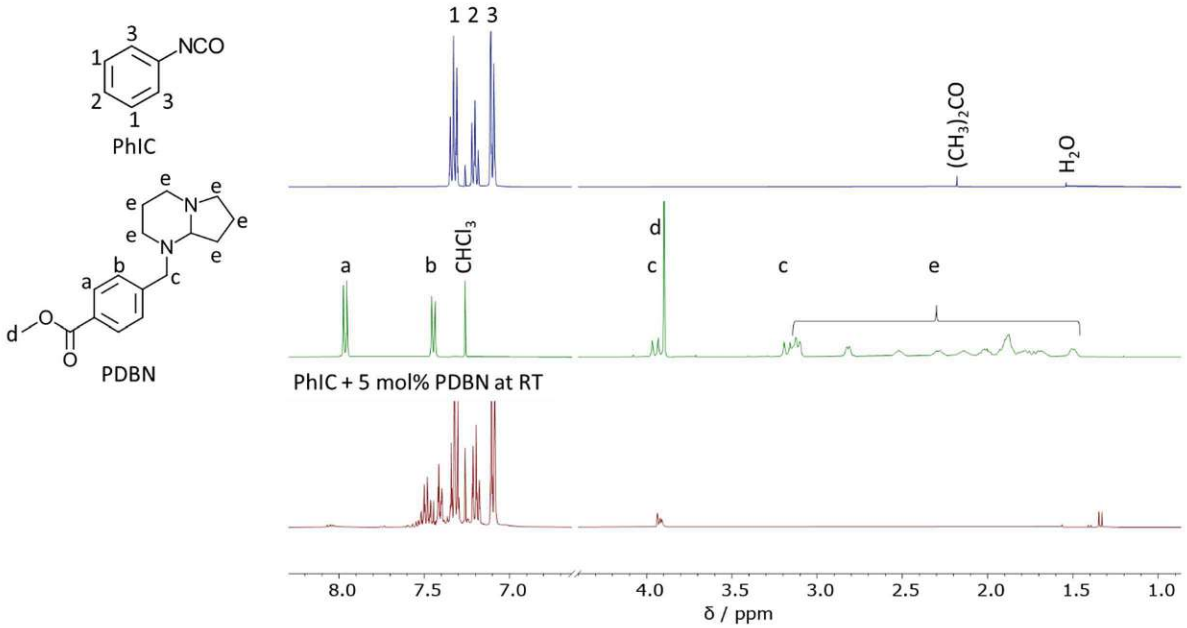

Figure 49: ^{1}H-NMR spectra (400 MHz, $CDCl_3$) of phenyl isocyanate (blue), PDBN (green) and reaction mixture with phenyl isocyanate and 5 mol% PDBN at ambient temperatures (red)

As concluded from the free base studies, in contrast to phenyl isocyanate, hexyl isocyanate does not show any cyclodimerization or cyclotrimerization with a catalytic amount of DBN but a cyclisation between one equivalent of hexyl isocyanate and two equivalents of DBN could be observed. To investigate a photochemical cyclisation reaction of PDBN and hexyl isocyanate, a reaction mixture with two equivalents of hexyl isocyanate with one equivalent of PDBN and 1 mol% ITX (according to the PDBN) was investigated. The reaction mixture needed to be heated to 85 °C because PDBN was not completely soluble in hexyl isocyanate. The stability of the reaction mixture was investigated with ^{1}H-NMR. The ^{1}H-NMR of the reaction mixture showed a reaction within 30 minutes without exposure to light.

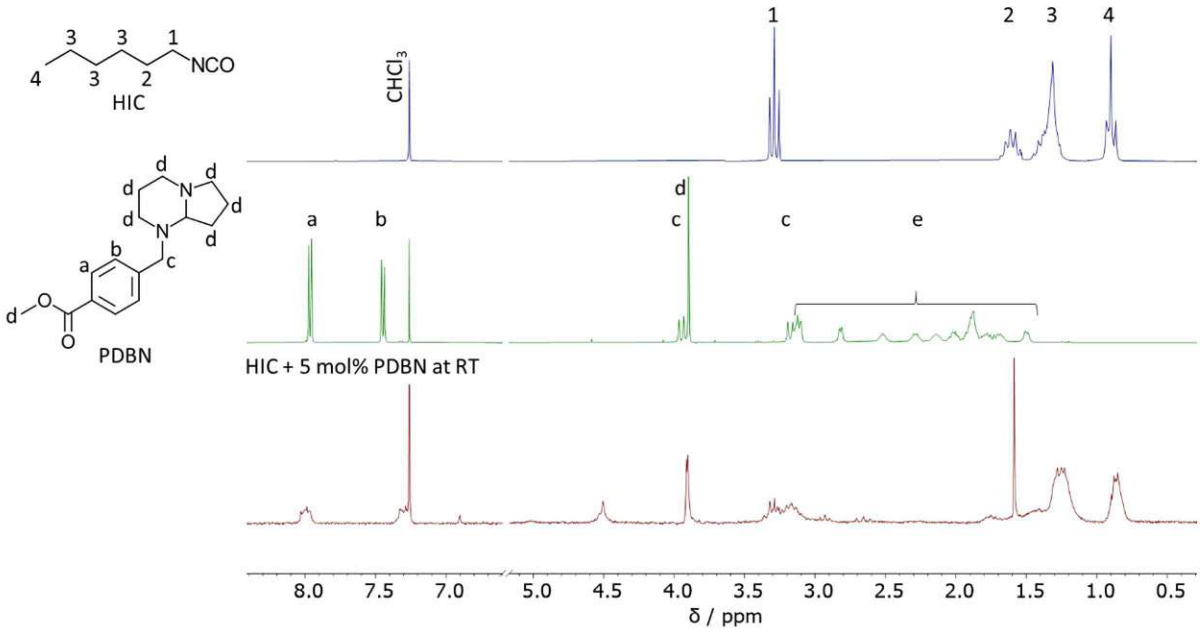

Figure 50: ^{1}H-NMR spectra (400 MHz, $CDCl_3$) of hexyl isocyanate (blue), PDBN (green) and reaction mixture with hexyl isocyanate and 5 mol% PDBN at 85 °C

The stability studies with PDBN and phenyl isocyanate or hexyl isocyanate exhibit a dark reaction, accompanying no stable reaction mixture with PDBN and phenyl isocyanate or hexyl isocyanate could be achieved.

2.3. Photo-tetramethyl guanidine salt

Regarding to the free base studies, where a cyclic adduct formation of phenyl isocyanate and hexyl isocyanate with TMG was proven, this reaction will further be investigated via a photochemical way. Because a PBG of TMG is not available commercially, the PBG was synthesized derived from literature.[110]

2.3.1. Synthesis of photo-tetramethyl guanidine salt

The PBG of TMG and ketoprofen was prepared via deprotonation of ketoprofen with tetramethyl guanidine to form a salt (Figure 51). Therefore, ketoprofen (1 eq.) and TMG (1 eq.) were dissolved in dry THF under argon atmosphere at ambient temperature. After one hour

the solvent was evaporated to obtain photo-keto-tetramethyl guanidine salt (PKTMG) as a highly viscous and sticky liquid, indicating that solvent was still present in the product.

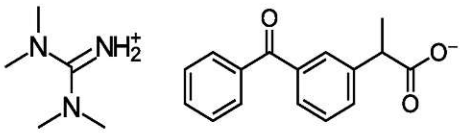

PKTMG
369.46 g/mol

Figure 51: Structure of the PBG of ketoprofen and TMG

2.3.2. Photoactivity and stability of photo-tetramethyl guanidine salt

The synthesized PKTMG was further investigated about the photoactivity. A ketoprofen based photobase generator conduct decarboxylation when irradiated with light and generate a carbanion. This generated carbanion further perform a proton transfer to obtain the free base (Scheme 23).[111] PKTMG showed photoactivity upon irradiation with light as a result of the decarboxylation and proton transfer in basic aqueous solution, which could be visible in the ^{1}H-NMR (Figure 52).

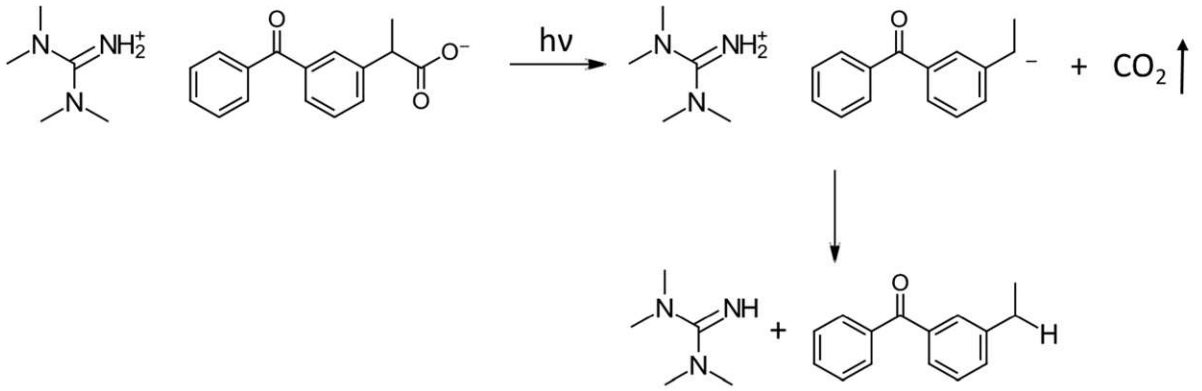

Scheme 23: The photodecarboxylation of PTMG and generation of the free base TMG shown as an example for a ketoprofen based photobase generator

Based on the photodecarboxylation and the proton transfer, the signal of the CH_3-group of PKTMG (**f**) changed from a doublet to a triplet and changed in chemical shifts. Additionally, the signal of the CH-group of ketoprofen (**d**) changed in multiplicity and chemical shift. The proton transfer was also indicated by the change of the NH_2^+-group integral from two to one (**a**).

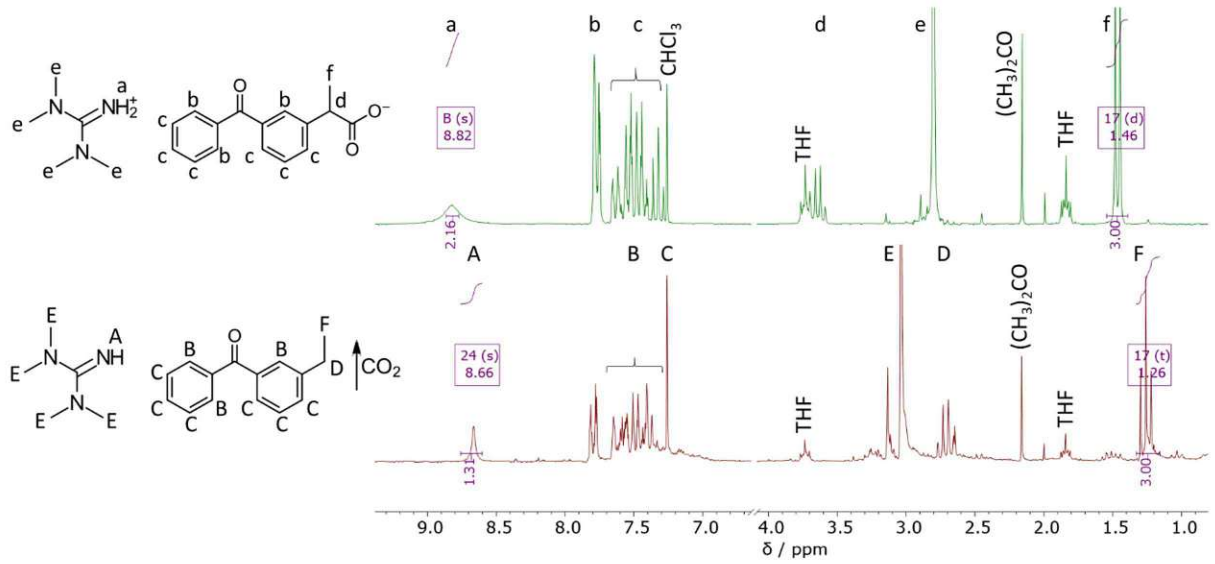

Figure 52: ^{1}H-NMR spectra (400 MHz, $CDCl_3$) of PKTMG (green) and PKTMG after irradiation of light and decarboxylation (red)

Since PKTMG showed photoactivity, further the reactivity of PKTMG and phenyl isocyanate or hexyl isocyanate were investigated. As concluded from the free base studies, phenyl isocyanate and hexyl isocyanate do not show any cyclodimerization or cyclotrimerization with catalytic amounts of TMG but a cyclisation between one equivalent of isocyanate and two equivalents of TMG could be observed. To investigate a photochemical cyclisation reaction between two equivalents of isocyanate and one equivalent of TMG, a reaction mixture with two equivalents of phenyl isocyanate or hexyl isocyanate with one equivalent of PKTMG and of 1 mol% ITX (according to the PKTMG) were investigated. The reaction mixtures were heated to 80 °C to lower the viscosity of PKTMG and to ensure homogeneity of the reaction mixture. The stability of the reaction mixture was investigated with ^{1}H-NMR. The ^{1}H-NMR of the reaction mixtures showed a reaction within 30 minutes without exposure to light, accompanying no stable reaction mixture with PKTMG and phenyl isocyanate or hexyl isocyanate could be achieved (Figure 53 and Figure 54).

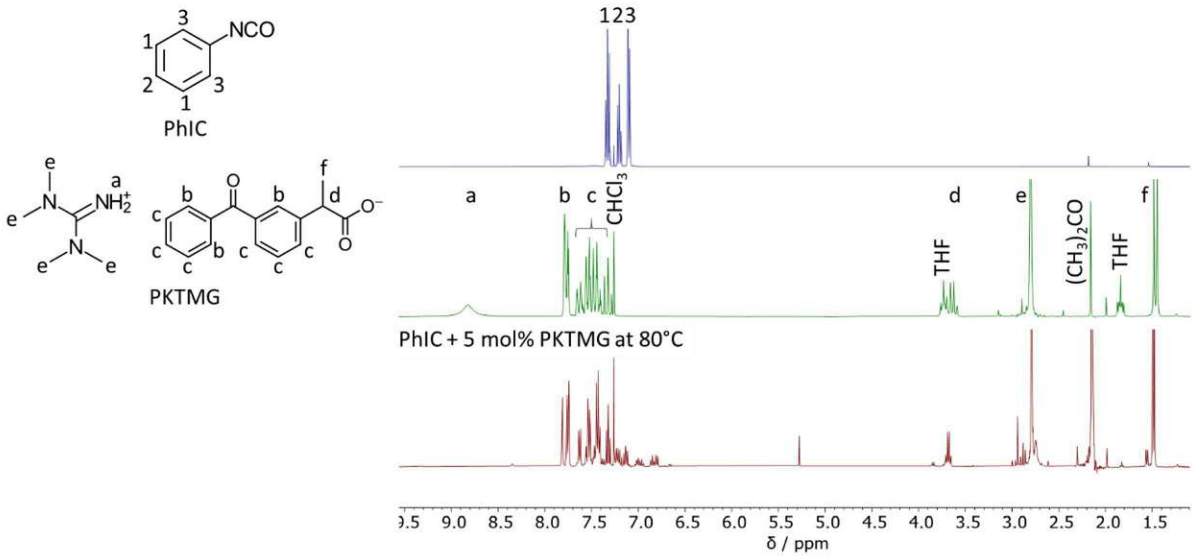

Figure 53: ^{1}H-NMR spectra (400 MHz, $CDCl_3$) of phenyl isocyanate (blue), PKTMG (green) and reaction mixture with phenyl isocyanate and 5 mol% PKTMG at 80 °C

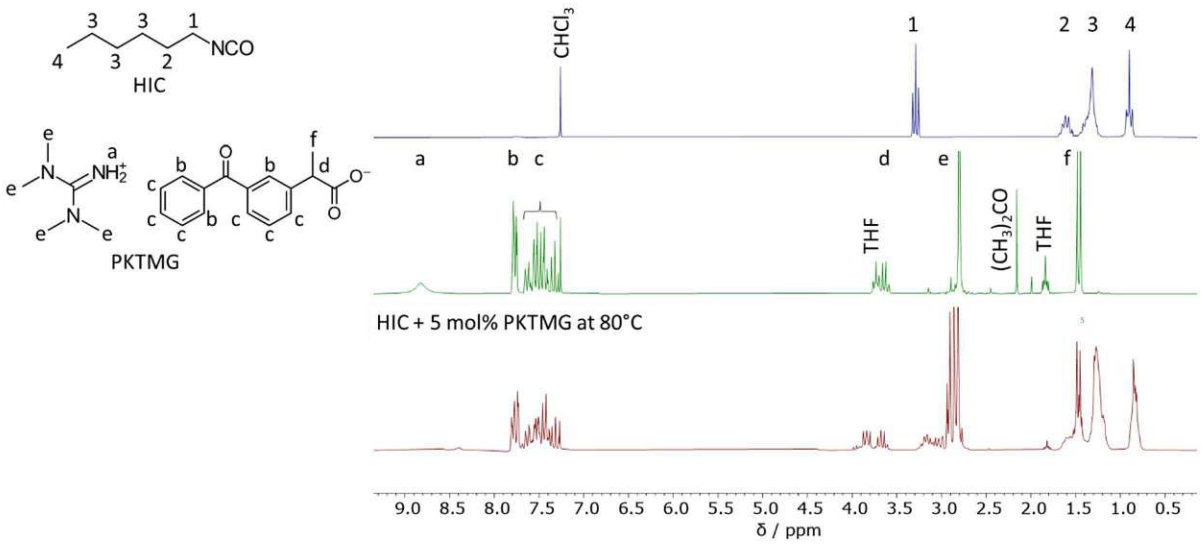

Figure 54: ^{1}H-NMR spectra (400 MHz, $CDCl_3$) of hexyl isocyanate (blue), PKTMG (green) and reaction mixture with hexyl isocyanate and 5 mol% PKTMG at 80 °C

2.4. Photo-tributylphosphine salts

The cyclodimerization and cyclotrimerization could be proven with TBP, as described in the free base studies. A corresponding PBG to TPB is not available commercially, therefore three different PBG of TBP were synthesized and studied about the reactivity and stability.

2.4.1. Synthesis of photo-tributylphosphine salts

2.4.1.1. Synthesis of photo-keto-tributylphosphine salt

A photobase generator was synthesized from ketoprofen and TBP via deprotonation to obtain the salt (Figure 55). Therefore, ketoprofen (1 eq.) and TBP (1 eq.) were dissolved in dry THF

and reacted at ambient temperatures for one hour. After removal of the solvent, photo-keto-tributylphosphine salt (PKTBP) was obtained as a highly viscous and sticky liquid, indicating that solvent was still present in the product. The synthesis of photo-keto-tributylphosphine salt (PKTBP) yield multiple products according to the ^{31}P-NMR, which exhibited multiple signals (Figure S 18). TBP is known for its easy oxidation to tributylphosphine oxide.[112] This oxidation could be observed in the ^{31}P-NMR. Therefore, TBP phosphine was distilled for purification to exclude impurities in the following PBG synthesis. After distillation of TBP, 10% of TBP oxidation was still evident. Accompanying a second attempt to obtain PKTBP was not performed due to the impurities of tributylphosphine oxide in TBP.

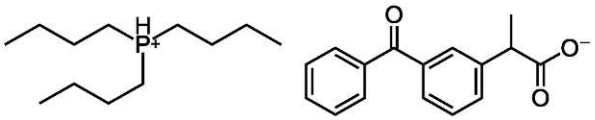

PKTBP

Figure 55: Structure of the PBG of TBP and ketoprofen

Therefore, new synthesis routs were investigated, in which the tributylphosphine oxide impurities of TBP does not interfere with the PGB synthesis and generated tributylphosphine oxide during the synthesis can be separated from the resulting PBG through several purification steps.

*2.4.1.2. Synthesis of photo-*borate*-tributylphosphine salt*

Tetraphenylborate salts and derivates are commonly used in photo base chemistry and generate upon irradiation via a proton transfer a free base (Scheme 24). These compounds precipitate during the synthesis and herein enable an easy purification of the obtain PBG.[26]

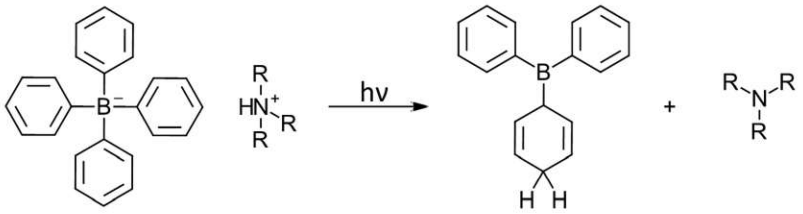

Scheme 24: Generation of a tertiary amine by irradiation of a tetraphenylborate-based PBG

The first synthesis route to obtain the PBG to TBP was conducted by exchanging the counterion triethylammonium from tetraphenylborate to tributylphosphomium with release of triethylamine to obtain photo-borate-tributylphosphine salt (PBTBP) (Scheme 25).

Therefore, triethylammonium tetraphenylborate (1 eq.) was dissolved in dry THF and tributylphosphine (1 eq.) was added to the solution. After 17 hours of stirring at ambient temperatures under argon atmosphere, still no precipitate could be observed. After removal of the solvent, the ^{1}H-NMR of the crude could be characterized as the starting material triethylammonium tetraphenylborate, rendering the synthesis unsuccessful.

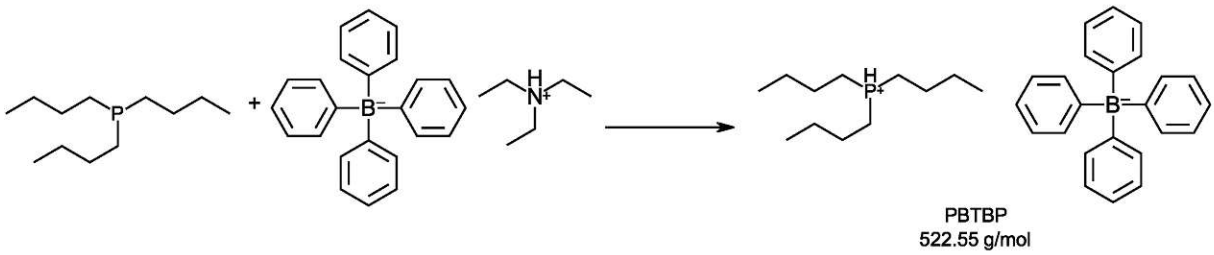

Scheme 25: Exchanging of the counterion triethylammonium to TBP to obtain the salt PBTBP

The second synthesis route was performed in a trifluoroacetic acid solution by exchanging the counterion of sodium tetraphenylborate to tributylphosphomium tetraphenylborate (PBTBP). PBTBP could be prepared under argon atmosphere by merging a solution of TBP (1 eq.) and trifluoroacetic acid (2 eq.) in dry ethanol with a solution of sodium tetraphenylborate (1 eq.) in dry ethanol. The formed precipitate was filtrated and washed to obtain the product PBTBP as a white salt (Figure 56).

Another couterion exchange of sodium tetraphenylborate (1 eq.) with TBP (1 eq.) was performed in 10% aqueous HCl to obtain tributylphosphomium tetraphenylborate. After 30 minutes at ambient temperatures, the formed precipitate was filtered and washed to obtain the product PBTBP as a white salt (Figure 56).

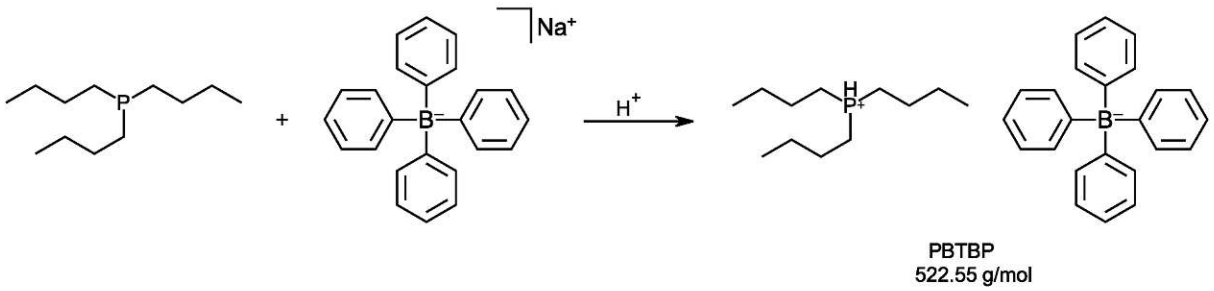

Figure 56: Exchanging of the sodium counterion to TBP to obtain the salt PBTBP

2.4.1.3. Synthesis of photo-benzophenone-tributylphosphine salt

The third synthesis route was investigated with benzophenone. Benzophenone is known to release the covalent bonded amine under irradiation with light to obtain the free tertiary amine.[26]

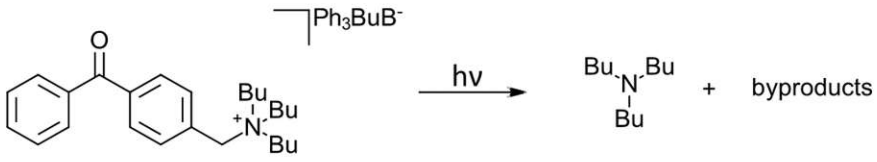

Scheme 26: Cleavage of a photo-benzophenone based salt by irradiation of light to obtain a tributyl amine

This cleavage mechanism was implemented to a covalent bonded phosphine and release of a tributylphosphine. Commercially available 4-bromomethylbenzophenone (1 eq.) and TBP (1 eq.) were dissolved in dry toluene under argon atmosphere. After a reaction time of 24 hours at 80 °C, the formed precipitate was filtered and washed to obtain the white solid phosphonium salt para-photo-benzophenone-tributylphosphine (p-PBPTBP) (Figure 57).

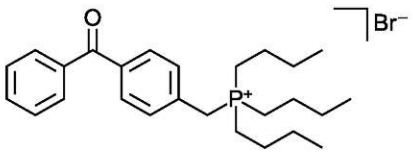

p-PBPTPB

Figure 57: Structure of the PBG of TBP and 4-(bromomethyl)benzophenone

Based on the results of *Blake et al,*[111] which reported the photo-inertness of para-substituted xanthone acetic acid, the same synthesis was performed with a benzophenone with the bromomethyl functionality in meta position to obtain meta-photo-benzophenone-tributylphosphine (m-PBPTBP) (Figure 58). M-PBPTBP was synthesised to avoid that the substitutions position leads to a photo-inert compound. According to literature, para-substituted xanthone acetic acid does not undergo decarboxylation when irradiated with light and accompanying no carbanion is generated with irradiation of light. Further para-substituted xanthone acetic acid is incapable of initiating a photochemical reaction (Scheme 27).[111]

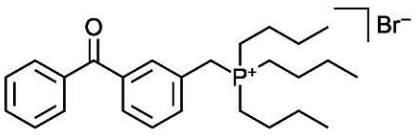

m-PBPTPB

Figure 58: Structure of the PBG of TBP and 3-(bromomethyl)benzophenone

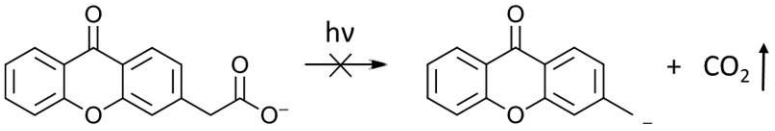

Scheme 27: Structure of para-substituted xanthone acetic acid and the photo-inertness as a result of the not occurring decarboxylation

2.4.2. Photoactivity and stability of photo-tributylphosphine salts

The successfully synthesized PGB to TBP (PBTBP, p-PBPTBP and m-PBPTBP) were studied with respect to their photoactivity. PBTBP, p-PBPTBP and m-PBPTBP showed no significant photoactivity upon irradiation because the signals from the unirradiated PBG and the irradiated PBG do not show any significant changes. The ^{1}H-NMR of the PBG before irradiation with light (green spectrum) and after irradiation with light (red spectrum) are depicted in the following Figure 59.

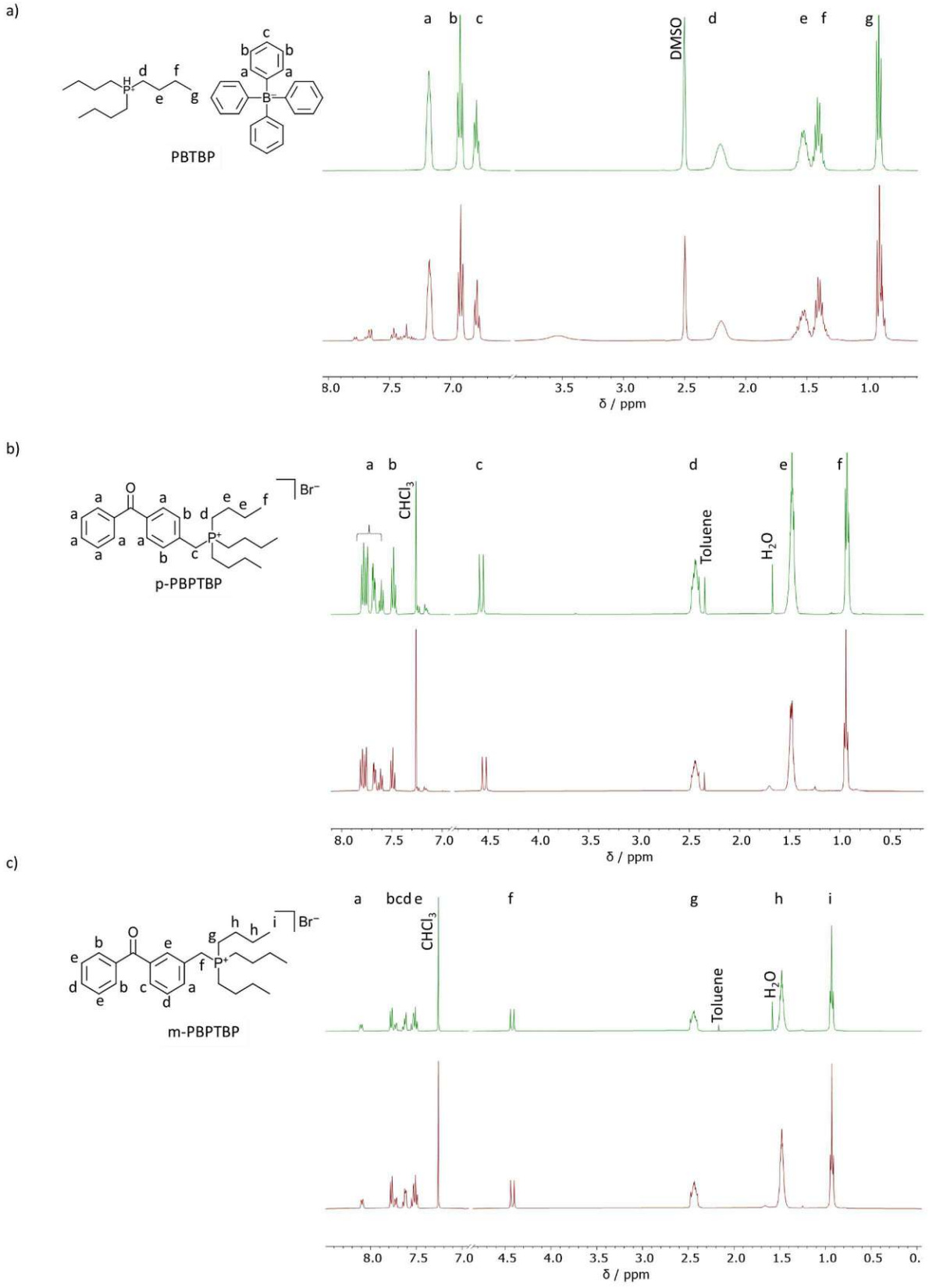

Figure 59: a) ^{1}H-NMR spectra (400 MHz,DMSO-d_6) of PBTBP (green) and PBTBP after irradiation of light (red), b) ^{1}H-NMR spectra (400 MHz, $CDCl_3$) of p-PBPTBP (green) and p-PBPTBP after irradiation of light (red), c) ^{1}H-NMR spectra (400 MHz, $CDCl_3$) of m-PBPTBP (green) and m-PBPTBP after irradiation of light (red)

2.5. Photo-dimethylimidazole salts

In chapter 1, the possibility of cyclodimerization and cyclotrimerization of phenyl isocyanate with the free base DMI was proven. Therefore, the corresponding PBG of DMI was synthesized with ketoprofen and sodium tetraphenylborate and investigated about their reactivity and stability.

2.5.1. Synthesis of photo-dimethylimidazole salt

2.5.1.1. Synthesis of photo-keto-dimethylimidazole salt

The photobase generator photo-keto-dimethylimidazole salt (PKDMI) could be prepared through a deprotonation of ketoprofen with DMI (Figure 60). Therefore, ketoprofen (1 eq.) and DMI (1 eq.) were dissolved in dry dichloromethane under argon atmosphere. After 16 hours stirring at ambient temperatures, the solvent was removed and PKDMI was obtained as a highly viscous and sticky liquid, indicating that solvent was still left in the product.

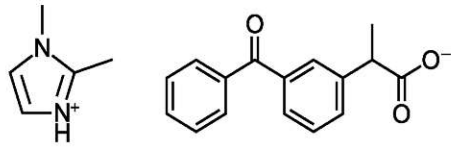

PKDMI

Figure 60: Structure of the PBG of DMI and ketoprofen

All syntheses containing ketoprofen yield a viscous and sticky PBGs, elicited to an insufficient drying process of the PBGs, even if high vacuum and elevated temperatures were used, and unavailable purification. In consequence of this, further PBGs based on ketoprofen were not synthesized.

2.5.1.2. Synthesis of photo-borate-dimethylimidazole salt

The second synthesis to obtain a PBG of DMI was performed by exchange the counterion of sodium tetraphenylborate (1 eq.) with DMI (1 eq.) at ambient temperatures in 10% aqueous HCl. The formed precipitation was immediately filtered and washed to obtain the product photo-borate-dimethylimidazole salt (PBDMI) as a white solid (Figure 61).

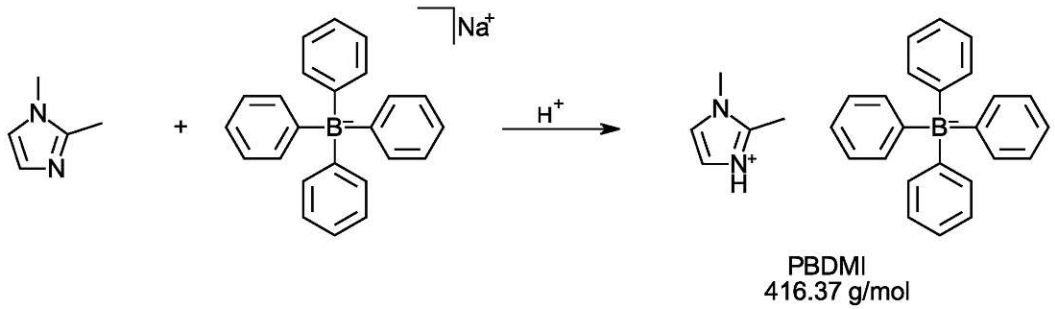

Figure 61: Exchanging of the sodium counterion to dimethyl imidazolium to obtain the salt PBDMI

2.5.2. Photoactivity and stability of photo-dimethylimidazole salt

The synthesized PBGs to DMI (PKDMI and PBDMI) were studied with respect to their photoactivity. PKDMI shows moderate photoactivity, which is visible via incomplete decarboxylation in the ^{1}H-NMR (Figure 62). Because of the decarboxylation the multiplicity of the CH_3-group changed from a doublet (**j**) to a triplet (**J**) as well as the upfield chemical shift of the triplet is visible (**J**). This is accompanied by the proton transfer from the nitrogen of the imidazole to the CH-group of ketoprofen as indicated by the disappearance of signal **a** and the change in multiplicity of the doublet to a triplet of the CH_3-group of the decarboxylated ketoprofen (**J**).

The ^{1}H-NMR of PBDMI also indicated photoactivity, as evident through the signals of the aromatic hydrogens of tetraphenylborate change in shifts and multiplicity, as well as the upfield chemical shift of the CH_3-groups (**e**, **f**) from the imidazole (Figure 62).

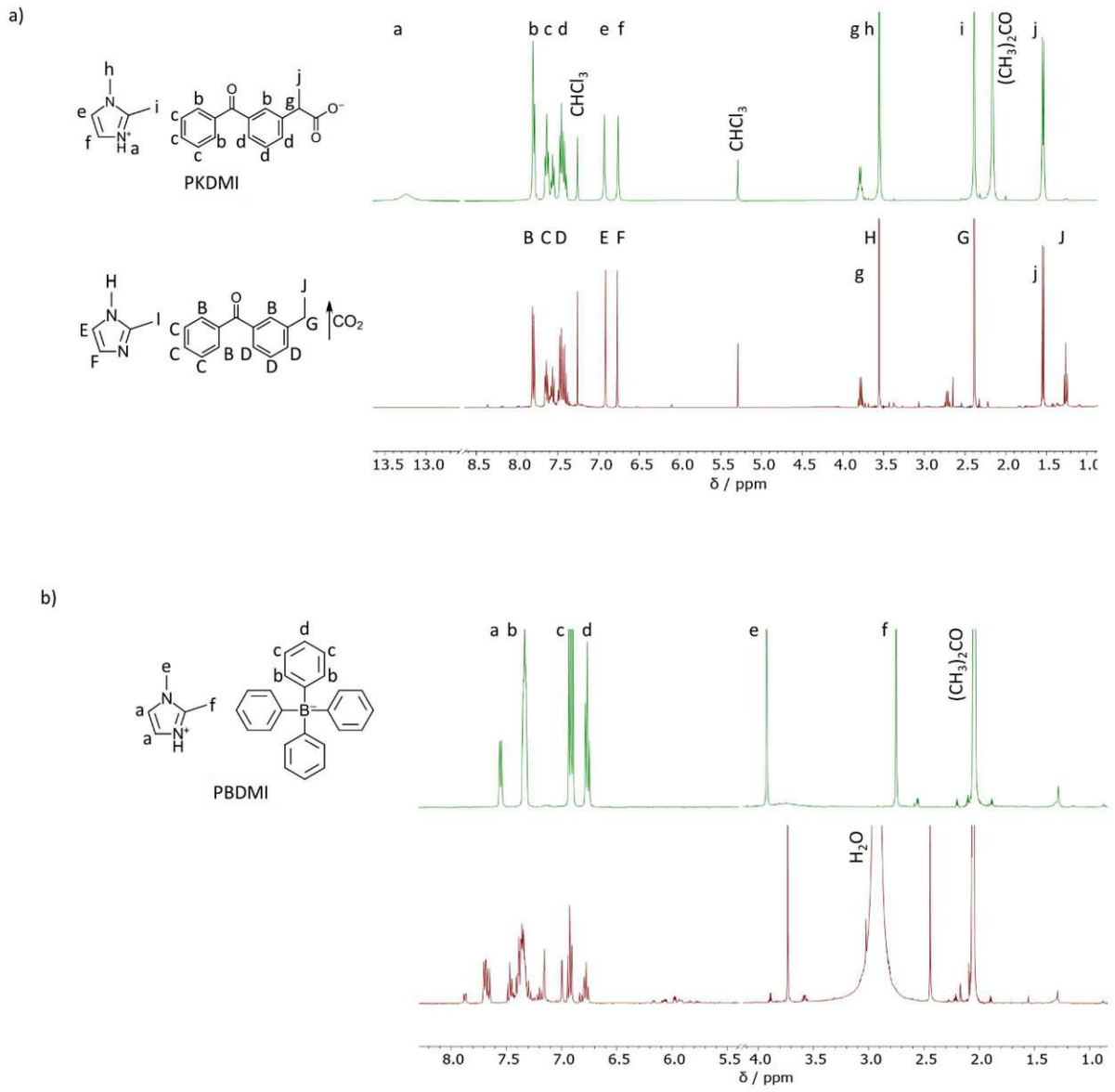

Figure 62: a) ^{1}H-NMR spectra (400 MHz, $CDCl_3$) of PKDMI (green) and PKDMI after irradiation of light (red), b) ^{1}H-NMR spectra (400 MHz, $(CD_3)_2CO$) of PBDMI (green) and PBDMI after irradiation of light (red)

To investigate a photochemical cyclodimerization and cyclotrimerization reaction and stability of the PBG of DMI with phenyl isocyanate, reaction mixtures containing 10 mol% of the PBG, 50 mol% ITX (according to the PBDMI) and one equivalent phenyl isocyanate were investigated. The amount of ITX was increased from 1 mol% to 50 mol% according to literature.[113] They reported the efficiency of a tetraphenylborate PBG was at highest with a molar ratio of 2:1 of PBG:ITX. Hence the prior used amount of 1 mol% was insufficient and caused by a misinterpretation of literture.[114]

The stability of a reaction mixture with phenyl isocyanate with PKDMI and ITX was investigated at ambient temperatures in bulk. After 10 minutes the reaction mixture solidified without exposure to light. The ^{1}H-NMR of the reaction mixture showed a reaction within 10 minutes

without exposure to light, and no stable reaction mixture with PKDMI and phenyl isocyanate could be achieved (Figure 63).

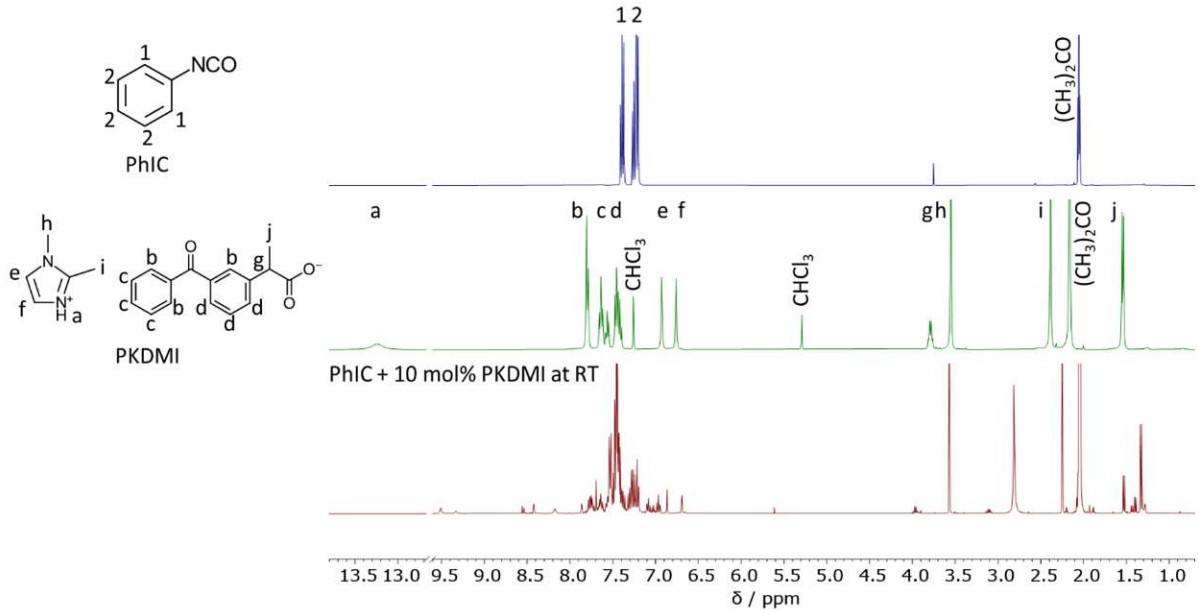

Figure 63: ^{1}H-NMR spectra (400 MHz, $(CD_3)_2CO$) of phenyl isocyanate in (blue), PKDMI (green) and reaction mixture with phenyl isocyanate and 10 mol% PKDMI at room temperature (RT)

The second reaction mixture containing the other synthesised PBG of DMI, PBDMI, could not fully be dissolved in phenyl isocyanate, although the reaction mixture was heated, placed in the ultrasonic bath and an excess of 300 mol% phenyl isocyanate was added. The ^{1}H-NMR of the suspension reaction mixture was stable without exposure to light (Figure 64).

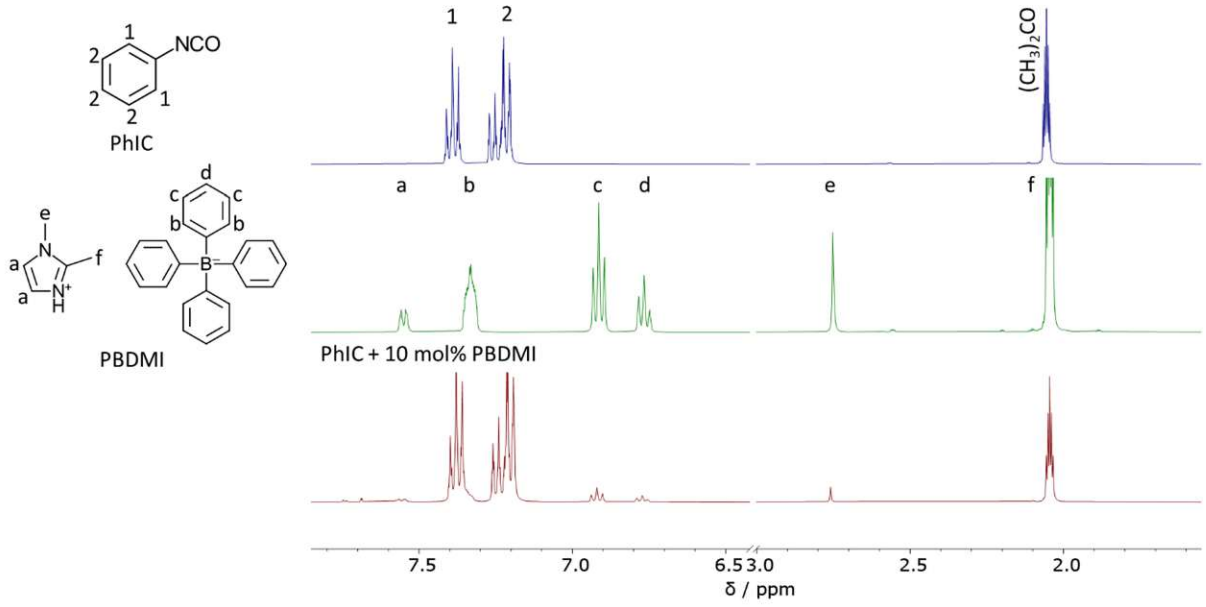

Figure 64: ^{1}H-NMR spectra (400 MHz, $(CD_3)_2CO$) of phenyl isocyanate (blue), PBDMI (green) and reaction mixture with phenyl isocyanate and 10 mol% PBDMI

To dissolve the PBG completely, a reaction mixture containing phenyl isocyanate, 10 mol% PBDMI (0.14 mmol, 7.15 mg,), ITX and acetone as dissolution-facilitating solvent, which should later be evaporated from the reaction mixture, was investigated. However, after adding 10 mL of acetone, the PBG could still not be dissolved, rendering the approach infeasible.

Therefore other solvents which facilitate dissolution of PBDMI were soughted. PBDMI could also be dissolved in N,N-dimethylformamide (DMF) and N,N-dimethylacetamide (DMA). In correlation to the boiling point of phenyl isocyanate (162 °C), the boiling points of DMF (153 °C) and DMA (165 °C) are quite similar. Consequently, the use of DMF and DMA as a solvent, which should be evaporated prior to bulk polymerization, would also cause evaporation of phenyl isocyanate. Therefore, DMF and DMA cannot be utilized for this approach. Another attempt to dissolve the PBDMI was tried by using a maximum of 20w% DMA or DMF as a co-solvent, which would remain in the formualtion. However, for complete solubility of PBDMI, 218 wt% DMF or 146 wt% of DMA were necessary. This clearly exceeds the maximum of potentially negligible amounts of co-solvent during bulk polymerization and leads to the conclusion that neither DMF nor DMA are suitable co-solvents.

The third attempt to improve the solubility of PBDMI was to replace the methyl substituents on the imidazole cycle with longer aliphatic chains to obtain a more polar and better soluble 2-butyl-1-ethylhexyl imidazole (Figure 65).

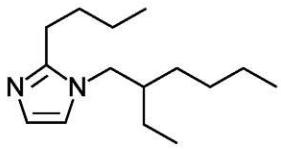

BEHI

Figure 65: Structure of 2-butyl-1-ethylhexyl imidazole (BEHI)

2.6. Photo-1-(2-ethyl hexyl)-2-butyl-imidazole) salt

2.6.1. Synthesis of photo-1-(2-ethyl hexyl)-2-butyl-imidazole) salt

After a successful synthesis of BEHI, the corresponding PBG of BEHI was synthesized by a counterion exchange from sodium tetraphenylborate (1 eq.) with BEHI (1 eq.) at ambient temperatures in 10% aqueous HCl to obtain the salt photo-borate-1-(2-ethyl hexyl)-2-butyl-imidazole (PBDMI) as a white solid (Figure 66).

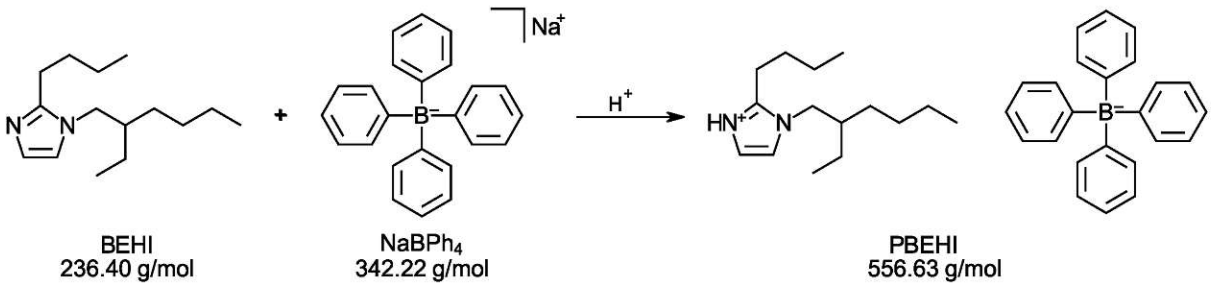

Figure 66: Exchanging of the sodium counterion to 1-(2-ethyl hexyl)-2-butyl-imidazolium to obtain the salt PBEHI

2.6.2. Photoactivity and stability of photo-1-(2-ethyl hexyl)-2-butyl-imidazole) salt

The photoactivity of the synthesized PBEHI was studied comparing ^{1}H-NMRs of the PBG bevor and after irradiation with UV light. The ^{1}H-NMR of PBEHI indicated photoactivity, according to the signals of the aromatic hydrogens of tetraphenylborate change in shifts and multiplicity, as well as the upfield chemical shift of the CH_2-groups (**e** and **f**) of the imidazole (Figure 67).

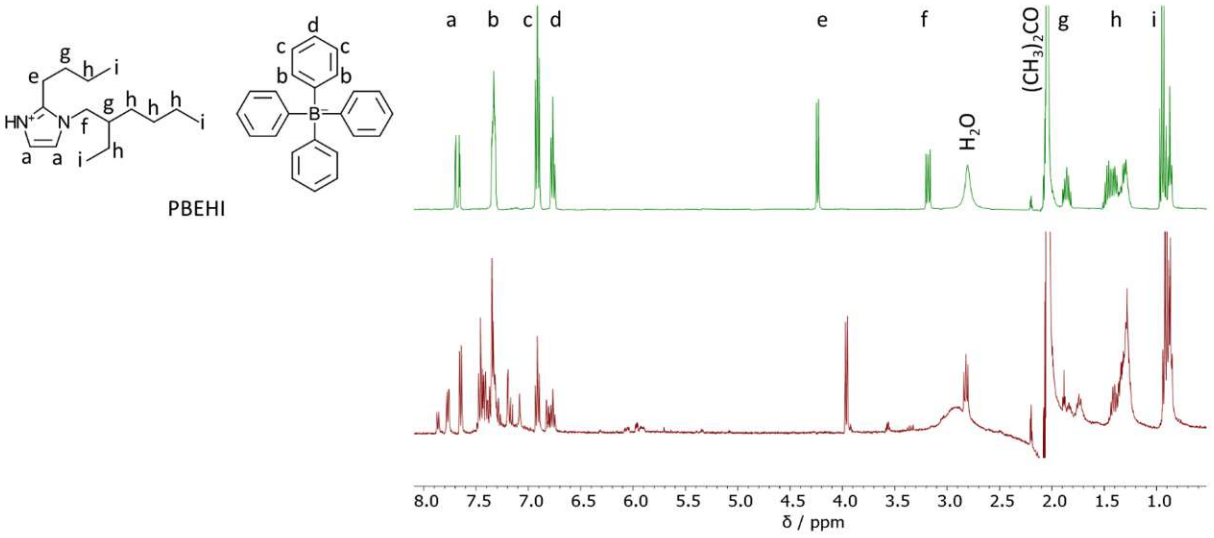

Figure 67: ^{1}H-NMR spectra (400 MHz, $(CD_3)_2CO$) of PBEHI (green) and PBEHI after irradiation of light (red)

After a successful photoactivity study of PBEHI, the stability of a phenyl isocyanate reaction mixture containing 10 mol% PBEHI and ITX (50 mol% according to PBEHI) in the absence of light was investigated. On account of the insufficient solubility at ambient temperatures, the reaction mixture was heated until PBEHI was completely dissolved and stored at 50 °C. After one hour, precipitation of the reaction mixture could be observed. In order to exclude that too low storing temperatures were the reason for the precipitation the reaction mixture was again heated and could be completely dissolved again. The reaction mixture was then stored at 70 °C. According to the ^{1}H-NMR, this setup results in a stable reaction mixture for 24 hours

at 70 °C without exposure to light because the reaction mixture was still liquid after 24 hours and the ^{1}H-NMR does not indicate any reaction (Figure 68).

The stable reaction mixture was further investigated with respect to their photochemical cyclodimerization and cyclotrimerization reaction. Therefore, 100 µm of the reaction mixture were placed on a glass plate in the UV-oven at 75 °C. The intensity of the UV light was 100 % and the exposure timer was 2x200 seconds. Although the ^{1}H-NMR of the irradiated reaction mixtures indicates a reaction between phenyl isocyanate and PBEHI, the reaction mixture remained liquid after irradiation (Figure 68).

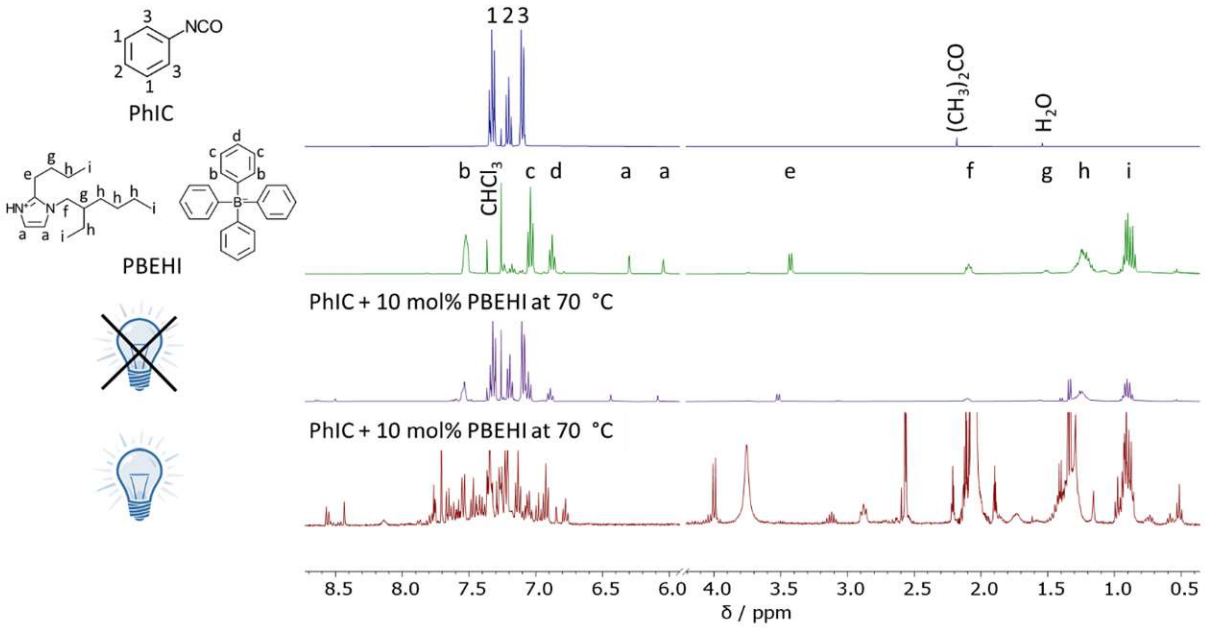

Figure 68: ^{1}H-NMR spectra (400 MHz, $CDCl_3$) of phenyl isocyanate (blue), PBEHI (green), reaction mixture with phenyl isocyanate and 10 mol% PBEHI at 70°C (purple) and reaction mixture with phenyl isocyanate and 10 mol% PBEHI after irradiation with light at 70°C (red)

As discussed in the free base study, the cyclodimerization and cyclotrimerization with BEHI was a very slow reaction and solidification of the reaction mixture occurred only after one hour. The reason for the slow reaction and associated slow solidification could be explained by the steric hindrance on the imidazole ring due to the longer and branched aliphatic substituents, causing only slow photochemical catalytic cyclodimerization and cyclotrimerization.

Experimental Part

1. Model systems for catalytic cyclodimerization and cyclotrimerization of isocyanates with free bases

1.1. General procedure for the investigation

Phenyl isocyanate (PhIC) (bp: 75 °C, 50 mbar) and hexyl isocyanate (HIC) (bp: 80 °C, 55 mbar) were distilled before use and maximal stored for five days at 5 °C under argon atmosphere and molecular sieve. The reaction mixtures were prepared under argon atmosphere at ambient temperatures in bulk. The liquid compounds (isocyanate, free base) were added via Eppendorf Pipettes to 1.5 mL brown glass vials, which were closed off and stored overnight at room temperature (25 °C). The 1.5 mL brown glass vials were prior purged with argon to ensure inert gas atmosphere. The reaction progress was monitored by ATR-FTIR, ^{1}H-NMR and LC-MS. The composition of the reaction mixtures, literature, temperatures and NMR solvents are listed in the following Table 4 - Table 10.

1.2. 1,5-Diazabicyclo[4.3.0]non-5-ene

Table 4: Composition, literature, temperatures and NMR solvent of the investigated reaction mixtures with DBN

	5 mol% DBN	PhIC	HIC	Lit.	DBN	HIC	Lit.	Temp.	NMR
eq.	0.05	1.00	1.00	100	2.00	1.00	105	RT	$CDCl_3$
mmol	0.05	1.00	1.00		2.00	1.00			
mg	6	117	125		250	125			

1.3. Tetramethyl guanidine

Table 5: Composition, literature, temperatures and NMR solvent of the investigated reaction mixtures with TMG

	5 mol% TMG	PhIC	HIC	Lit.	Temp.	NMR
eq.	0.05	1.00	1.00	80	RT	$CDCl_3$
mmol	0.05	1.00	1.00			
mg	6	117	125			

1.4. Triethylamine

Table 6: Composition, literature, temperatures and NMR solvent of the investigated reaction mixtures with TEA

	5 mol% TEA	PhIC	HIC	Lit.	Temp.	NMR
eq.	0.05	1.00	1.00	101	RT	$CDCl_3$
mmol	0.05	1.00	1.00			
mg	5	117	125			

1.5. Tributylphosphine

Table 7: Composition, literature, temperatures and NMR solvent of the investigated reaction mixtures with TBP

	5 mol% TBP	PhIC	NMR	5 mol% TBP	HIC	NMR	Lit.	Temp.
eq.	0.05	1.00	DMSO	0.05	1.00	C_6D_6	106	RT 60 °C
mmol	0.07	1.37		0.05	1.04			
mg	14	163		11	132			

1.6. Triphenylphosphine

Table 8: Composition, literature, temperatures and NMR solvent of the investigated reaction mixtures with TPhP

	5 mol% TphP	PhIC	5 mol% TphP	HIC	NMR	Lit.	Temp.
eq.	0.05	1.00	0.05	1.00	C_6D_6	106	RT 60 °C
mmol	0.07	1.37	0.05	1.04			
mg	18	163	14	132			

1.7. 1,2-Dimethylimidazole

Table 9: Composition, literature, temperatures and NMR solvent of the investigated reaction mixtures with DMI

	10 mol% DMI	PhIC	10 mol% DMI	HIC	NMR	Lit.	Temp.
eq.	0.10	1.00	0.10	1.00	$CDCl_3$	103	RT
mmol	0.14	1.37	0.10	1.04			
mg	13	163	11	132			

1.8. 1-(2-Ethyl hexyl)-2-butyl-imidazole)

1.8.1. Synthesis of 1-(2-ethyl hexyl)-2-butyl-imidazole)

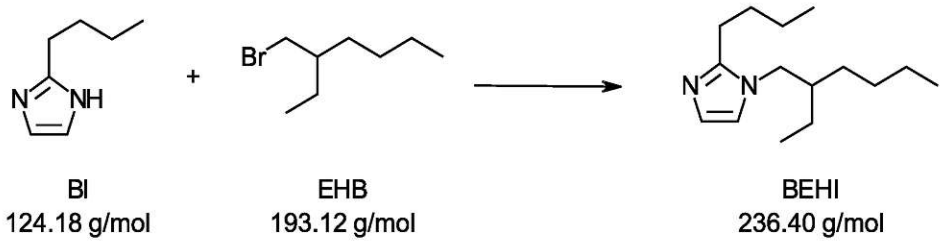

BI
124.18 g/mol

EHB
193.12 g/mol

BEHI
236.40 g/mol

Scheme 28: Reaction of 2-butyl-1H-imidazole (BI) and 2-ethylhexylbromide (EHB) to obtain 2-butyl-1-ethylhexyl imidazole (BEHI).

The approach was conducted in analogy to literature.[107] 2-Butyl-1H-imidazole (1 eq., 16.0 mmol, 1.99 g) and tetrabutylammoniumbromide (0.02 eq., 0.32 mmol, 1013 mg) were dissolved under vigorous stirring in an aqueous solution of sodium hydroxide (1.2 eq., 2.4 mmol, 96 mg) in 10 mL water. 2-Ethylhexylbromide (1.1 eq., 19.2 mmol, 768 mg) was added dropwise at ambient temperatures, then the reaction mixture was heated to 75°C. After 24 hours the resulting two phases were separated. The upper organic phase (2 mL) of the reaction mixture was merged with 10 mL ethyl acetate, washed once with water and birne, dried over Na_2SO_4 and the solvent was evaporated to obtain a yellow oil. The crude was purified by column chromatography in $CHCl_3$ containing 3% (w/v) methanol. ^{1}H-NMR, ^{13}C-NMR and thin layer chromatography were measured of the product.

Yield: 1.98 g (53% th.)

^{1}H-NMR (400 MHz, $(CD_3)_2CO$) δ = 6.90 (d, J = 1.3 Hz, 1H, H^{ar}), 6.76 (d, J = 1.3 Hz, 1H, H^{ar}), 3.80 (d, J = 7.5 Hz, 2H, N-*CH_2*-CH), 2.65 – 2.55 (t, 2H, Ar-*CH_2*-CH_2), 1.79 – 1.64 (m, 3H, Ar-CH_2-*CH_2*-CH_2, N-CH_2-*CH*-), 1.46 – 1.19 (m, 12H, -CH-*CH_2*-*CH_2*-*CH_2*-CH_3, *CH_2*-CH_3), 0.95 – 0.81 (m, 9H, CH_2-*CH_3*) ppm.

^{13}C NMR (101 MHz, $(CD_3)_2CO$) δ: 126.83, 119.15, 49.31, 40.54, 30.24, 29.95, 28.40, 26.44, 23.52, 22.76, 22.45, 13.82, 13.69, 10.41 ppm.

TLC: R_f = 0.32 ($CHCl_3$:MeOH, 1:0.03).

1.8.2. Investigation of 2-butyl-1-ethylhexyl imidazole

Table 10: Composition, literature, temperatures and NMR solvent of the investigated reaction mixtures with BEHI

	10 mol% BEHI	PhIC	10 mol% BEHI	HIC	Lit.	Temp.
eq.	0.10	1.00	0.10	1.00	103	RT
mmol	0.08	0.82	0.06	1.62		
mg	19	98	15	80		

2. Synthesis and stability of Photobase Generators

2.1. General procedure for the investigation

The stability studies were conducted under exclusion of light in the orange light lab with phenyl isocyanate and hexyl isocyanate. Phenyl isocyanate and hexyl isocyanate were distilled before use and stored under argon and molecular sieve for maximal five days at 5 °C. The reaction mixtures were prepared in bulk under argon atmosphere and stored at different temperatures. The PBG of TMG, TBP, DMI and BEHI needed to be synthesised, PDBN was already synthesised by co-workers. The corresponding literatures for the synthesis are mentioned in the respective chapters.

The investigated concentrations and temperatures are derived from the free base studies. The mol% of ITX are in relation to the photobase generator. The composition of the studied reaction mixtures and the stabilities are listed in the following Table 11. The stability was monitored by ^{1}H-NMR in $CDCl_3$ or $(CD_3)_2CO$.

Table 11: Composition of the studied reaction mixtures and stability

PDBN	PhIC		HIC		ITX	Temp.	stability
0.05 eq.	2 eq.	3.66 mmol	-	-	1 mol%	80 °C	NO
1 eq.	-	-	2 eq.		1 mol%	80 °C	NO

PTMG	PhIC		HIC		ITX	Temp.	stability
1 eq.	2 eq.	3.66 mmol	-	-	1 mol%	75 °C	NO
1 eq.	-	-	2 eq.	2.75 mmol	1 mol%	75 °C	NO

PKDMI	PhIC		HIC		ITX	Temp.	stability
0.1 eq.	1 eq.	1.4 mmol	-	-	50 mol% [113]	25 °C	NO

PBDMI	PhIC		HIC		ITX	Temp.	stability
0.1 eq.	1 eq.	1.4 mmol	-	-	50 mol% [113]	80 °C	not soluble

PBEHI	PhIC		HIC		ITX	Temp.	stability
0.1 eq.	1 eq.	1.4 mmol	-	-	50 mol% [113]	70 °C	YES

2.3. Photo-tetramethyl guanidine salt

2.3.1. Synthesis of photo-tetramethyl guanidine salt

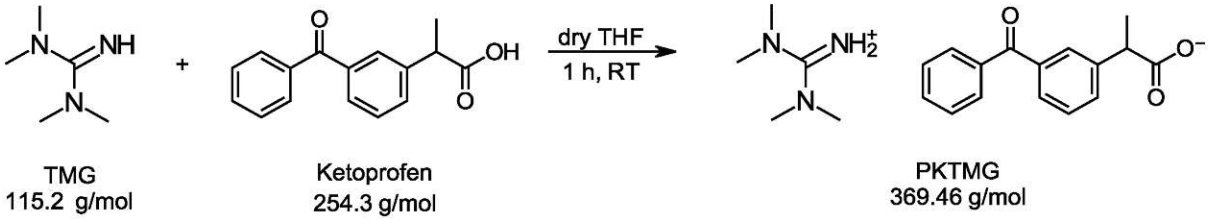

Scheme 29: Reaction of 1,1,3,3-tetramethylguanidin (TMG) with ketoprofen in dry THF for 1 hour at room temperature (RT)

The synthesis was performed under light exclusion, in analogy to literature.[110] Therefore, ketoprofen (1 eq., 15 mmol, 1.73 g) and 1,1,3,3-tetramethylguanidin (1 eq., 15 mmol, 3.88 mg) were transferred into a 100 mL round bottom flask. Standard Schlenk techniques were applied to remove any residual moisture. 20 mL dry THF were added with a syringe via a septum and the yellow suspension was stirred at ambient temperature for 1 h. The solvent was removed using the rotary evaporator at 40 °C. To remove residual THF from the obtained yellow high viscous liquid, it was dried using the high vacuum pump. A ^{1}H-NMR of the product was measured (Figure S 17). The yield of the reaction could not be obtained because the substance could not be dried sufficiently.

^{1}H NMR (200 MHz, $CDCl_3$) δ = 8.82 (s, 2H, N-H_2), 7.84 – 7.70 (m, 3H, H^{ar}), 7.69 – 7.27 (m, 6H, H^{ar}), 3.62 (q, J = 7.1 Hz, 1H, C_{arom}-C*H*-CH_3), 2.80 (s, 12H, N-CH_3), 1.46 (d, J = 7. Hz, 3H, CH-CH_3) ppm.

2.4. Photo-tributylphosphine salts

2.4.1. Synthesis of photo- tributylphosphine salts

2.4.1.1. Synthesis of photo-keto-tributylphosphine salts

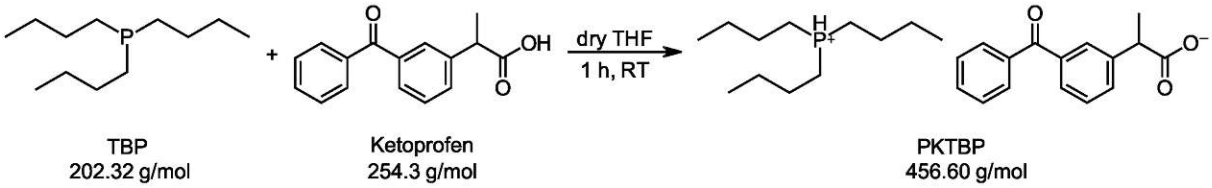

Scheme 30: Reaction of tributylphosphine (TBP) with ketoprofen in dry THF for 1 hour at room temperature (RT)

The synthesis was performed under light exclusion, in analogy to literature.[110] Therefore, ketoprofen (1 eq., 15 mmol, 3.81 g) were transferred into a 100 mL three-necked round bottom flask fitted with a septum. Standard Schlenk techniques were applied to remove any residual moisture. 20 mL dry THF and tributylphosphine (1 eq., 15 mmol, 3.03 g) were added and the solution was stirred at ambient temperature for 1 h. The solvent was removed using the rotary evaporator with a water bath at 40 °C. To remove residual THF, the viscous solution was dried using the high vacuum pump, resulting in a phase separation. After separation of the two phases, ^{31}P-NMR were measured of the upper phase, indicating the presence of by-products (Figure S 18).

2.4.1.2. Synthesis of photo-borate-tributylphosphine salts

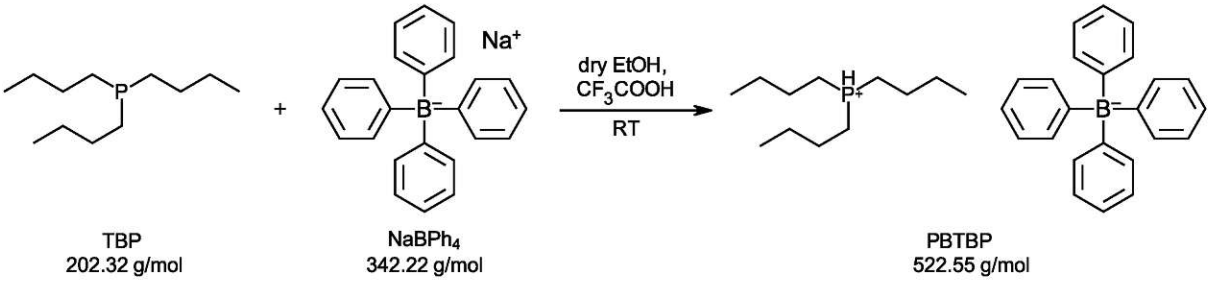

Scheme 31: Reaction of tributylphosphine (TBP) with sodium tetraphenylborate ($NaBPh_4$) and trifluoroacetic acid in ethanol for 21 hours at RT

The approach was conducted under light exclusion, in analogy to literature.[107] Therefore, tributylphosphine (1 eq., 1 mmol, 202 mg) and trifluoroacetic acid (CF_3COOH) (2 eq., 2.0 mmol, 228 mg) were dissolved in 3 mL dry ethanol under argon atmosphere. An ethanolic

solution of sodium tetraphenylborate (1 eq., 1.0 mmol, 342 mg) in 3 mL ethanol was added slowly. After 2 h the resulting white crystalline precipitate was filtered, washed with 3 mL ethanol three times and dried under high vacuum. A ^{1}H-NMR and a ^{31}P-NMR in DMSO were measured of the obtained white crystalline product (Figure S 19 and Figure S 20).

Yield: 156 mg (30% th.)

^{1}H-NMR (400 MHz, DMSO) δ = 7.18 (m, 8H, H^{ar}), 6.92 (t, J = 7.3 Hz, 8H, H^{ar}), 6.79 (t, J = 7.2 Hz, 4H, H^{ar}), 2.21 (s, 6H, P^{+}-*CH_2*-), 1.53 (m, 6H, -CH_2-*CH_2*-CH_2-), 1.40 (m, 6H, -CH_2-*CH_2*-CH_3), 0.91 (t, J = 7.3 Hz, 9H, -CH_2-*CH_3*) ppm.

^{31}P-NMR (162 MHz, DMSO) δ = 12.25 ppm.

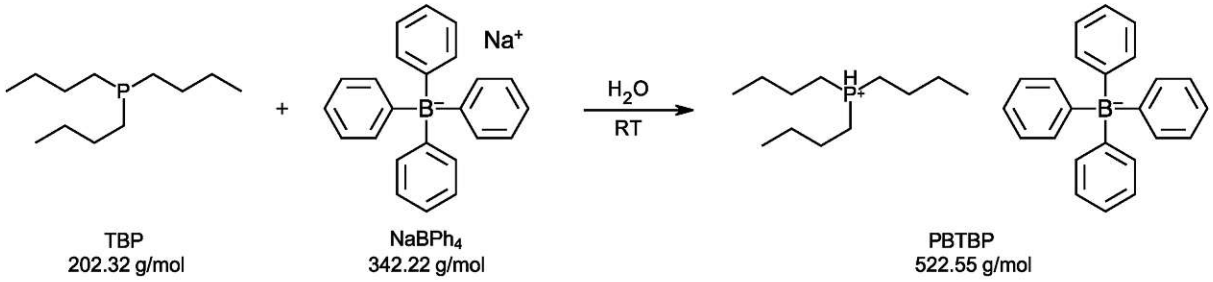

Scheme 32: Reaction of tributylphosphine (TBP) with sodium tetraphenylborate ($NaBPh_4$) in H_2O for at RT

The second approach was conducted in analogy to literature.[112] Therefore, tributylphosphine (1 eq., 1 mmol, 202 mg) was dissolved in 10 mL 10% HCl (aq) under argon atmosphere. An aqueous solution of sodium tetraphenylborate (1 eq., 1 mmol, 342 mg) in 1 mL water was added slowly. After 30 min the white crystalline precipitate was filtered, washed three times with 3 mL water and dried under high vacuum. ^{1}H-NMR and a ^{31}P-NMR in DMSO of the obtained product was measured (Figure S 19 and Figure S 20).

Yield: 407 mg (78% th.)

^{1}H-NMR (400 MHz, DMSO) δ = 7.18 (m, 8H, H^{ar}), 6.92 (t, J = 7.3 Hz, 8H, H^{ar}), 6.79 (t, J = 7.2 Hz, 4H, H^{ar}), 2.21 (s, 6H, P^{+}-*CH_2*-), 1.53 (m, 6H, -CH_2-*CH_2*-CH_2-), 1.40 (m, 6H, -CH_2-*CH_2*-CH_3), 0.91 (t, J = 7.3 Hz, 9H, -CH_2-*CH_3*) ppm.

^{31}P-NMR (162 MHz, DMSO) δ = 12.25 ppm.

2.4.1.3. Synthesis of photo-benzophenone-tributylphosphine salt

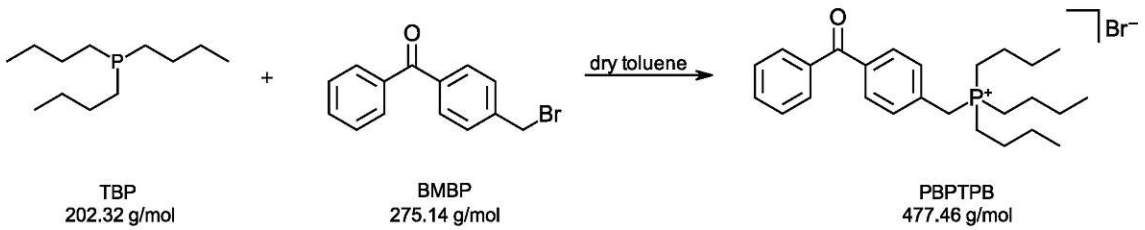

Scheme 33: Reaction of tributylphosphine (TBP) with 4-(bromomethyl)benzophenone in dry toluene for 24 hours at 80 °C

The synthesis was performed under light exclusion, in analogy to literature.[115] Therefore, 4-(bromomethyl)bonzophenone (1 eq., 1.0 mmol, 275 mg) and tributylphosphine (1 eq., 1.0 mmol, 202 mg) was dissolved in 6 mL dry toluene under argon atmosphere and stirred at 80 °C for 24 h. After cooling to room temperature and further cooling with an ice bath the precipitate was filtered and washed tree times with toluene and dried under vacuum. ^{1}H-NMR and ^{31}P-NMR of the white crystalline product were measured (Figure S 21 and Figure S 22).

Yield: 380 mg (79% th.)

^{1}H-NMR (400 MHz, CDCl3) δ = 7.82 – 7.56 (m, 7H, H^{ar}), 7.48 (dd, J = 8.3, 2H, H^{ar}), 4.57 (d, J = 15.8 Hz, 2H, Ar-CH_2-P^+-), 2.50 – 2.38 (m, 6H, -P^+-CH_2-CH_2-), 1.48 (tt, J = 10.5, 12H, -CH_2-CH_2-CH_2-CH_3), 0.97 – 0.89 (m, 9H, -CH_2-CH_3) ppm.

^{31}P-NMR (162 MHz, $CDCl_3$) δ = 31.89 ppm.

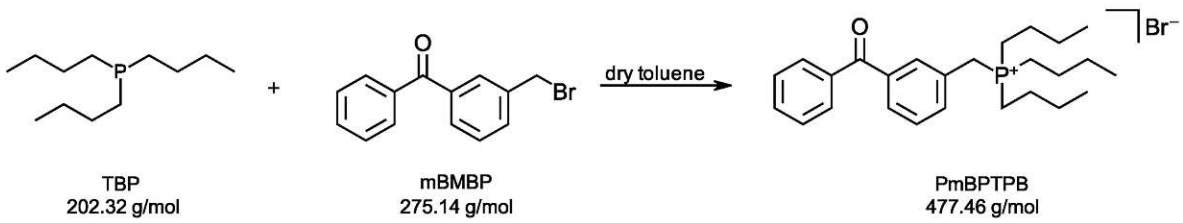

Scheme 34: Reaction of tributylphosphine (TBP) with 3-(bromomethyl)benzophenone in dry toluene for 1 hour at 80 °C

The reaction was conducted under light exclusion, in analogy to literature.[115] Therefore, 3-(bromomethyl)bonzophenone (1 eq., 1.0 mmol, 275 mg) and tributylphosphine (1.5 eq., 1.5 mmol, 304 mg) were dissolved in 5 mL dry toluene under argon atmosphere and stirred at 80 °C for 1 h. After cooling to room temperature and further cooling in an ice bath, the precipitate was filtered, washed tree times with toluene tree times and dried under vacuum. ^{1}H-NMR and ^{31}P-NMR were measured of the white crystalline product (Figure S 23 and Figure S 24).

Yield: 427 mg (89% th.)

^{1}H-NMR (400 MHz, CDCl3) δ = 8.11 (dd, J = 7.9, 1H, H^{ar}), 7.81 – 7.75 (m, 2H, H^{ar}), 7.73 (dq, 1.5 Hz, 1H, H^{ar}), 7.67 – 7.58 (m, 2H, H^{ar}), 7.52 (dt, J = 9.1, 3H, H^{ar}), 4.42 (d, J = 15.2 Hz, 2H, , Ar-*CH_2*-P^+-), 2.50 – 2.38 (m, 6H, -P^+-*CH_2*-CH_2-), 1.47 (dq, J = 6.7, 12H, -CH_2-*CH_2*-*CH_2*-CH_3), 0.97 – 0.89 (m, 9H, -*CH_2*-*CH_3*) ppm.

^{31}P-NMR (162 MHz, $CDCl_3$) δ = 31.99 ppm.

2.5. Photo-dimethylimidazole salts

2.5.1. Synthesis of photo-dimethylimidazole salts

2.5.1.1. Synthesis of photo-keto-dimethylimidazole salts

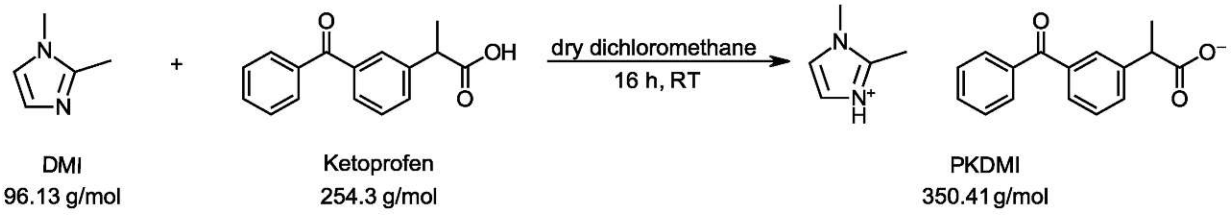

DMI
96.13 g/mol

Ketoprofen
254.3 g/mol

PKDMI
350.41 g/mol

Scheme 35: Reaction of 1,2-dimethylimidazole (DMI) with ketoprofen in dry DCM for 16 hours at RT

The reaction was performed under light exclusion, in analogy to literature.[110] Therefore, ketoprofen (1 eq., 1 mmol, 254 mg) were dissolved in 4 mL dry dichloromethane and 1,2-dimethylimidazole (1 eq., 1 mmol, 96 mg) were added and the solution was stirred under argon atmosphere at ambient temperature for 16 h. The solvent was removed under reduced pressure with a water bath at 40 °C. To remove residual THF form the obtained product, it was dried using the high vacuum pump. ^{1}H-NMR was measured of the clear highly viscous product (Figure S 25).

Yield: 310 mg (89 % of th.)

^{1}H-NMR (400 MHz, $CDCl_3$) δ = 7.80 (d, J = 7.5 Hz, 3H, H^{ar}), 7.60 (dt, J = 28.4, 3H, H^{ar}), 7.44 (dt, J = 15.9, 3H, H^{ar}), 6.93 (s, 1H, N-*CH*=), 6.76 (s, 1H, N^+-*CH*=), 3.55 (s, 3H, N-*CH_3*), 2.39 (s, 3H, C-*CH_3*, DMI), 1.54 (d, J = 7.1 Hz, 3H, C-*CH_3*, KP) ppm.

2.5.1.2. *Synthesis of photo-borate-dimethylimidazole salts*

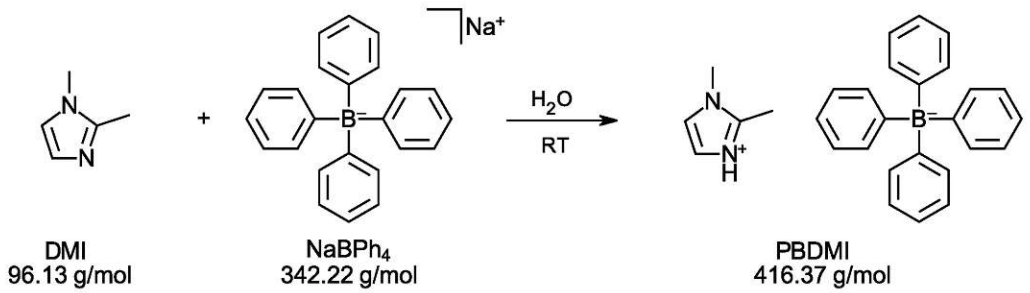

Scheme 36: Reaction of 1,2-dimethylimidazole (DMI) with sodium tetraphenylborate ($NaBPh_4$) in H_2O at room temperature (RT)

The reaction was performed under light exclusion, in analogy to literature.[112] Therefore, 1,2-dimethyl imidazole (1 eq., 1.0 mmol, 202 mg) was dissolved in 2 mL 10% HCL (aq) under argon atmosphere. An aqueous solution of sodium tetraphenylborate (1 eq., 1.0 mmol, 342 mg) in 6 mL water was added slowly. The formed white precipitate was immediately filtered and washed three times with 2 mL water. The precipitate was dried at high vacuum with a water bath at 70 °C. ^{1}H-NMR was measured of the white crystalline product (Figure S 26).

Yield: 261 mg (62 % of th.)

^{1}H-NMR (400 MHz, CDCl3) δ = 7.55 – 7.47 (m, 2H, -N-*CH*-*CH*-N-), 7.33 (ddt, J = 6.6, 4.4, 2.1 Hz, 8H, H^{ar}), 6.92 (t, J = 7.4 Hz, 8H, H^{ar}), 6.81 – 6.72 (m, 4H, H^{ar}), 3.89 (s, 3H, -N-*CH_3*), 2.72 (s, 3H, -C-*CH_3*) ppm.

2.6. Photo-1-(2-ethyl hexyl)-2-butyl-imidazole) salt

2.6.1. *Synthesis of photo-1-(2-ethyl hexyl)-2-butyl-imidazole) salt*

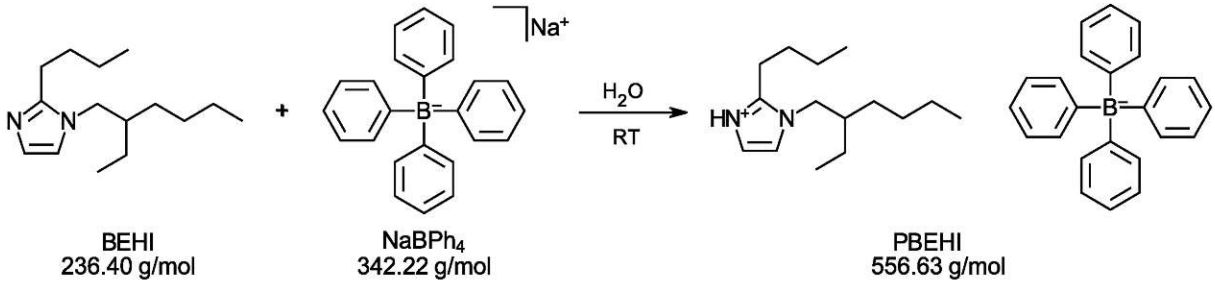

Figure 69: Reaction of 2-butyl-1-ethylhexyl imidazole (BEHI) with sodium tetraphenylborate ($NaBPh_4$) in H_2O at room temperature (RT)

The reaction was performed under light exclusion, in analogy to literature.[112] Therefore, 2-butyl-1-ethylhexyl imidazole (1 eq., 1.0 mmol, 236 mg) was dissolved in 10 mL 10% HCL (aq).

An aqueous solution of sodium tetraphenylborate (1 eq., 1.0 mmol, 342 mg) in 10 mL water was added slowly. The formed white precipitate was immediately filtered and washed three times with 5 mL water. The precipitate was dried at high vacuum with a water bath at 70 °C. ^{1}H-NMR was measured of the white crystalline product (Figure S 27).

Yield: 393 mg (93 % of th.)

^{1}H-NMR (400 MHz, $(CD_3)_2CO$) δ 7.68 (dd, *J* = 14.9, 2.1 Hz, 2H, -N-*CH*-*CH*-N-), 7.33 (m, 8H, H^{ar}), 6.91 (t, *J* = 7.4 Hz, 8H, H^{ar}), 6.77 (ddt, *J* = 8.9, 7.4, 1.6 Hz, 4H, H^{ar}), 4.24 (d, *J* = 7.7 Hz, 2H, -N-C-*CH_2*-CH_2-CH_2-CH_3), 3.23 – 3.14 (m, 2H, -N-*CH_2*-CH-), 1.90 – 1.80 (m, 3H, -N-CH_2-*CH*-, -N-C-CH_2-*CH_2*-CH_2-CH_3), 1.52 – 1.22 (m, 10H,-*CH_2*-), 0.98 – 0.77 (m, 9H,-CH_2-*CH_3*) ppm.

Summary and Conclusion

This work focuses on the investigation of new isocyanate-based high performance materials via photopolymerization. Radiation-based polyisocyanurate formation offers efficient production conditions in curing industries or lithographic additive manufacturing. Time savings, energy efficiency and environmental friendliness are among the advantages of radiation-based chemistry. The resultant polyisocyanurate exhibits outstanding thermal and mechanical properties, potentially opening a new pathway to high-performance materials through photopolymerization.

The catalytic cyclodimerization and cyclotrimerization of phenyl isocyanate and hexyl isocyanate with 1,5-diazabicyclo(4.3.0)non-5-ene (DBN), 1,1,3,3-tetramethylguanidin (TMG), triethylamine (TEA), tributylphosphine (TBP), triphenylphosphine (TPhP), 1,2-dimethyl imidazole (DMI) and 2-butyl-1-ethylhexyl imidazole (BEHI) were investigated (Scheme 37 and Figure 70).

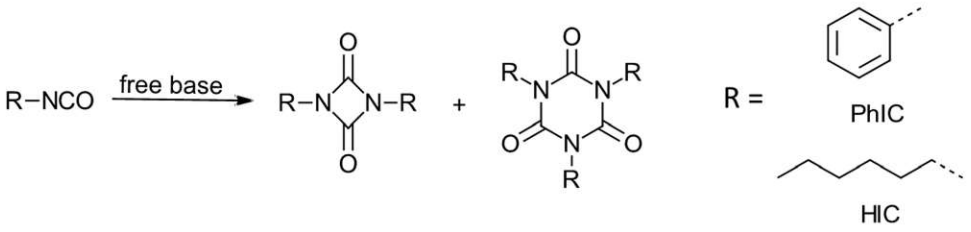

Scheme 37: Reaction of phenyl isocyanate (PhIC) or hexyl isocyanate (HIC) with the free base to obtain the corresponding cyclodimer or cyclotrimer

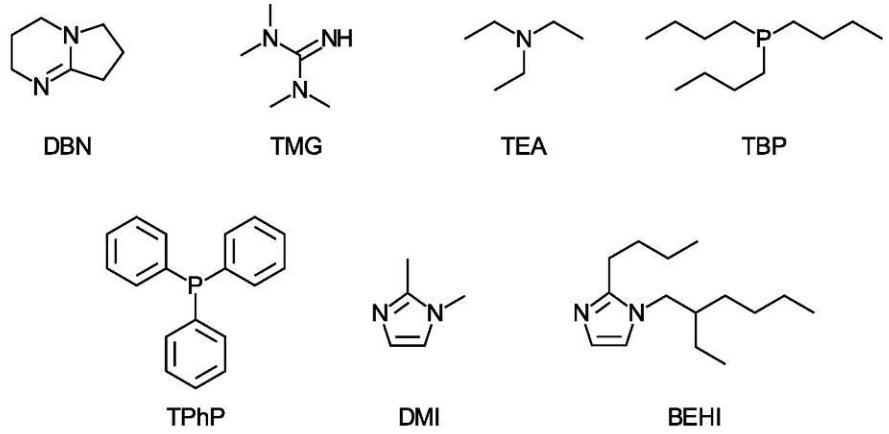

Figure 70: Structures of the free bases used for investigation of the cyclodimerization and cyclotrimerization: 1,5-diazabicyclo(4.3.0)non-5-ene (DBN), 1,1,3,3-tetramethylguanidin (TMG), triethylamine (TEA), tributylphosphine (TBP), triphenylphosphine (TPhP), 1,2-dimethyl imidazole (DMI) and 2-butyl-1-ethylhexyl imidazole (BEHI)

The nitrogen based free base TEA and triarylphosphine TPhP did not catalyse the di- or trimerization reactions. According to NMR-analysis, with TEA no reaction occurs and with

TPhP the hydrolysis of the phenyl isocyanate and hexyl isocyanate to the amines, aniline and hexylamine was proven.

As well the nitrogen based free bases DBN and TMG did not catalyse the di- or trimerization reactions according to the NMR-analysis. The results with the nitrogen based free bases DBN and TMG show adduct formation between one equivalent of DBN or TMG and two equivalents of isocyanate (Scheme 38). This adduct formation facilitate an interesting approach to obtain a photocurable stoichiometric copolymer of isocyanates and DBN or TMG.

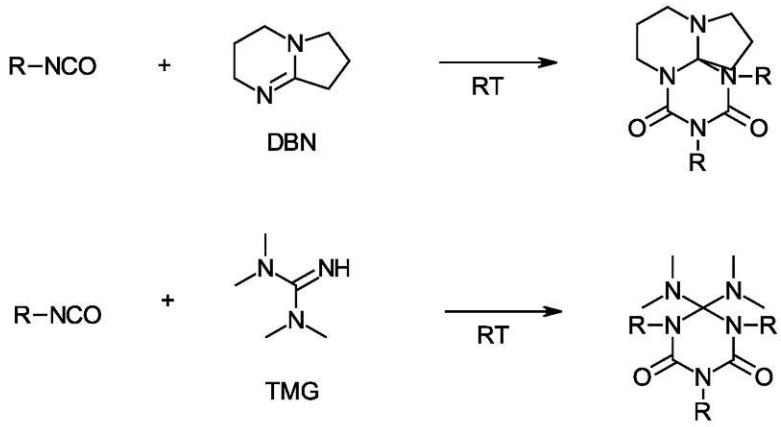

Scheme 38: Adduct formation between DBN or TMG with isocyanates at RT

The experiments with the trialkylphosphine TBP and the imidazole based free bases DMI and BEHI prove the possible cyclodimerization and cyclotrimerization of isocyanates. TBP catalyzes the cyclodimerization and cyclotrimerization of phenyl isocyanate and hexyl isocyanate at ambient temperatures and 60 °C with a catalyst loading of 5 mol% (Scheme 39).

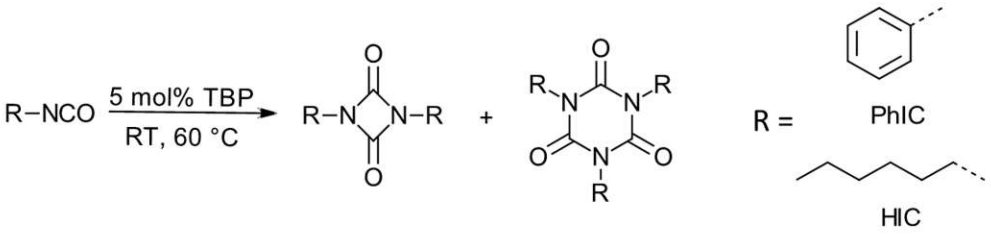

Scheme 39: Cyclodimerization and Cyclotrimerization of phenyl isocyanate and hexyl isocyanate withe 5 mol% TBP at ambient temperatures (RT) and 60 °C

The imidazole based free bases DMI and BEHI catalyzes the cyclodimerization and cyclotrimerization of phenyl isocyanate at ambient temperatures with a catalyst loading of 10 mol% (Scheme 40). Hexyl isocyanate does not show any conversion with 10 mol% DMI. Additionally, the catalytic dimerization and trimerization with the imidazole based free base BEHI was very slow in comparison to the imidazole based free base DMI.

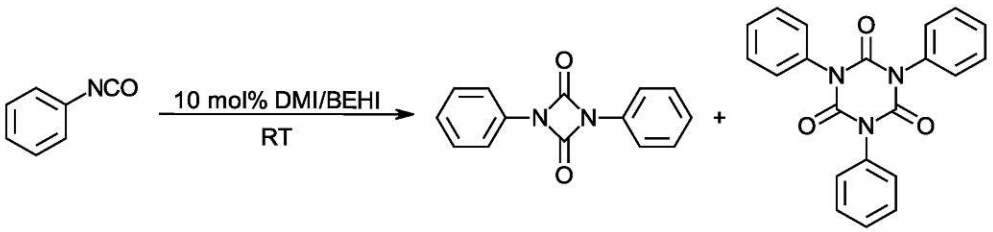

Scheme 40: Cyclodimerization and Cyclotrimerization of phenyl isocyanate withe 10 mol% DMI or BEHI at ambient temperatures (RT).

Whereas the nitrogen based free bases DBN and TMG facilitate a stoichiometric adduct formation of the free base and isocyanates, the trialkylphosphine and imidazole based free bases (TBP, DMI and BEHI) catalyzes a cyclodimerization and cyclotrimerization of isocyanates. To investigate a photochemical approach of the observed reactions, the photobase generators corresponding to the free bases DBN, TMG, TBP, DMI and BEHI were studied about their photoactivity and stability in darkness at elevated temperatures (Figure 71). In contrast to the photobase generator of DBN, which is commercially available, a corresponding photobase generator of TMG, TBP, DMI and BEHI are not commercially available. Therefore the photobase generators of TMG (PKTMG), TBP (PKTBP, PBTBP, p-PBPTBP and m-PBPTBP), DMI (PKDMI and PBDMI) and BEHI (PBEHI) were synthesized.

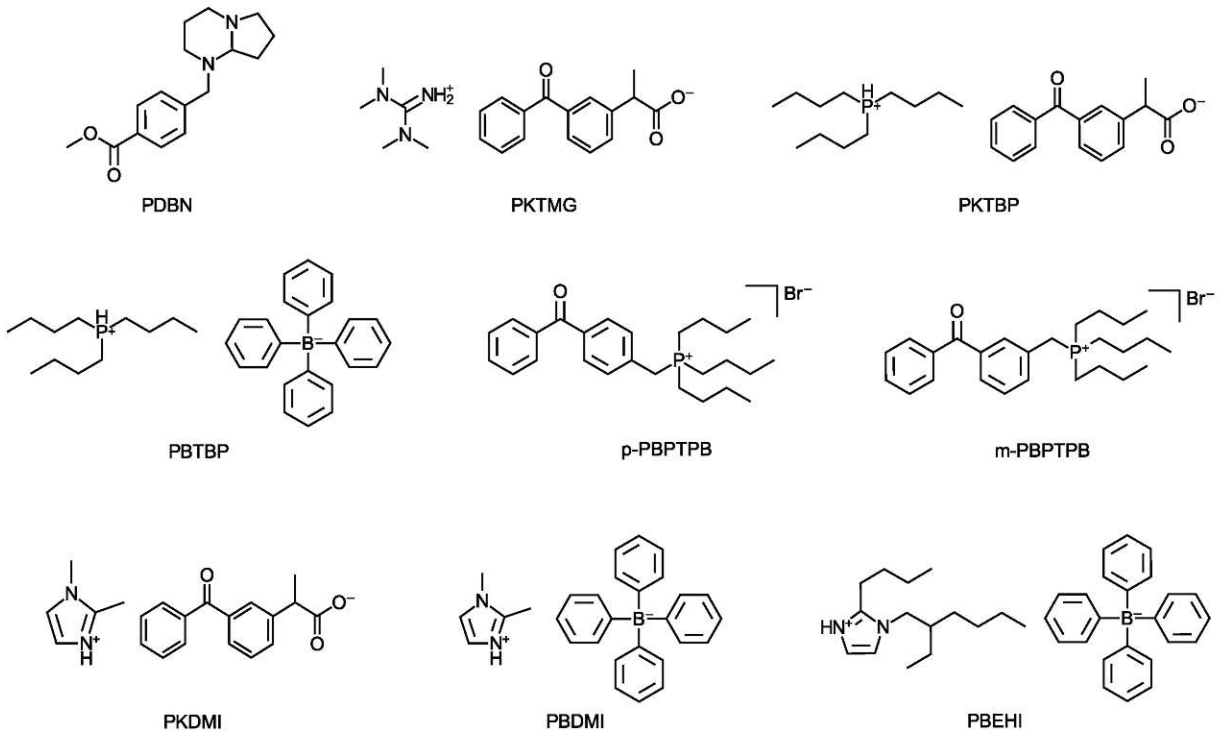

Figure 71: Structures of the photobase generator used for investigation of the photochemical cyclodimerization and cyclotrimerization

The photobase generators corresponding to TBP were synthesized as salts of TBP and ketoprofen, sodium tetraphenylborate or benzophenone. The ^{31}P-NMR analysis of the ketoprofen based PBG of TBP (PKTBP) exhibited impurities and could not be purified further. Therefore the photoactivity and stability of PKTBP was not investigated. The PBG corresponding to TBP with tetraphenylborate (PBTBP) or the two benzophenone based PBG of TBP with substitution in para or meta position (p-PBPTBP and m-PBPTBP) were investigated about their photoactivity and stability. The three PBG derived from TBP do not show any photoactivity according to NMR analysis, and therefore were not suitable for the photocatalytic cyclodimerization and cyclotrimerization of isocyanates.

According to NMR analysis the synthesized ketoprofen based PBG of TMG and DMI (PKDMI, PBDMI) and the tetraphenylborate based PBG of DMI and BEHI (PBDMI, PBEHI) exhibit photoactivity upon irradiation with light. Corresponding to the photoactivity the stability in darkness at elevated temperatures of PKTMG, PKDMI, PBDMI and PBEHI, as well as the commercially available PBG of DBN (PDBN) were investigated.

As concluded from the free base studies, the adduct formation of DBN and TMG with phenyl isocyanate and hexyl isocyanate was investigated in a photochemical approach (Scheme 38). The stability of a stoichiometric reaction mixture of phenyl isocyanate or hexyl isocyanate with the PBG of DBN and the ketoprofen PBG of TMG (PDBN, PKTMG) and 1 mol% ITX were investigated at ambient temperatures. According to NMR analysis PDBN and PKTMG reacts with phenyl isocyanate and hexyl isocyanate even without exposure to light. Corresponding to the occurring dark reaction of PDBN and PKTMG, no stable reaction mixture could be achieved. Accompanying the PBG of DBN and the ketoprofen PBG of TMG are not suitable for a photochemical approach of adduct formation between PDBN or PKTMG with isocyanates.

Further the dark stability studies of a catalytic amount of the ketoprofen based PBG of DMI (PKDMI) in phenyl isocyanate with 50 mol% ITX (in relation to PKDMI) resulted in a dark reaction. Accompanying PKDMI is not suitable for a photochemical cyclodimerization and cyclotrimerization of phenyl isocyanates, corresponding to an instable reaction mixture.

In contrast to the PBG of DBN and the ketoprofen PBG of TMG and DMI (PDBN, PKTMG, PKDMI) the synthesized tetraphenylborate photobase generator PBDMI provided a stable reaction mixture with phenyl isocyanate and 50 mol% ITX (in relation to PBDMI). Although PBDMI was not completely soluble in phenyl isocyanate. Further attempts with a co-solvent to completely dissolve PBDMI were not successful.

To improve the solubility of the tetraphenylborate photobase generator PBDMI, the tetraphenylborate photobase generator PBEHI, which provide longer aliphatic chains and accompanying increased polarity and solubility was synthesized. A reaction mixture with phenyl isocyanate, 10 mol% PBEHI and 50 mol% ITX (in relation to PBEHI) yield a stable reaction mixture over 24 hours at 70 °C. Further the reaction mixture was investigated about the cyclodimerization and cyclotrimerization via exposure to UV light. The irradiated reaction mixture remained liquid and no solidification could be observed. The cyclodimerization and cyclotrimerization with BEHI was a very slow reaction and solidification, which indicated the formation of the cyclodimer or cyclotrimer occurs after one hour. The slow reaction and delayed solidification may be attributed to steric hindrance because of the branched aliphatic substituents on the imidazole ring. This steric hindrance significantly reduces the speed of potential photochemical catalytic cyclodimerization and cyclotrimerization.

Although, the cyclodimerization and cyclotrimerization of isocyanates suitable for potential industrial applications could not be achieved, fundamental knowledge of promising imidazole photobase generators could be obtained. These fundamental knowledge establishes the groundwork for future investigations, to optimize the solubility and the reactivity of imidazole photobase generators suitable for the cyclodimerization and cyclotrimerization of isocyanates.

Reaction mixture preparation protocol for reactivity testing with the free bases: phenyl isocyanate and hexyl isocyanate were distilled before use and maximal five days stored under argon and molecular sieve. Under argon atmosphere at ambient temperatures and via an Eppendorf Pipette, first the isocyanate and immediately the free base was added to a brown glass vail, which was closed off. The brown glass vail was purged with argon prior and after addition of the isocyanate and the free base stored at ambient temperatures without light exclusion.

PBG photoreactivity testing procedure: The photoactivity of the PBGs under UV irradiation were studied via ^{1}H-NMR. The PBG was dissolved in the corresponding NMR solvent under light exclusion. The dissolved PBG were placed in the UV oven and for 2x200 seconds with 100% intensity irradiated with light. To investigate the photoactivity of the PBGs, a ^{1}H-NMR bevor irradiation with light and after irradiation with light were compared.

Dark stability testing procedure: The dark stability studies were performed in the orange lab. The sensitizer ITX was weighted in a prior purged brown glass vail. Further the PBG were weighted in a weighing paper and added to the brown glass vail. At least the isocyanate were added via an Eppendorf Pipette under constant argon flow. After complete addition of all reactants, the brown glass vail was closed off and stored in a metal block with defined temperature.

All commercially available chemicals were used as received unless noted otherwise. Solvents and reagents were purchased at least in 96 % purity and purified according to common organic procedures if noted in the experimental section. Commercial grade methylene chloride (CH_2Cl_2,), toluene, ethanol (EtOH) and tetrahydrofuran (THF, Donau Chemie), were all obtained from Donau Chemie and dried with a PureSolvsystem (Inert, Amesbury, MA).

Orange light lab: all weigh-ins, reactions and measurements of light sensitive substances were carried out in an orange light lab. The windows are laminated with Asmetec metolight SF-UV-foils (type ASR-SF-LY5) and all lamps are of the type Osram lumix with chip controlled light color 62.

UV chamber: A Uvitron International INTELLI-RAY 600 with a Hg broad bond UV lamp (600 W, UV-A: 125 mW/cm², Vis: 125 mW/cm²) was utilized for all photoreactions, unless noted otherwise.

ATR-FTIR was performed on a PerkinElmer Spectrum 65 FT-IR Spectrometer equipped with a Specac MKII Golden Gate Single Reflection ATR System at ambient temperature.

^{1}H-, ^{13}C- and ^{31}P-NMR spectra were measured with a BRUKER Avance DRX-400 FT-NMR spectrometer. The chemical shift was reported in ppm (s = singlet, d = doublet, t = triplet, q = quartet, m = multiplet). Deuterated chloroform ($CDCl_3$, 99.5% deuteration), deuterated benzene (C_6D_6, 99.9% deuteration) deuterated acetone ($(CD_3)_2CO$, 99.8% deuteration) and deuterated DMSO (DMSO-d_6, 99.8% deuteration) were used as solvents. Analysis of the spectra was performed with the software MestrReNova (version number: 14.1.0-24037).

Ultra High Pressure Liquid Chromatography-mass spectroscopy (UHPLC-MS): HPLC analysis was performed on a Nexera X2® UHPLC system (Shimadzu®) comprised of LC- 30AD pumps, SIL-30AC autosampler, CTO-20AC column oven and DGU-20A5/3 degasser module. Detection was done using an SPD-M20A photo diode array, an RF-20Axs fluorescence detector, and ELS-2041 evaporative light scattering detector (JASCO®) and an LC-MS-2020 mass spectrometer (ESI/APCI). If not stated otherwise, all separations were performed using a Waters® XSelect® CSHTM C18 2,5 µm (3.0 x 50 mm) column XP at 40 °C, and a flowrate of 1.7 mL/min with water/acetonitrile + 0.1% formic acid gradient elution.

Silica column chromatography was performed with a Büchi MPLC-system equipped with the control unit C-620, fraction collector C-660, RI detector and UV-photometer C-635. As stationary phase Merck silica gel 60 (0.040-0.063 mm) was used.

Thin Layer Chromatography was carried out by using TL-aluminum foils coated with silica gel (60 F245) from Merck.

References

(1) The introduction was revised with the help of ChatGPT in terms of word choice, grammar and syntax.
(2) Dworak, C., Novel concepts for photoinitiating moieties, Dissertation, 2009.
(3) Abliz, D.; Duan, Y.; Steuernagel, L.; Xie, L.; Li, D.; Ziegmann, G. Curing methods for advanced polymer composites-a review. Polymers and Polymer Composites 2013, 21 (6), 341.
(4) Srivatsan, T.; Sudarshan, T. Additive manufacturing: innovations, advances, and applications. 2015; p: 2-3
(5) Gebhardt, A.; Hötter, J.-S. Additive manufacturing: 3D printing for prototyping and manufacturing; Carl Hanser Verlag GmbH Co KG, 2016; p: 1-43
(6) Awad, R. H.; Habash, S. A.; Hansen, C. J. In 3D Printing Applications in Cardiovascular Medicine; Elsevier, 2018.
(7) Ligon, S. C.; Liska, R.; Stampfl, J. r.; Gurr, M.; Mülhaupt, R. Polymers for 3D printing and customized additive manufacturing. Chemical reviews 2017, 117 (15), 10212.
(8) Bikas, H.; Stavropoulos, P.; Chryssolouris, G. Additive manufacturing methods and modelling approaches: a critical review. The International Journal of Advanced Manufacturing Technology 2016, 83, 389.
(9) Han, D.; Lee, H. Recent advances in multi-material additive manufacturing: methods and applications. Current Opinion in Chemical Engineering 2020, 28, 158.
(10) Pfaffinger, M. Hot Lithography–New Possibilities in Polymer 3D Printing: A newly developed stereolithography-based additive manufacturing technology combines good material properties with outstanding manufacturing precision. Laser Technik Journal 2018, 15 (4), 45.
(11) Steyrer, B.; Neubauer, P.; Liska, R.; Stampfl, J. Visible light photoinitiator for 3D-printing of tough methacrylate resins. Materials 2017, 10 (12), 1445.
(12) Husár, B.; Hatzenbichler, M.; Mironov, V.; Liska, R.; Stampfl, J.; Ovsianikov, A. In Biomaterials for Bone Regeneration; Elsevier, 2014.
(13) Husár, B.; Heller, C.; Schwentenwein, M.; Mautner, A.; Varga, F.; Koch, T.; Stampfl, J.; Liska, R. Biomaterials based on low cytotoxic vinyl esters for bone replacement application. Journal of Polymer Science Part A: Polymer Chemistry 2011, 49 (23), 4927.
(14) Fouassier, J.; Allonas, X.; Burget, D. Photopolymerization reactions under visible lights: principle, mechanisms and examples of applications. Progress in organic coatings 2003, 47 (1), 16.
(15) Fouassier, J.-P.; Lalevée, J. Photoinitiators for polymer synthesis: scope, reactivity, and efficiency; John Wiley & Sons, 2012; p: XXV-XXVIII
(16) Kirchmayr, R.; Berner, G.; Rist, G. Photoinitiators for UV curing of paints. Farbe und Lack 1980, 86 (3), 224.
(17) Mautner, A., Technische Universität Wien, Development of low cytotoxic Photopolymers, Dissertation, 2012.
(18) Peer, G.; Dorfinger, P.; Koch, T.; Stampfl, J. r.; Gorsche, C.; Liska, R. Photopolymerization of cyclopolymerizable monomers and their application in hot lithography. Macromolecules 2018, 51 (22), 9344.
(19) Kaur, M.; Srivastava, A. Photopolymerization: A review. Journal of Macromolecular Science, Part C: Polymer Reviews 2002, 42 (4), 481.
(20) Saleh, T. Polymer science and polymerization methods toward hybrid materials. Polymer Hybrid Materials and Nano-Composites; Elsevier: Amsterdam, The Netherlands 2021, 59.
(21) Dellago, B., Technische Universität Wien, Toughness enhancing additives for additive manufactured bone replacement materials, Dissertation, 2023.
(22) Schörpf, S., Technische Universität Wien, Novel monomers with stress relaxing and shrinkage reducing characteristics for dental restorations, Dissertation, 2020.
(23) Ravve, A.; Ravve, A. Ionic Chain-Growth Polymerization. Principles of Polymer Chemistry 2012, p: 151-251.
(24) Yilmaz, G.; Yagci, Y. Light-induced step-growth polymerization. Progress in Polymer Science 2020, 100, 101178.
(25) Suyama, K.; Shirai, M. Photobase generators: Recent progress and application trend in polymer systems. Progress in Polymer Science 2009, 34 (2), 194.
(26) Zivic, N.; Kuroishi, P. K.; Dumur, F.; Gigmes, D.; Dove, A. P.; Sardon, H. Recent advances and challenges in the design of organic photoacid and photobase generators for polymerizations. Angewandte Chemie International Edition 2019, 58 (31), 10410.

(27) Cameron, J. F.; Frechet, J. M. Base catalysis in Imaging Materials. 1. Design and synthesis of novel light-sensitive urethanes as photoprecursors of amines. The Journal of Organic Chemistry 1990, 55 (23), 5919.
(28) Zivic, N.; Kuroishi, P. K.; Dumur, F.; Gigmes, D.; Dove, A. P.; Sardon, H. Recent Advances and Challenges in the Design of Organic Photoacid and Photobase Generators for Polymerizations. Angew Chem Int Ed Engl 2019, 58 (31), 10410.
(29) Lopez de Pariza, X.; Varela, O.; Catt, S. O.; Long, T. E.; Blasco, E.; Sardon, H. Recyclable photoresins for light-mediated additive manufacturing towards Loop 3D printing. Nature Communications 2023, 14 (1), 5504.
(30) GmbH., F. W. C. E.; FUJIFILM, https://specchem-wako.fujifilm.com/europe/en/photo-base-generators/index.htm.
(31) Hergenrother, P. M. The use, design, synthesis, and properties of high performance/high temperature polymers: an overview. High Performance Polymers 2003, 15 (1), 3.
(32) Al Christopher, C.; da Silva, Í. G.; Pangilinan, K. D.; Chen, Q.; Caldona, E. B.; Advincula, R. C. High performance polymers for oil and gas applications. Reactive and Functional Polymers 2021, 162, 104878.
(33) GmbH, K., https://krempel.com/de/produkte/elektroisolierstoffe/kapton-folien#:~:text=Kapton%C2%AE%2DPolyimidfolien%20zeichnen%20sich,hohe%20Best%C3%A4ndigkeit%20gegen%C3%BCber%20Koronaentladungen%20auf.
(34) Dupont, https://www.dupont.de/kevlar/what-is-kevlar.html.
(35) Krause, E.; Yang, G.; Sessler, G. Charge dynamics and morphology of Ultem 1000 and Ultem 5000 PEI grade films. Polymer international 1998, 46 (1), 59.
(36) Kunststofftechnik, P., https://www.polytron-gmbh.de/ultem-pei.aspx.
(37) Liaw, D.-J.; Wang, K.-L.; Huang, Y.-C.; Lee, K.-R.; Lai, J.-Y.; Ha, C.-S. Advanced polyimide materials: Syntheses, physical properties and applications. Progress in Polymer Science 2012, 37 (7), 907.
(38) Sezer Hicyilmaz, A.; Celik Bedeloglu, A. Applications of polyimide coatings: A review. SN Applied Sciences 2021, 3, 1.
(39) Plenco, https://www.plenco.com/phenolic-novolac-resol-resins.htm.
(40) Asim, M.; Saba, N.; Jawaid, M.; Nasir, M.; Pervaiz, M.; Alothman, O. Y. A review on phenolic resin and its composites. Current Analytical Chemistry 2018, 14 (3), 185.
(41) Delebecq, E.; Pascault, J.-P.; Boutevin, B.; Ganachaud, F. On the versatility of urethane/urea bonds: reversibility, blocked isocyanate, and non-isocyanate polyurethane. Chemical reviews 2013, 113 (1), 80.
(42) Islam, M. R.; Beg, M. D. H.; Jamari, S. S. Development of vegetable-oil-based polymers. Journal of applied polymer science 2014, 131 (18).
(43) Zia, K. M.; Bhatti, H. N.; Bhatti, I. A. Methods for polyurethane and polyurethane composites, recycling and recovery: A review. Reactive and functional polymers 2007, 67 (8), 675.
(44) Chattopadhyay, D. K.; Raju, K. Structural engineering of polyurethane coatings for high performance applications. Progress in polymer science 2007, 32 (3), 352.
(45) Szycher, M. Szycher's handbook of polyurethanes; CRC press, 1999; pp: 11-3
(46) Akindoyo, J. O.; Beg, M.; Ghazali, S.; Islam, M.; Jeyaratnam, N.; Yuvaraj, A. Polyurethane types, synthesis and applications–a review. Rsc Advances 2016, 6 (115), 114453.
(47) More, A. S.; Lebarbé, T.; Maisonneuve, L.; Gadenne, B.; Alfos, C.; Cramail, H. Novel fatty acid based di-isocyanates towards the synthesis of thermoplastic polyurethanes. European Polymer Journal 2013, 49 (4), 823.
(48) Palaskar, D. V.; Boyer, A.; Cloutet, E.; Alfos, C.; Cramail, H. Synthesis of biobased polyurethane from oleic and ricinoleic acids as the renewable resources via the AB-type self-condensation approach. Biomacromolecules 2010, 11 (5), 1202.
(49) Claeys, B.; Vervaeck, A.; Hillewaere, X. K.; Possemiers, S.; Hansen, L.; De Beer, T.; Remon, J. P.; Vervaet, C. Thermoplastic polyurethanes for the manufacturing of highly dosed oral sustained release matrices via hot melt extrusion and injection molding. European Journal of Pharmaceutics and Biopharmaceutics 2015, 90, 44.
(50) Johnson, T. J.; Gupta, K. M.; Fabian, J.; Albright, T. H.; Kiser, P. F. Segmented polyurethane intravaginal rings for the sustained combined delivery of antiretroviral agents dapivirine and tenofovir. European Journal of Pharmaceutical Sciences 2010, 39 (4), 203.
(51) Rogers, M. E.; Long, T. E.; Turner, S. R. Introduction to Synthetic Methods in Step-Growth Polymers. Synthetic Methods in Step-Growth Polymers 2003, p: 1-16.
(52) Datta, J.; Kasprzyk, P. Thermoplastic polyurethanes derived from petrochemical or renewable resources: A comprehensive review. Polymer Engineering & Science 2018, 58 (S1), E14.

(53) Viney, C. In Structural Biological Materials (Edited by M. Elices), Pergamon/Elsevier Science, Oxford, 2000, 2000.
(54) Cinelli, P.; Anguillesi, I.; Lazzeri, A. Green synthesis of flexible polyurethane foams from liquefied lignin. European Polymer Journal 2013, 49 (6), 1174.
(55) Energie, W., 2022, https://positionen.wienenergie.at/grafiken/energieverbrauch-eu-haushalte/.
(56) Chen, T.; Qiu, J.; Zhu, K.; Li, J. Electro-mechanical performance of polyurethane dielectric elastomer flexible micro-actuator composite modified with titanium dioxide-graphene hybrid fillers. Materials & Design 2016, 90, 1069.
(57) Maamoun, A. A.; Barakat, M. A. Y.; El-Wakil, A. E.-A. A.; Zulfiqar, S.; Oghenekohwo, V. J. Valorization of eggshell waste in designing flexible polyurethane-based piezoelectric composite materials for ultrasonic transducers. Journal of Polymer Research 2023, 30 (7), 286.
(58) Modesti, M.; Lorenzetti, A. An experimental method for evaluating isocyanate conversion and trimer formation in polyisocyanate–polyurethane foams. European Polymer Journal 2001, 37 (5), 949.
(59) Modesti, M.; Lorenzetti, A. Flame retardancy of polyisocyanurate–polyurethane foams: use of different charring agents. Polymer Degradation and Stability 2002, 78 (2), 341.
(60) Driest, P. J.; Dijkstra, D. J.; Stamatialis, D.; Grijpma, D. W. The Trimerization of Isocyanate-Functionalized Prepolymers: An Effective Method for Synthesizing Well-Defined Polymer Networks. Macromolecular rapid communications 2019, 40 (9), 1800867.
(61) Qian, X.; Liu, Q.; Zhang, L.; Li, H.; Liu, J.; Yan, S. Synthesis of reactive DOPO-based flame retardant and its application in rigid polyisocyanurate-polyurethane foam. Polymer Degradation and Stability 2022, 197, 109852.
(62) Samborska-Skowron, R.; Balas, A. An overview of developments in poly (urethane-isocyanurates) elastomers. Polymers for Advanced Technologies 2002, 13 (9), 653.
(63) Špirkova, M.; Budinski-Simendic, J.; Ilavský, M.; Špaček, P.; Dušek, K. Formation of poly (urethane-isocyanurate) networks from poly (oxypropylene) diols and diisocyanate. Polymer bulletin 1993, 31, 83.
(64) Brocas, A.-L.; Mantzaridis, C.; Tunc, D.; Carlotti, S. Polyether synthesis: From activated or metal-free anionic ring-opening polymerization of epoxides to functionalization. Progress in Polymer Science 2013, 38 (6), 845.
(65) Bailosky, L. C.; Bender, L. M.; Bode, D.; Choudhery, R. A.; Craun, G. P.; Gardner, K. J.; Michalski, C. R.; Rademacher, J. T.; Stella, G. J.; Telford, D. J. Synthesis of polyether polyols with epoxidized soy bean oil. Progress in Organic Coatings 2013, 76 (12), 1712.
(66) Mishra, A. K.; Valodkar, M. C.; Patel, A. M.; Sanchapara, N. K.; Vaishnav, P. B. Synthesis of Polyester Polyol from Cyclohexanone plant wash water. Materials Today: Proceedings 2023, 77, 136.
(67) Shelke, N. B.; Nagarale, R. K.; Kumbar, S. G. In Natural and Synthetic Biomedical Polymers; Elsevier, 2014.
(68) Saunders, J.; Slocombe, R. The chemistry of the organic isocyanates. Chemical reviews 1948, 43 (2), 203.
(69) Rafiee, Z.; Keshavarz, V. Synthesis and characterization of polyurethane/microcrystalline cellulose bionanocomposites. Progress in Organic Coatings 2015, 86, 190.
(70) Zia, K. M.; Anjum, S.; Zuber, M.; Mujahid, M.; Jamil, T. Synthesis and molecular characterization of chitosan based polyurethane elastomers using aromatic diisocyanate. International journal of biological macromolecules 2014, 66, 26.
(71) Prisacariu, C. Polyurethane elastomers: from morphology to mechanical aspects; Springer Science & Business Media, 2011; pp: viii
(72) Ionescu, M. Chemistry and technology of polyols for polyurethanes; iSmithers Rapra Publishing, 2005; pp: 477
(73) Madbouly, S. A.; Otaigbe, J. U. Recent advances in synthesis, characterization and rheological properties of polyurethanes and POSS/polyurethane nanocomposites dispersions and films. Progress in polymer science 2009, 34 (12), 1283.
(74) Vermette, P.; Griesser, H. J.; Laroche, G.; Guidoin, R. Biomedical applications of polyurethanes; Landes Bioscience Georgetown, TX, 2001; pp: 8
(75) Howard, G. T. Biodegradation of polyurethane: a review. International Biodeterioration & Biodegradation 2002, 49 (4), 245.
(76) Romaškevič, T.; Budrienė, S.; Pielichowski, K.; Pielichowski, J. Application of polyurethane-based materials for immobilization of enzymes and cells: a review. Chemija 2006, 17 (4), 74.
(77) Golling, F. E.; Pires, R.; Hecking, A.; Weikard, J.; Richter, F.; Danielmeier, K.; Dijkstra, D. Polyurethanes for coatings and adhesives–chemistry and applications. Polymer International 2019, 68 (5), 848.
(78) Guo, Y.; Muuronen, M.; Lucas, F.; Sijbesma, R. P.; Tomović, Ž. Catalysts for Isocyanate Cyclotrimerization. ChemCatChem 2023, e202201362.

(79) Siebert, M.; Sure, R.; Deglmann, P.; Closs, A. C.; Lucas, F.; Trapp, O. Mechanistic investigation into the acetate-initiated catalytic Trimerization of aliphatic isocyanates: a bicyclic ride. The Journal of Organic Chemistry 2020, 85 (13), 8553.
(80) Wu, L.; Liu, W.; Ye, J.; Cheng, R. Fast cyclotrimerization of a wide range of isocyanates to isocyanurates over acid/base conjugates under bulk conditions. Catalysis Communications 2020, 145, 106097.
(81) Zeng, J.; Yang, Y.; Tang, Y.; Xu, X.; Chen, X.; Li, G.; Chen, K.; Li, H.; Ouyang, P.; Tan, W. Synthesis, monomer removal, modification, and coating performances of biobased pentamethylene diisocyanate isocyanurate trimers. Industrial & Engineering Chemistry Research 2022, 61 (6), 2403.
(82) Dekamin, M. G.; Varmira, K.; Farahmand, M.; Sagheb-Asl, S.; Karimi, Z. Organocatalytic, rapid and facile cyclotrimerization of isocyanates using tetrabutylammonium phthalimide-N-oxyl and tetraethylammonium 2-(carbamoyl) benzoate under solvent-free conditions. Catalysis Communications 2010, 12 (3), 226.
(83) Kogon, I. New Reactions of Phenyl Isocyanate and Ethyl Alcohol1. Journal of the American Chemical Society 1956, 78 (19), 4911.
(84) Musin, B. Synthesis of N-aminosulfenylcarbamates. Russian Journal of General Chemistry 2000, 70 (2), 271.
(85) Moghaddam, F. M.; Koozehgiri, G. R.; Dekamin, M. G. Solvent-free efficient synthesis of symmetrical isocyanurates by a combination catalyst: Sodium saccharin and tetrabutylammonium iodide. Monatshefte für Chemie/Chemical Monthly 2004, 135, 849.
(86) Moghaddam, F. M.; Dekamin, M. G.; Khajavi, M. S.; Jalili, S. Efficient and selective trimerization of aryl and alkyl isocyanates catalyzed by sodium p-toluenesulfinate in the presence of TBAI in a solvent-free condition. Bulletin of the Chemical Society of Japan 2002, 75 (4), 851.
(87) Dekamin, M. G.; Mallakpour, S.; Ghassemi, M. Sulfate catalysed multicomponent cyclisation reaction of aryl isocyanates under green conditions. Journal of Chemical Research 2005, 2005 (3), 177.
(88) Dekamin, M. G.; Mallakpour, S.; Ghassemi, M. Combination of sulfite anion and phase transfer catalysts for green cyclotrimerization of aryl isocyanates. Synthetic communications 2005, 35 (3), 427.
(89) Khajavi, M. S.; Dakamin, M. G.; Hazarkhani, H. Solvent-free cyclotrimerization of isocyanates catalysed by sodium or potassium piperidinedithiocarbamate or nitrite under conventional or microwave heating: preparation of aryl or alkyl isocyanurates. Journal of Chemical Research 2000, 2000 (3), 145.
(90) Nambu, Y.; Endo, T. Synthesis of novel aromatic isocyanurates by the fluoride-catalyzed selective trimerization of isocyanates. The Journal of Organic Chemistry 1993, 58 (7), 1932.
(91) Tang, J. S.; Verkade, J. G. [P (MeNCH2CH2) 3N] as a Superior Catalyst for the Conversion of Isocyanates to Isocyanurates. Angewandte Chemie International Edition in English 1993, 32 (6), 896.
(92) Tang, J.; Mohan, T.; Verkade, J. G. Selective and efficient syntheses of perhydro-1, 3, 5-triazine-2, 4, 6-triones and carbodiimides from isocyanates using ZP (MeNCH2CH2) 3N catalysts. The Journal of Organic Chemistry 1994, 59 (17), 4931.
(93) Raders, S. M.; Verkade, J. G. An electron-rich proazaphosphatrane for isocyanate trimerization to isocyanurates. The Journal of Organic Chemistry 2010, 75 (15), 5308.
(94) Pusztai, Z.; Vlád, G.; Bodor, A.; Horváth, I. T.; Laas, H. J.; Halpaap, R.; Richter, F. U. In Situ NMR Spectroscopic Observation of a Catalytic Intermediate in Phosphine-Catalyzed Cyclo-Oligomerization of Isocyanates. Angewandte Chemie International Edition 2006, 45 (1), 107.
(95) Duong, H. A.; Cross, M. J.; Louie, J. N-Heterocyclic carbenes as highly efficient catalysts for the cyclotrimerization of isocyanates. organic letters 2004, 6 (25), 4679.
(96) Pawar, G. M.; Buchmeiser, M. R. Polymer-Supported, Carbon Dioxide-Protected N-Heterocyclic Carbenes: Synthesis and Application in Organo-and Organometallic Catalysis. Advanced Synthesis & Catalysis 2010, 352 (5), 917.
(97) Li, C.; Zhao, W.; He, J.; Zhang, Y. Highly efficient cyclotrimerization of isocyanates using N-heterocyclic olefins under bulk conditions. Chemical Communications 2019, 55 (83), 12563.
(98) Giuglio-Tonolo, A. G.; Spitz, C.; Terme, T.; Vanelle, P. An expeditious method for the selective cyclotrimerization of isocyanates initiated by TDAE. Tetrahedron Letters 2014, 55 (16), 2700.
(99) Richter, R.; Ulrich, H. Four-Membered Rings Containing Two Nitrogen Heteroatoms. Chemistry of Heterocyclic Compounds 1983, 42, pp: 524
(100) Schwetlick, K.; Noack, R. Kinetics and catalysis of consecutive isocyanate reactions. Formation of carbamates, allophanates and isocyanurates. Journal of the Chemical Society, Perkin Transactions 2 1995, (2), 395.
(101) Taguchi, Y.; Shibuya, I.; Yasumoto, M.; Tsuchiya, T.; Yonemoto, K. The synthesis of isocyanurates on the trimerization of isocyanates under high pressure. Bulletin of the Chemical Society of Japan 1990, 63 (12), 3486.

(102) Helberg, J.; Oe, Y.; Zipse, H. Mechanistic Analysis and Characterization of Intermediates in the Phosphane-Catalyzed Oligomerization of Isocyanates. Chemistry–A European Journal 2018, 24 (54), 14387.
(103) QUELL, A., THOMAS, HAns-Josef, ELING, Berend, 2022.
(104) Spectral Database for Organic Compounds SDBS, https://sdbs.db.aist.go.jp/sdbs/cgi-bin/direct_frame_top.cgi.
(105) Polenz, I.; Laue, A.; Uhrin, T.; Rueffer, T.; Lang, H.; Schmidt, F.; Spange, S. Thermally cleavable imine base/isocyanate adducts and oligomers suitable as initiators for radical homo-and copolymerization. Polymer Chemistry 2014, 5 (23), 6678.
(106) Helberg, J.; Oe, Y.; Zipse, H. Mechanistic Analysis and Characterization of Intermediates in the Phosphane-Catalyzed Oligomerization of Isocyanates. Chemistry 2018, 24 (54), 14387.
(107) Cai, J.; Liu, J.; Mu, S.; Liu, J.; Hong, J.; Zhou, X.; Ma, Q.; Shi, L. Corrosion inhibition effect of three imidazolium ionic liquids on carbon steel in chloride contaminated environment. International Journal of Electrochemical Science 2020, 15 (2), 1287.
(108) Dakin, J. M.; Whitney, R. A.; Parent, J. S. Imidazolium Bromide Derivatives of Brominated Poly (isobutylene-co-para-methylstyrene): Synthesis of Peroxide-Curable Ionomeric Elastomers. Industrial & Engineering Chemistry Research 2014, 53 (45), 17527.
(109) Li, J.-X.; Liu, L.; Liu, A.-H. Study on synthesis and photoactivity of N-substituted diazabicyclononane derivatives with different substituents. International Journal of Adhesion and Adhesives 2015, 57, 118.
(110) Arimitsu, K.; Endo, R. Application to photoreactive materials of photochemical generation of superbases with high efficiency based on photodecarboxylation reactions. Chemistry of Materials 2013, 25 (22), 4461.
(111) Blake, J. A.; Gagnon, E.; Lukeman, M.; Scaiano, J. Photodecarboxylation of xanthone acetic acids: C– C bond heterolysis from the singlet excited state. Organic letters 2006, 8 (6), 1057.
(112) Zhang, X.; Wang, X.; Chatani, S.; Bowman, C. N. Phosphonium Tetraphenylborate: A Photocatalyst for Visible-Light-Induced, Nucleophile-Initiated Thiol-Michael Addition Photopolymerization. ACS Macro Letters 2020, 10 (1), 84.
(113) Catt, S. O.; Long, T. E.; Blasco, E.; Sardon, H. Loop 3D printing: recyclable photoresins for light-mediated additive manufacturing. 2023.
(114) Elliott, L. D.; Kayal, S.; George, M. W.; Booker-Milburn, K. Rational design of triplet sensitizers for the transfer of excited state photochemistry from UV to visible. Journal of the American Chemical Society 2020, 142 (35), 14947.
(115) Sugiura, T.; Yajima, D.; Shoji, K.; Ohta, Y.; Yokozawa, T. Control of chain ends of polyesters in polycondensation of AA and BB monomers by use of solid-phase reagent. Journal of Polymer Science Part A: Polymer Chemistry 2015, 53 (11), 1379.

Appendix

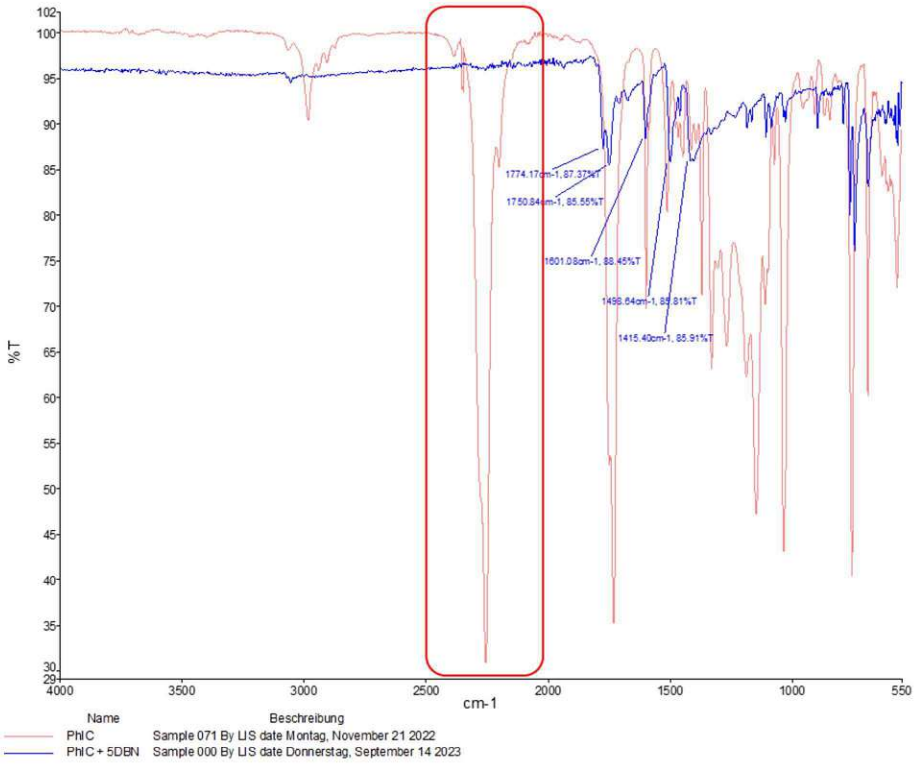

Figure S 1: ATR-FTIR of phenyl isocyanate (PhIC, orange) and reaction mixture with phenyl isocyanate and 5 mol% 1,5-diazabicyclo[4.3.0]non-5-ene (DBN) at ambient temperatures (blue). The isocyanate vibration at 2260 cm^{-1} is enframed in red.

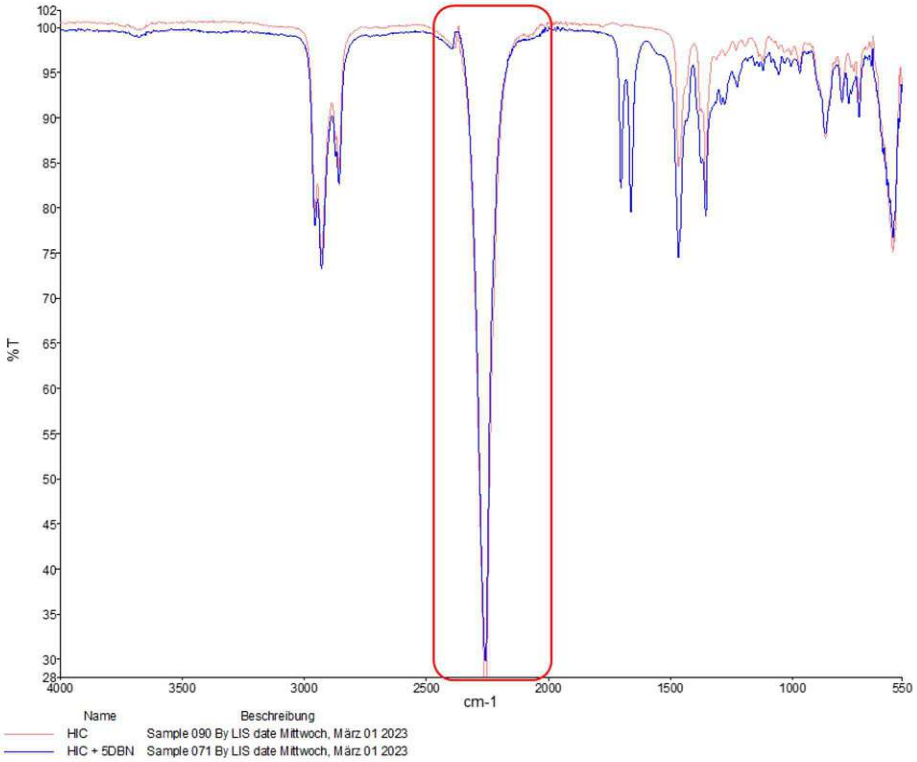

Figure S 2: ATR-FTIR of hexyl isocyanate (HIC, orange) and reaction mixture with hexyl isocyanate and 5 mol% 1,5-diazabicyclo[4.3.0]non-5-ene (DBN) at ambient temperatures (blue). The isocyanate vibration at 2260 cm^{-1} is enframed in red.

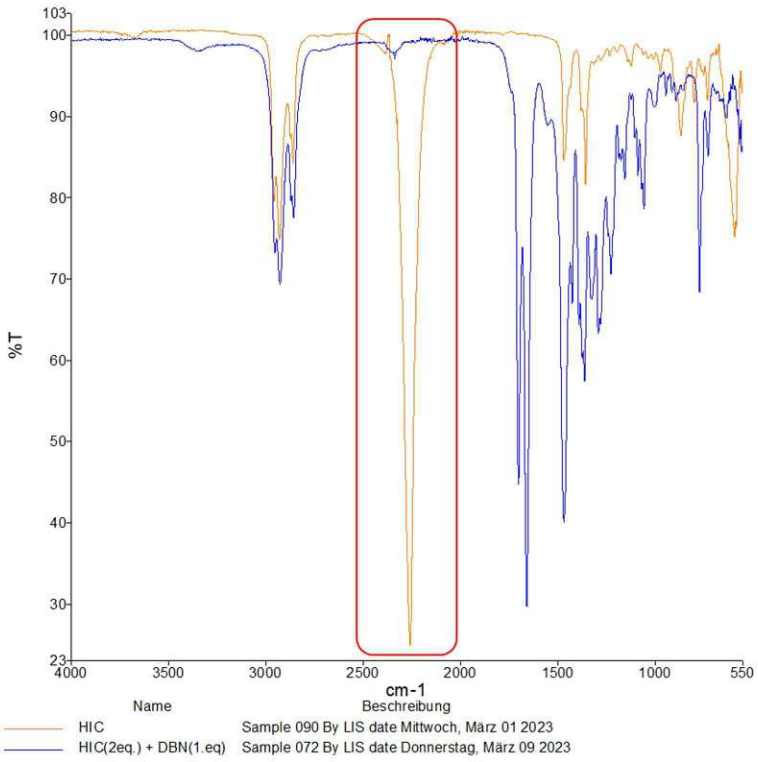

Figure S 3: ATR-FTIR of hexyl isocyanate (HIC, orange) and reaction mixture with 2 eq. hexyl isocyanate and 1 eq. 1,5-diazabicyclo[4.3.0]non-5-ene (DBN) at ambient temperatures (blue). The isocyanate vibration at 2260 cm-1 is enframed in red.

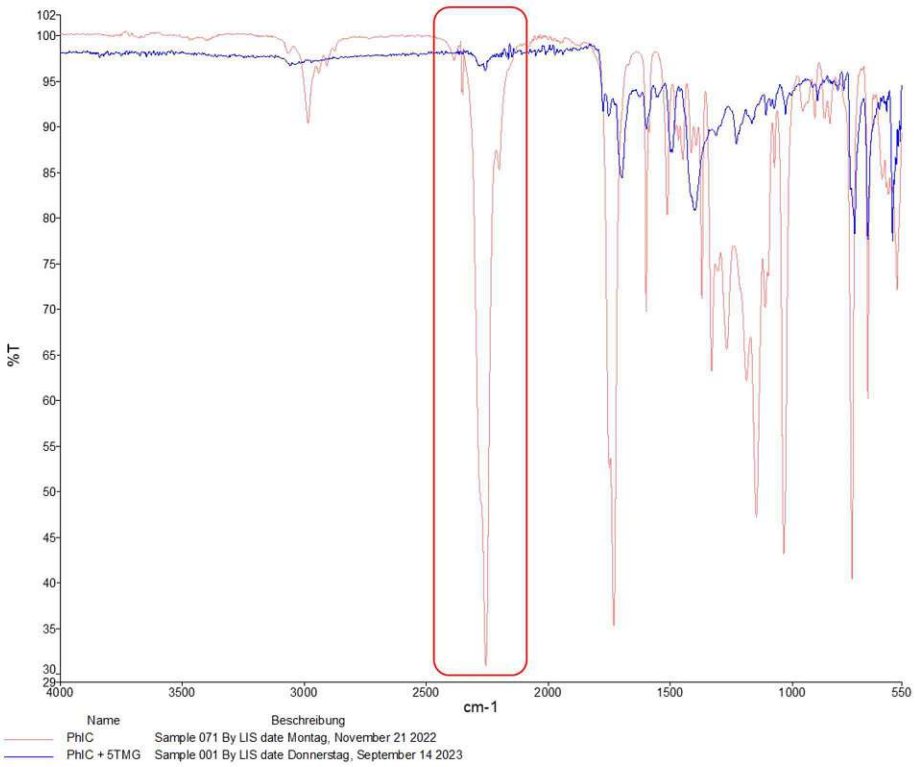

Figure S 4: ATR-FTIR of phenyl isocyanate (PhIC, orange) and reaction mixture with phenyl isocyanate and 5 mol% tetramethyl guanidine (TMG) at ambient temperatures (blue). The isocyanate vibration at 2260 cm^{-1} is enframed in red.

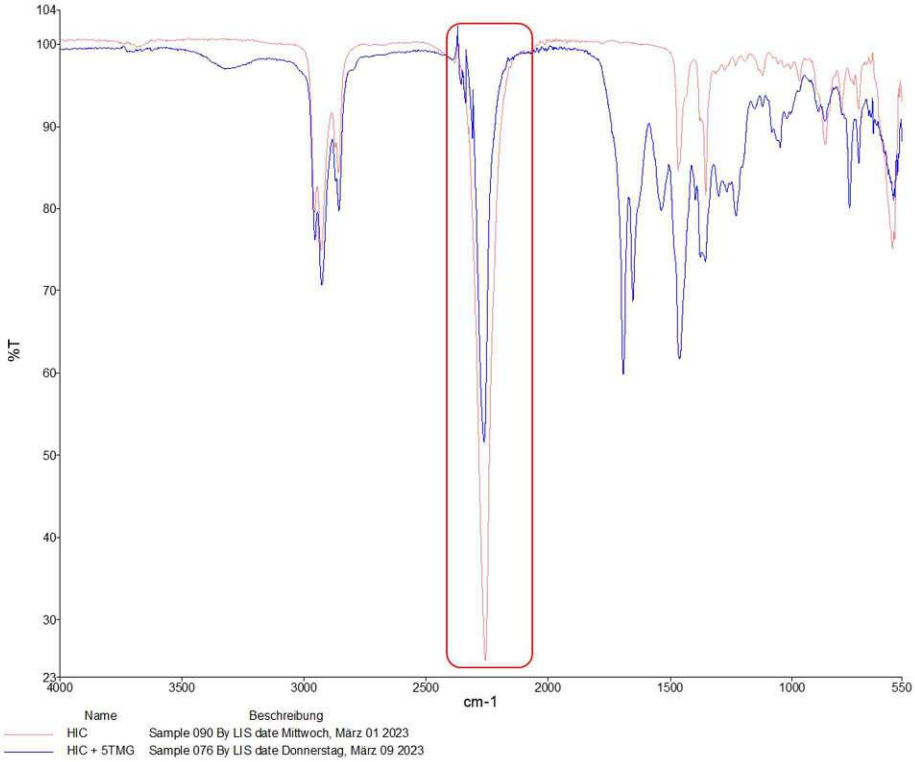

Figure S 5: ATR-FTIR of hexyl isocyanate (HIC, orange) and reaction mixture with hexyl isocyanate and 5 mol% tetramethyl guanidine (TMG) at ambient temperatures (blue). The isocyanate vibration at 2260 cm^{-1} is enframed in red.

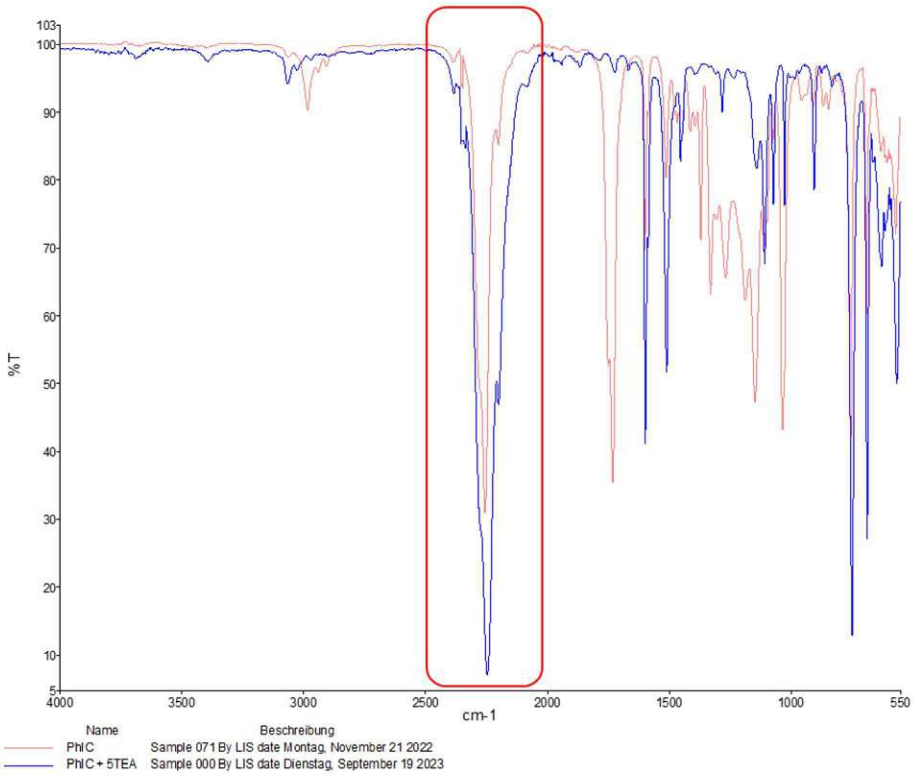

Figure S 6: ATR -FTIR of phenyl isocyanate (PhIC, orange) and reaction mixture with phenyl isocyanate and 5 mol triethylamine (TEA) at ambient temperatures (blue). The isocyanate vibration at 2260 cm^{-1} is enframed in red.

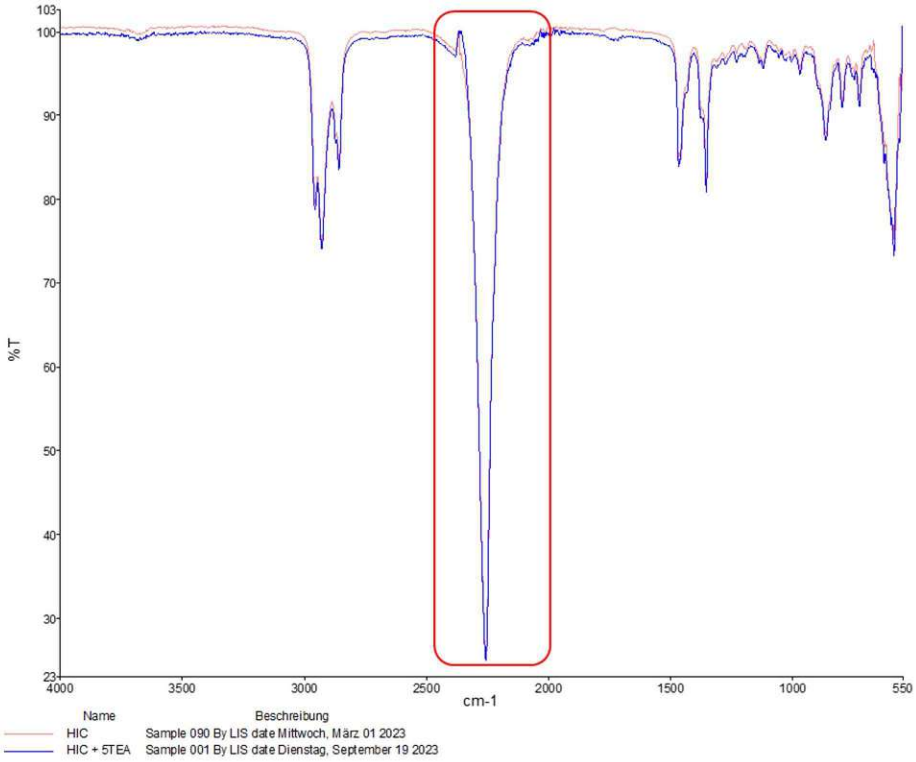

Figure S 7: ATR-FTIR of hexyl isocyanate (HIC, orange) and reaction mixture with hexyl isocyanate and 5 mol% triethylamine (TEA) at ambient temperatures (blue). The isocyanate vibration at 2260 cm^{-1} is enframed in red.

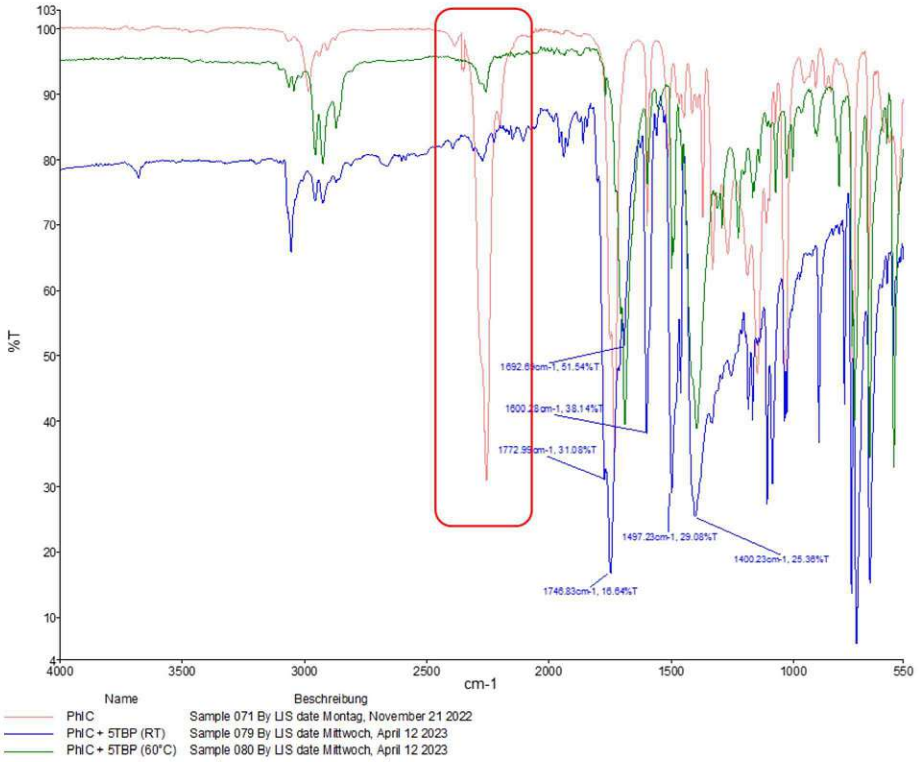

Figure S 8: ATR-FTIR of phenyl isocyanate (PhIC, orange), reaction mixture with phenyl isocyanate and 5 mol% tributylphosphine (TBP) at ambient temperatures (blue) and at 60 °C (green). The isocyanate vibration at 2260 cm^{-1} is enframed in red.

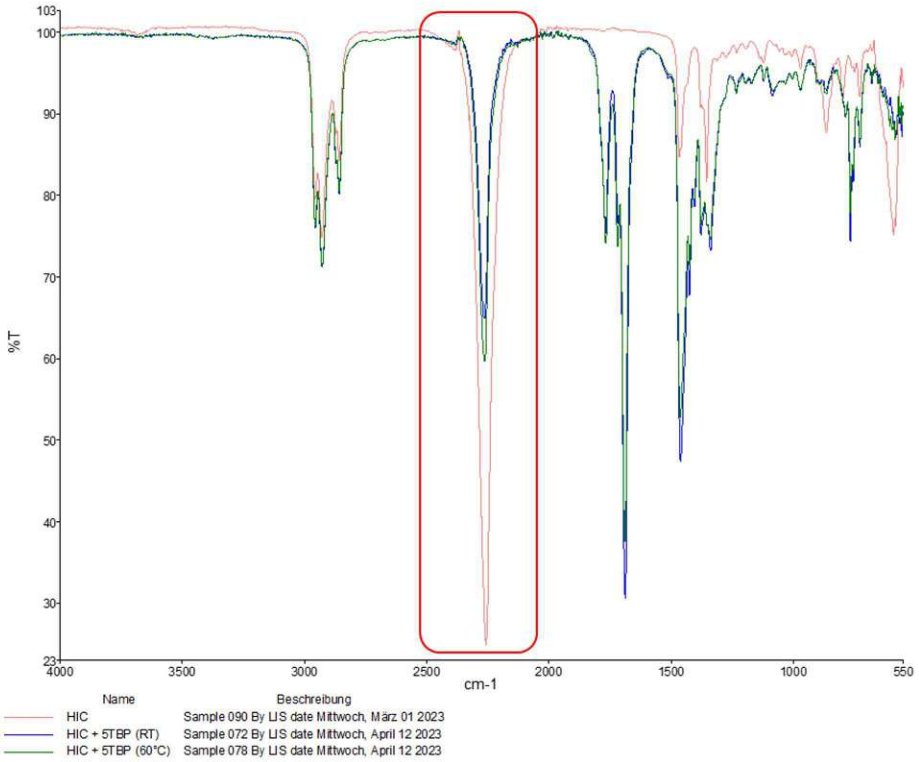

Figure S 9: ATR-FTIR of hexyl isocyanate (HIC, orange), reaction mixture with hexyl isocyanate and 5 mol% tributylphosphine (TBP) at ambient temperatures (blue) and at 60 °C (green). The isocyanate vibration at 2260 cm^{-1} is enframed in red.

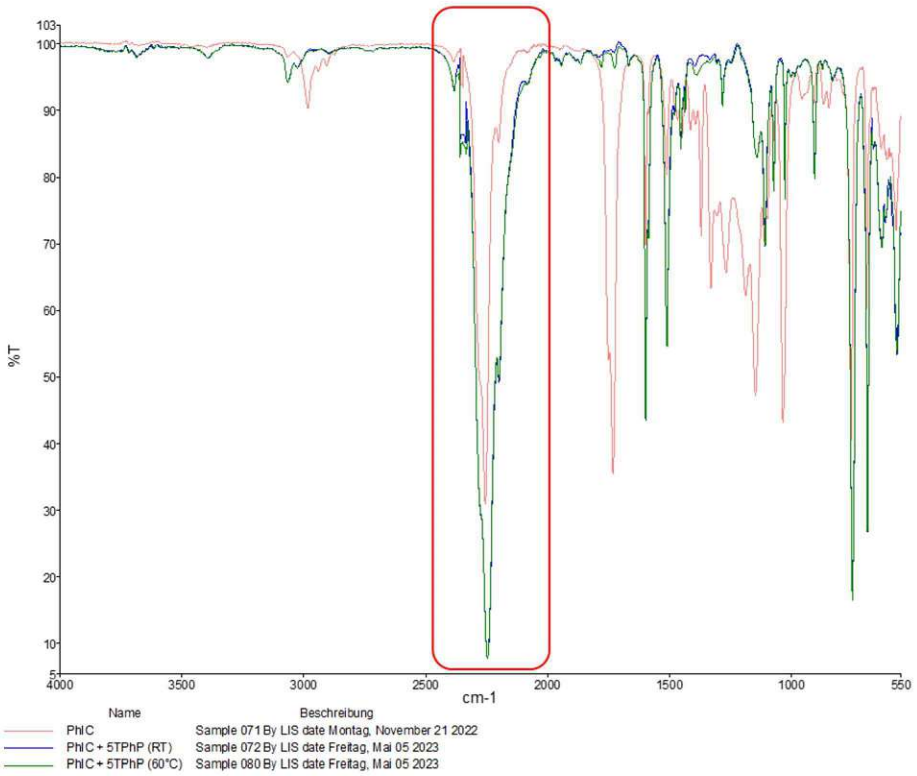

Figure S 10: ATR-FTIR of phenyl isocyanate (PhIC, orange), reaction mixture with phenyl isocyanate and 5 mol% triphenylphosphine (TPhP) at ambient temperatures (blue) and at 60 °C (green). The isocyanate vibration at 2260 cm^{-1} is enframed in red.

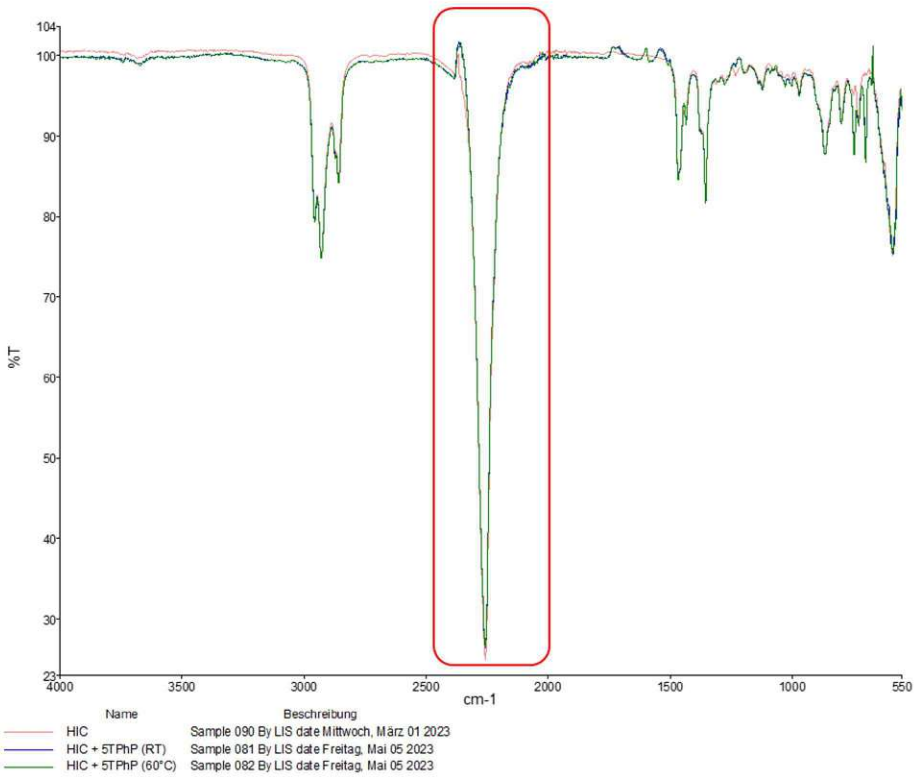

Figure S 11: ATR-FTIR of hexyl isocyanate (HIC, orange), reaction mixture with hexyl isocyanate and 5 mol% triphenylphosphine (TPhP)at ambient temperatures (blue) and at 60 °C (green). The isocyanate vibration at 2260 cm^{-1} is enframed in red.

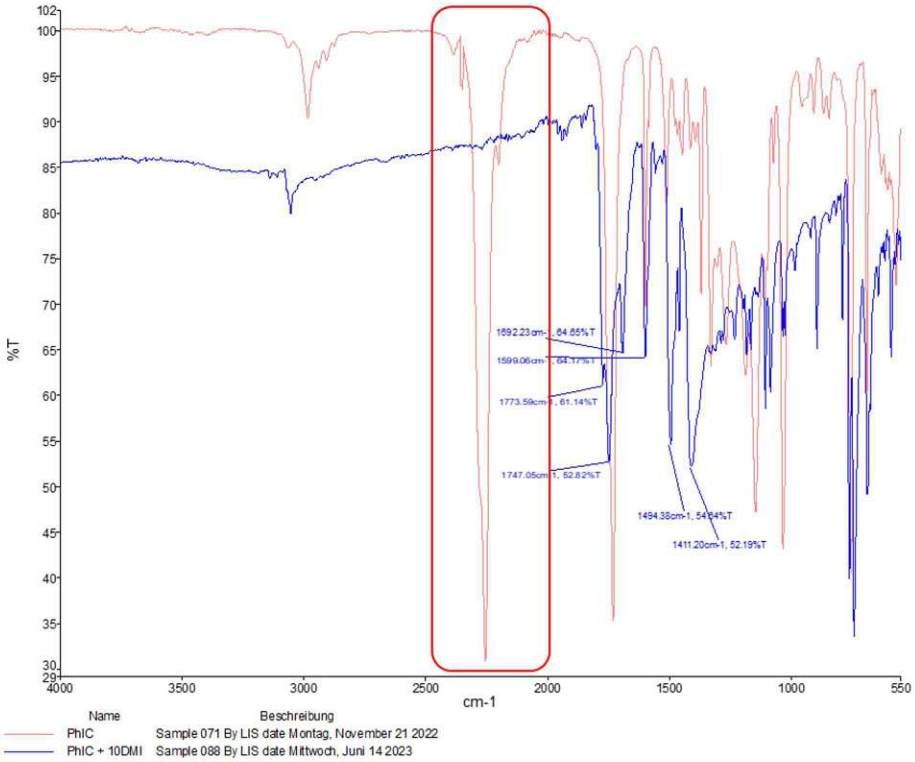

Figure S 12: ATR-FTIR of phenyl isocyanate (PhIC, orange) and reaction mixture with phenyl isocyanate and 10 mol% 1,2-dimethylimidazole (DMI) at ambient temperatures (blue). The isocyanate vibration at 2260 cm^{-1} is enframed in red.

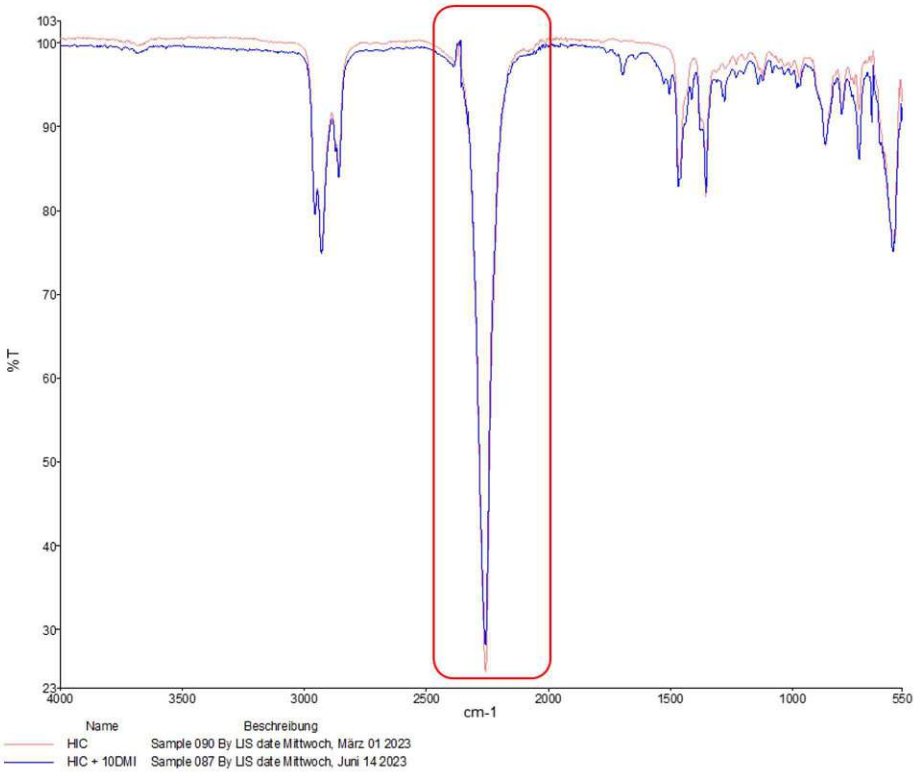

Figure S 1372: ATR-FTIR of hexyl isocyanate (HIC, orange) and reaction mixture with hexyl isocyanate and 10 mol% 1,2-dimethylimidazole (DMI) at ambient temperatures (blue). The isocyanate vibration at 2260 cm^{-1} is enframed in red.

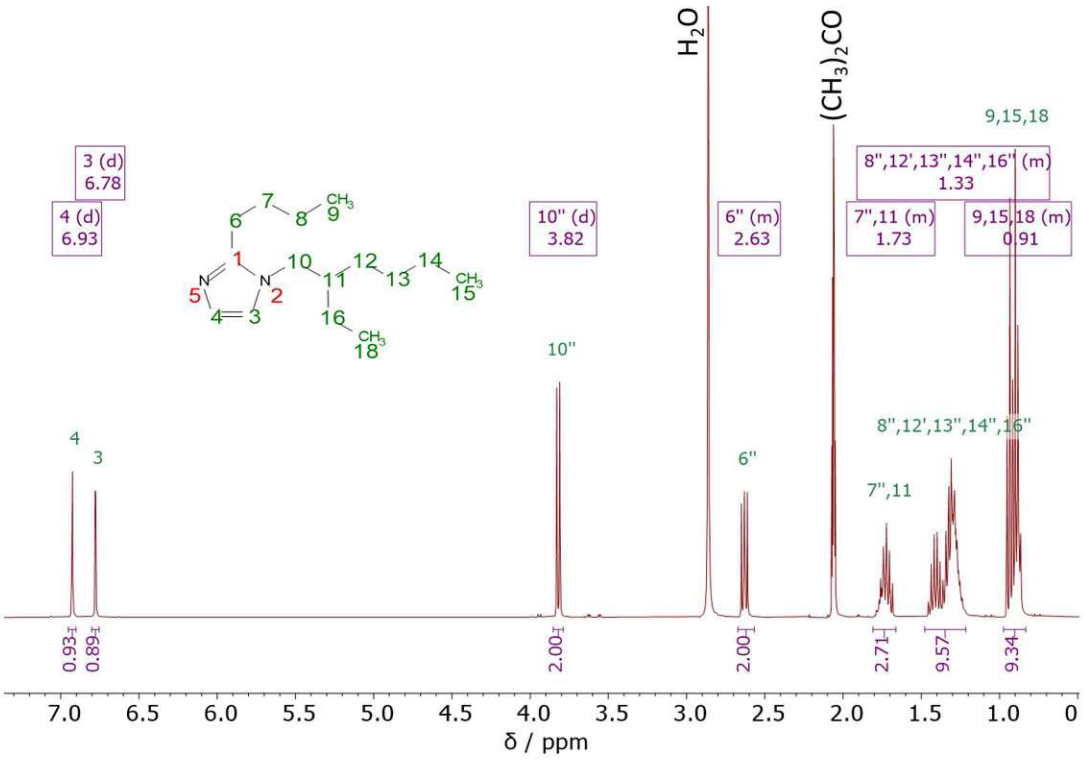

Figure S 14: ^{1}H-NMR (400 MHz, $(CD_3)_2CO$) of 1-(2-ethyl hexyl)-2-butyl-imidazole) (BEHI)

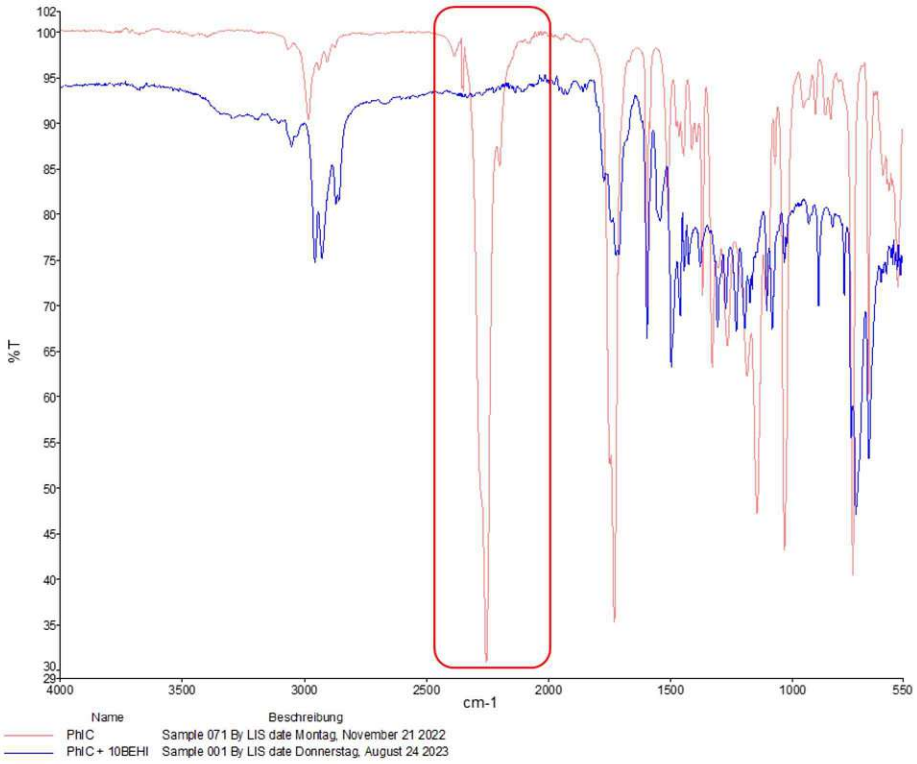

Figure S 15: ATR-FTIR of phenyl isocyanate (PhIC, orange) and reaction mixture with phenyl isocyanate and 10 mol% 1-(2-ethyl hexyl)-2-butyl-imidazole) (BEHI) at ambient temperatures (blue). The isocyanate vibration at 2260 cm^{-1} is enframed in red.

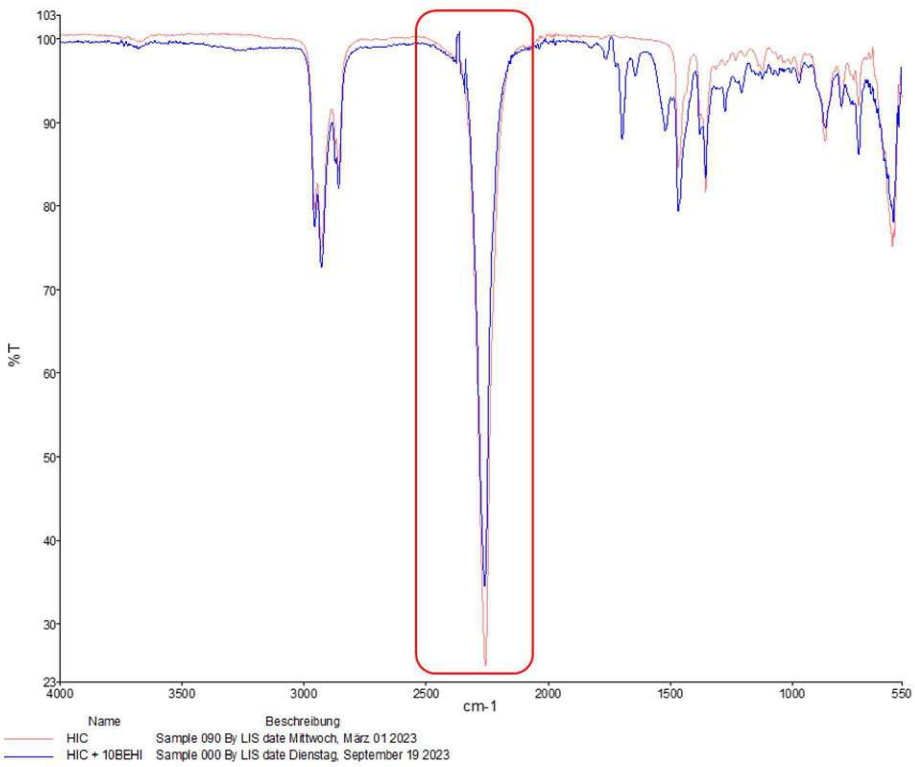

Figure S 16: ATR-FTIR of hexyl isocyanate (HIC, orange) and reaction mixture with hexyl isocyanate and 10 mol% 1-(2-ethyl hexyl)-2-butyl-imidazole) (BEHI) at ambient temperatures (blue). The isocyanate vibration at 2260 cm^{-1} is enframed in red.

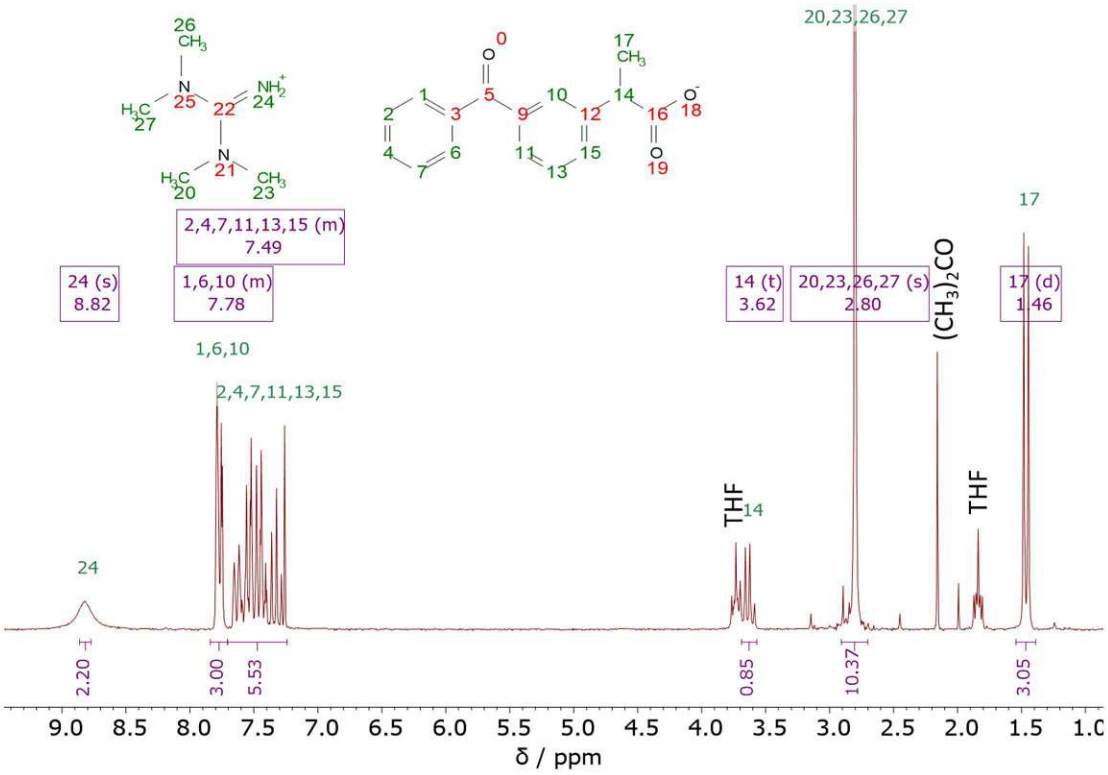

Figure S 17: ^{1}H-NMR (200 MHz, $CDCl_3$) of photo-keto-tetramethyl guanidine (PKTMG)

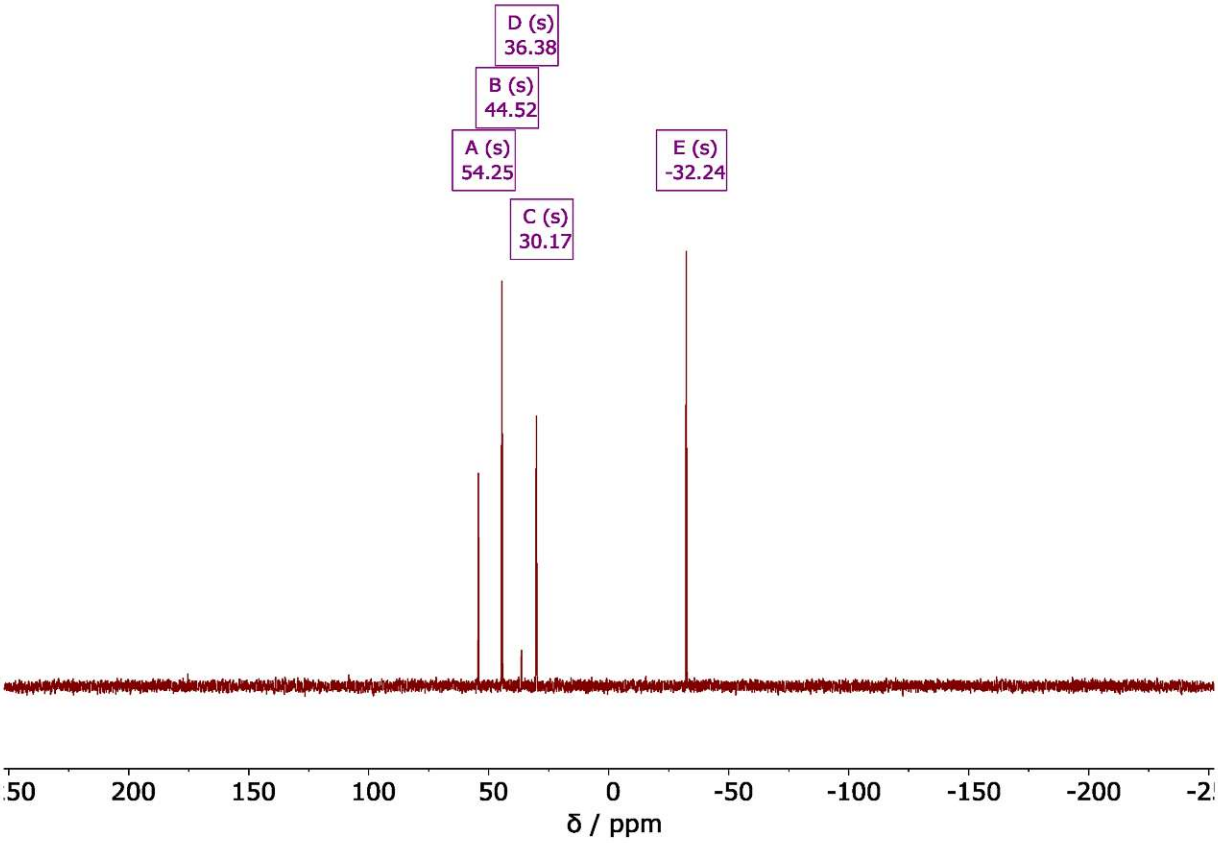

Figure S 18: ^{31}P-NMR (162 MHz, $CDCl_3$) of photo-keto-tributylphosphine (PKTBP)

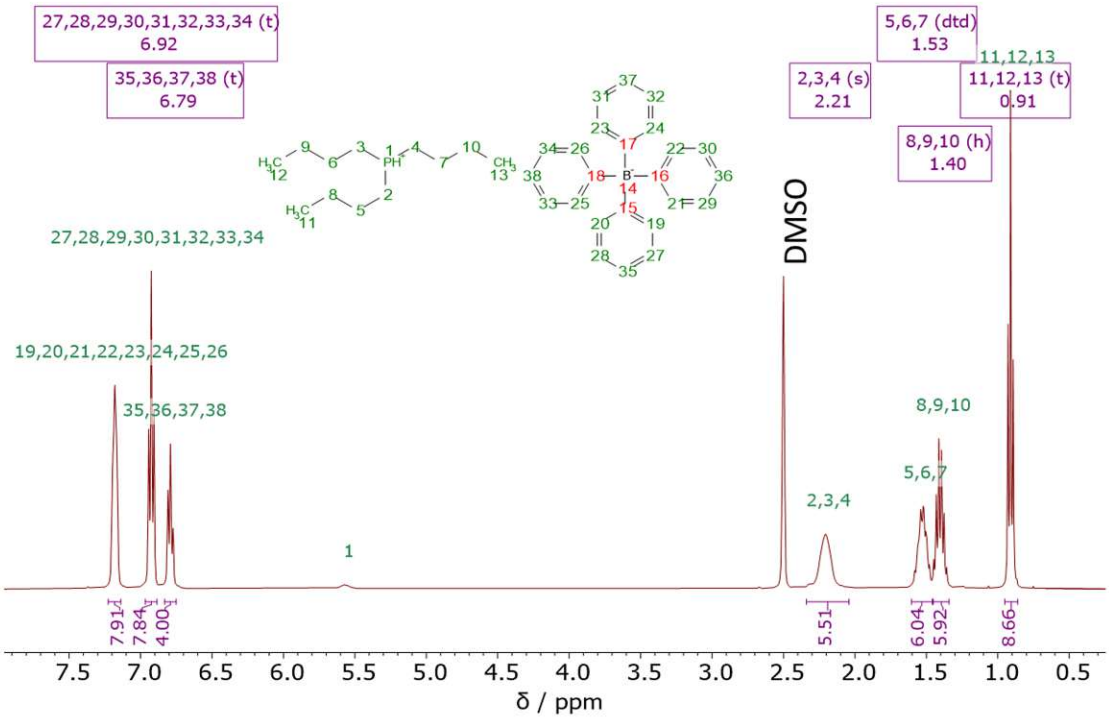

Figure S 19: ^{1}H-NMR (400 MHz, DMSO) of photo-borate-tributylphosphine (PBTBP)

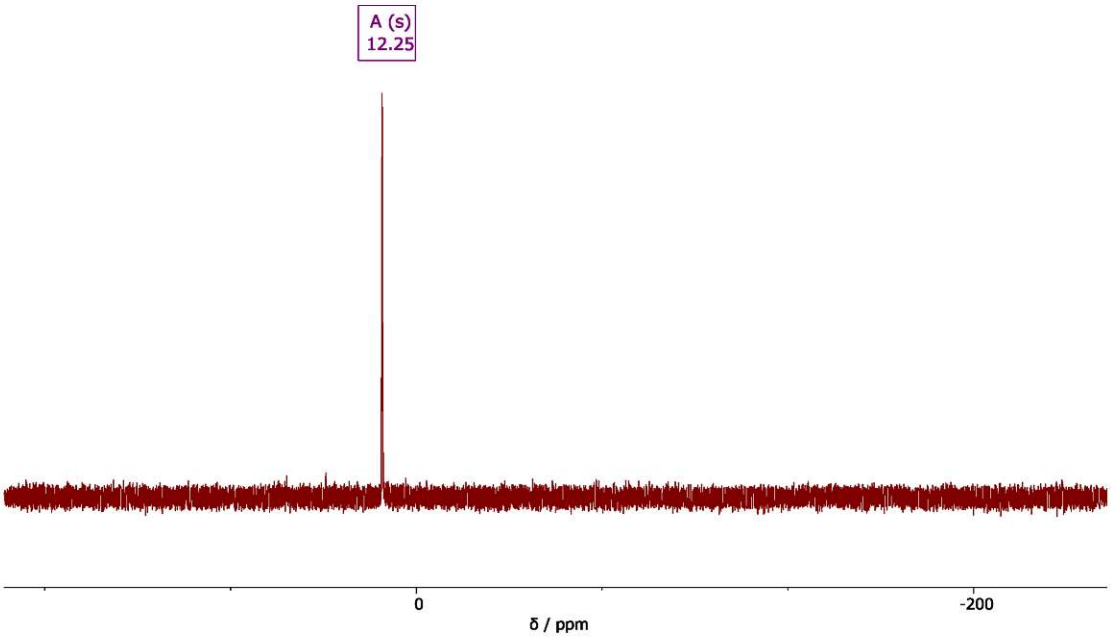

Figure S 20: ^{31}P-NMR (162 MHz, DMSO) of photo-borate- tributylphosphine (PBTBP))

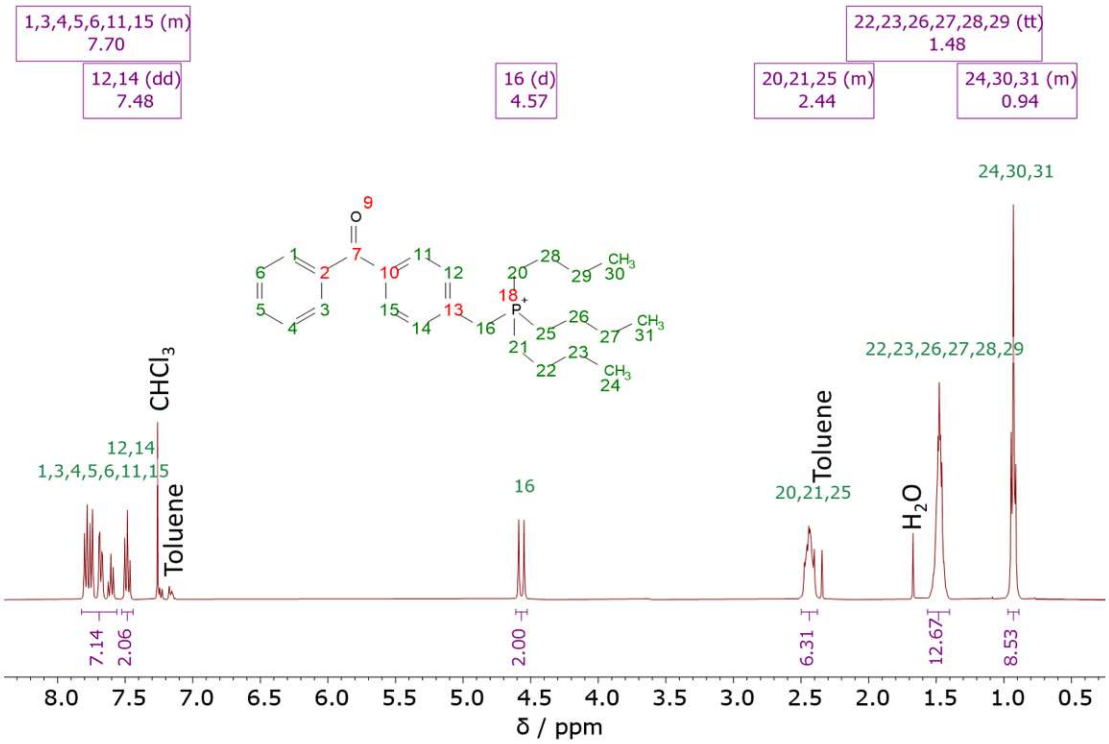

Figure S 21: ^{1}H-NMR (400 MHz, $CDCl_3$) of para-photo-benzophenone-tributylphosphine (p-PBPTBP)

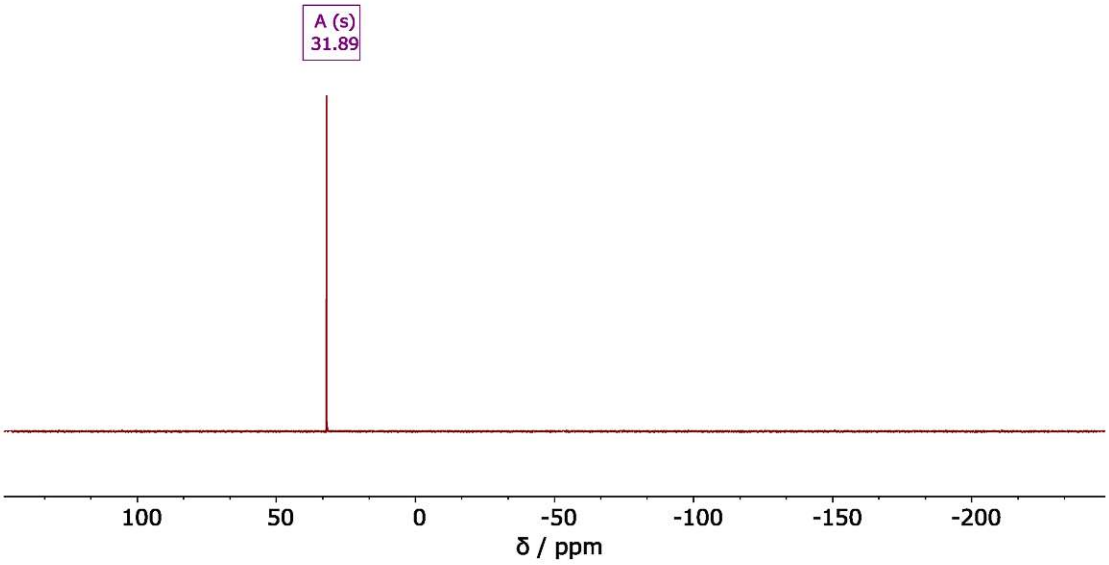

Figure S 22: ^{31}P-NMR (162 MHz, $CDCl_3$) of para-photo-benzophenone-tributylphosphine (p-PBPTBP)

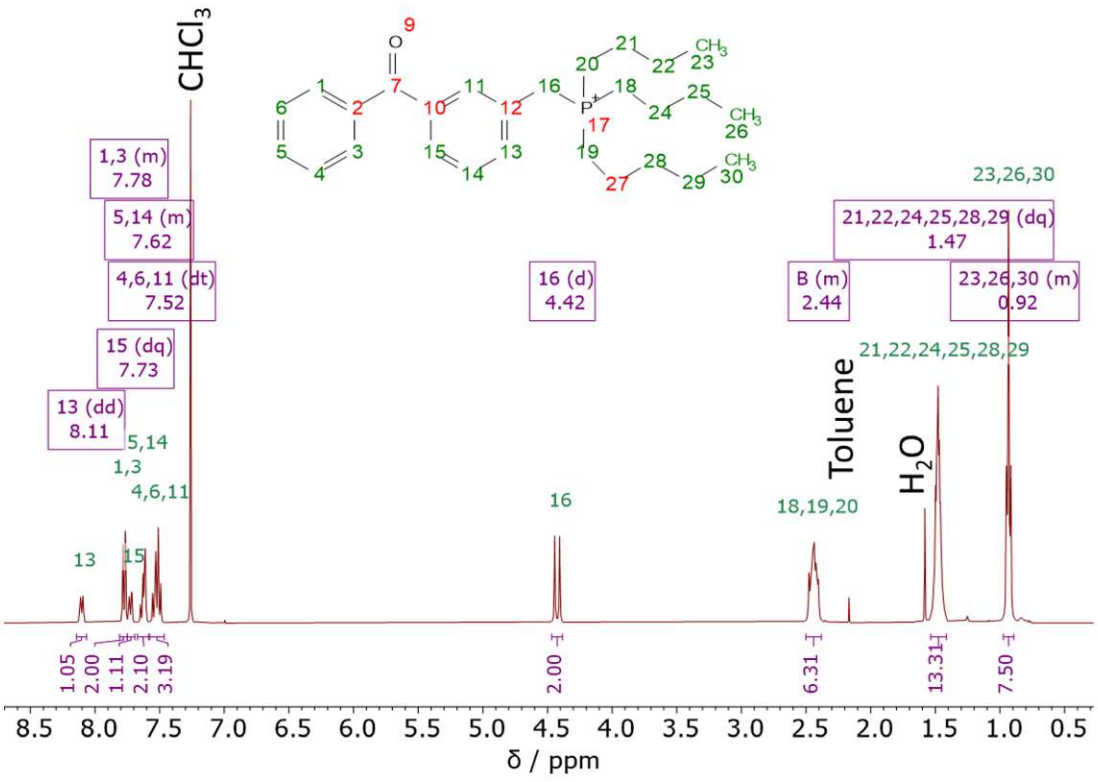

Figure S 23: ^{1}H-NMR (400 MHz, $CDCl_3$) of meta-photo-benzophenone-tributylphosphine (m-PBPTBP)

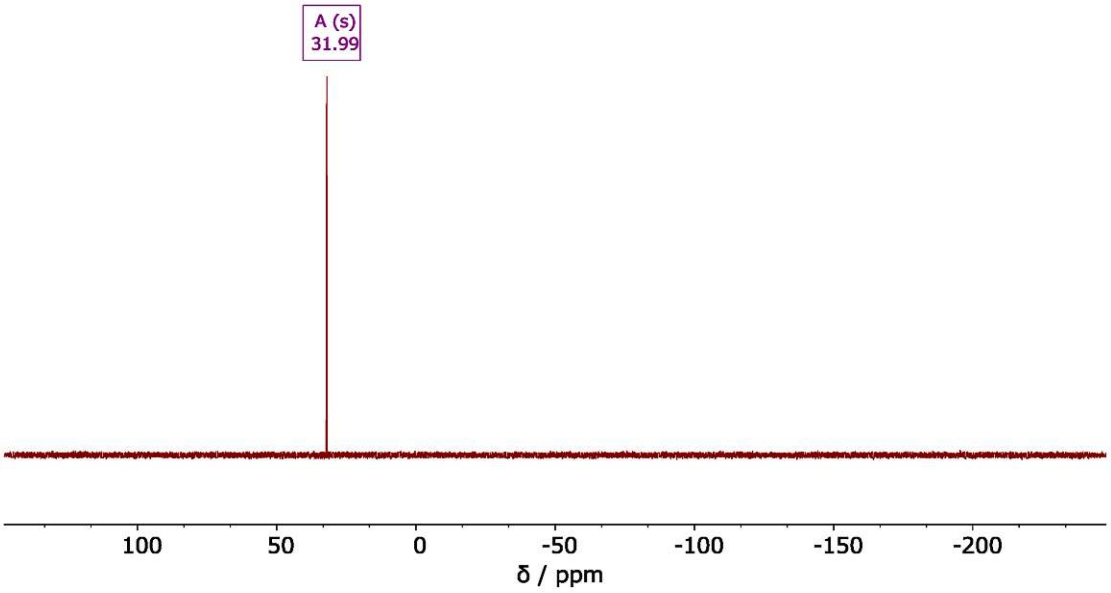

Figure S 24: ^{31}P-NMR (162 MHz, $CDCl_3$) of meta-photo-benzophenone-tributylphosphine (m-PBPTBP)

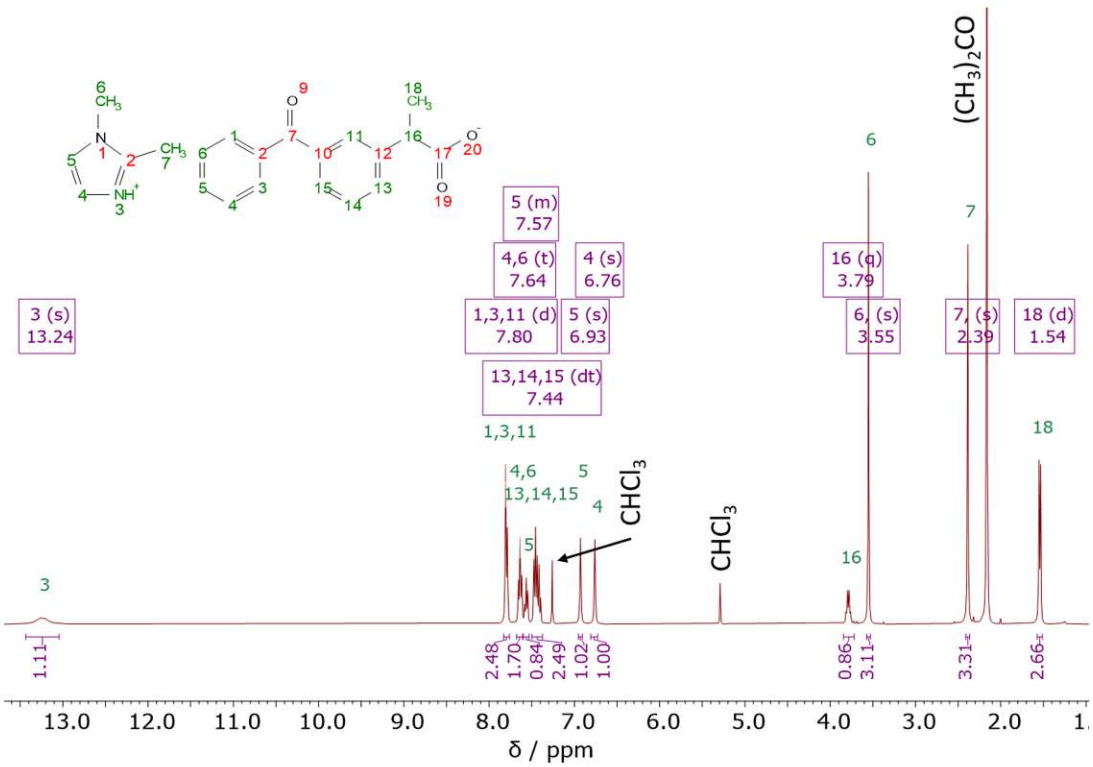

Figure S 25: ^{1}H-NMR (400 MHz, $CDCl_3$) of photo-keto-dimethylimidazole (PKDMI)

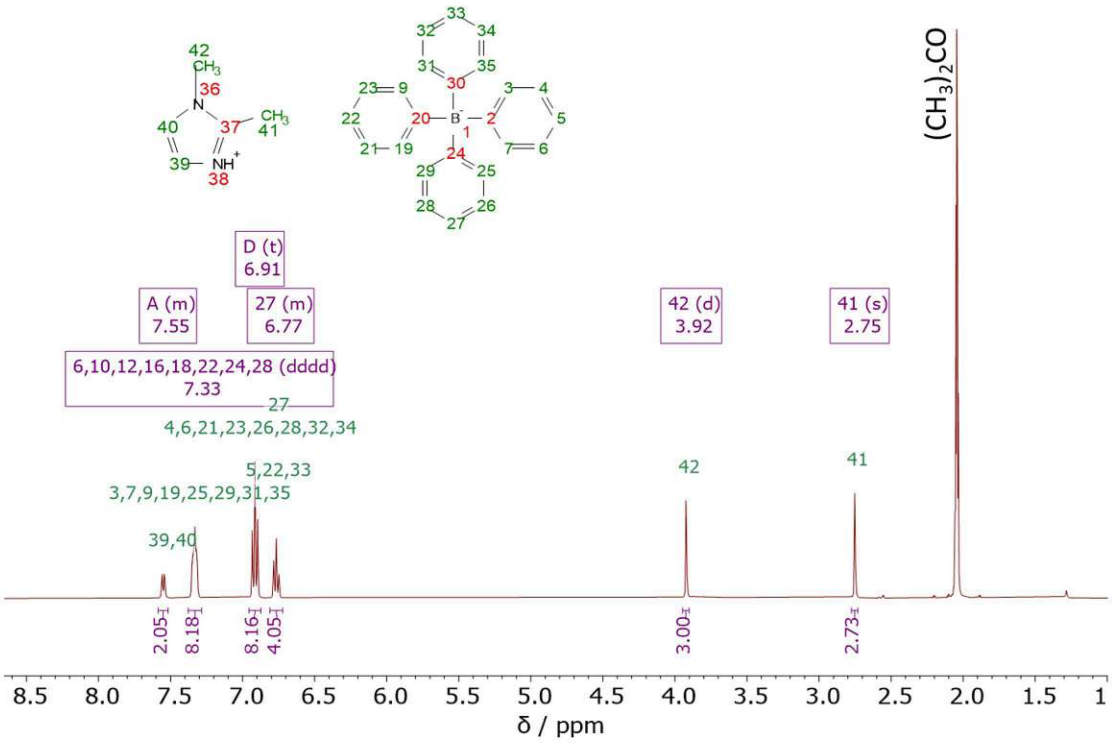

Figure S 26: ^{1}H-NMR (400 MHz, $(CD_3)_2CO$) of photo-borate-dimethylimidazole (PBDMI)

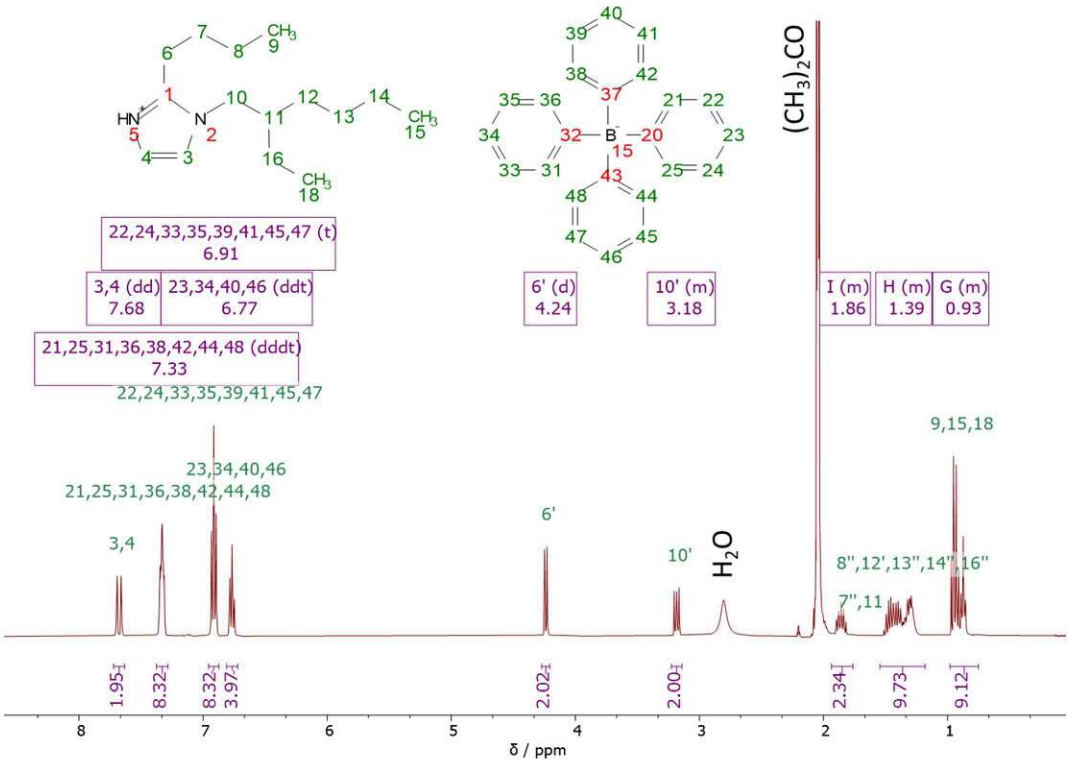

Figure S 27: ^{1}H-NMR (400 MHz, $(CD_3)_2CO$) of photo-borate-1-(2-ethyl hexyl)-2-butyl-imidazole) (PBEHI)